UCRL-16888

University of California

Ernest O. Lawrence Radiation Laboratory

NUCLEAR SPECTROSCOPIC STUDIES OF SOME VERY HEAVY ODD-MASS NUCLIDES

Berkeley, California

UCRL-16888

UNIVERSITY OF CALIFORNIA

Lawrence Radiation Laboratory
Berkeley, California

AEC Contract No. W-7405-eng-48

NUCLEAR SPECTROSCOPIC STUDIES OF SOME VERY HEAVY ODD-MASS NUCLIDES

Irshad Ahmad

(Ph.D. Thesis)

September 20, 1966

NUCLEAR SPECTROSCOPIC STUDIES OF SOME VERY HEAVY ODD-MASS NUCLIDES

Contents

NUCLEAR SPECTROSCOPIC STUDIES OF SOME VERY HEAVY ODD-MASS NUCLIDES

Irshad Ahmad

Lawrence Radiation Laboratory
University of California
Berkeley, California

September 20, 1966

ABSTRACT

The nuclear radiations of nuclides: U^{233}, Pu^{239}, Bk^{243}, Bk^{244}, Bk^{245}, Bk^{246}, Bk^{249}, Cf^{249}, and Fm^{255} were investigated with high-resolution spectrometers. The α-particle spectra of all nuclides except Bk^{249} were measured with 6 mm diameter surface-barrier detectors. Bk^{249} α-particles were analyzed with a double-focusing magnetic spectrograph. The γ-singles were examined with the recently developed Ge(Li) and Si(Li) detectors coupled with very-low noise "internal FET" preamplifiers. Weak alpha groups were observed in coincidence with γ-rays, detected with a NaI(Tl) scintillation spectrometer. To improve the over-all coincidence efficiency a new coincidence apparatus was designed and built. This instrument consisted of a cooled 4.5 cm diameter semiconductor detector for α-particle detection and a 3 cm diameter by 2.7 cm long Ge(Li) detector for γ-ray analysis. The Ge(Li) detector could also be replaced with a NaI(Tl) detector. Cf^{249} conversion electrons were measured with a cooled Si(Li) detector coupled with an internal FET preamplifier.

On the basis of the present work and previous information, energy-level diagrams of the daughter nuclei have been contructed. The levels have been grouped into rotational bands built on Nilsson single-particle states. Because of identification of several rotational members of the bands, definite Nilsson quantum number assignments have been made in most cases. The alpha intensity calculations of Poggenburg were found quite helpful in making these assignments.

A strong Coriolis effect was observed in the Am^{245} levels populated by the alpha groups of Bk^{249}. Calculations were made with Nilsson wave-functions, and these were found to agree with the experimental results. The Coriolis interaction was found important in almost all cases; the effect was very noticeable in the level spacings between the rotational members of the bands.

High-lying bands in Cm^{245} (at 644 keV) and Cf^{251} (at 550 keV) were observed and 4 rotational members of each were identified. The modes of de-excitation of these levels indicate very small or no vibrational characters in them. This suggests that the vibrational bands, in this region lie at very high energies (~1 MeV) above the ground state.

I. INTRODUCTION

Most of the information available about the energy levels of deformed odd-mass nuclei have been explained[1,2] in terms of the Nilsson[3] model. The Nilsson diagrams have been found very useful in the assignment of spin and parity of the ground state and the low-lying excited states of these nuclei. The rotational band structure associated with the intrinsic states is well established and has been explained in terms of the collective[4] motion of the deformed nuclei.

In radioactive decay, however, only a few of the Nilsson states receive enough population to be observed by the usual experimental techniques. This is especially true in the measurements of alpha spectra where the amount of the sample and the efficiency of the detecting system must be limited in order to achieve good resolution. In the case of α-particle detection by semiconductor detectors, each peak tails off at about $10^{-2}\%$ of the peak counts and thus masks the low-intensity alpha groups. Also, when trying to detect such weak transitions very little impurity can make the experiment almost impossible. Both of these problems can be avoided by doing α-γ and γ-α coincidence experiments.

In recent years the experimental techniques in the field of nuclear spectroscopy have been greatly improved to make this kind of work possible. The high resolution Ge(Li) γ-ray detectors[5] and high resolution Si(Li) electron detectors have been extremely helpful in γ-singles and electron singles measurements. In the coincidence measurements the development of the digital gain stabilizer[6] made longer experimental runs possible, and thus one could devote time in the search of the weakly populated states.

In establishing an energy-level diagram it is sometimes useful to show that certain γ-rays or conversion electrons are in coincidence with a specific alpha group. This kind of work requires high resolution and large efficiency for both detectors. It was the purpose of this work to get such an instrument built and use it in the study of decay schemes of odd-mass nuclei.

The present study has shown that the α-γ coincidence technique in which the α-particles gates or the γ-ray gates are carefully selected, is by far the most useful method of studying complex decay schemes. In some of the isotopes studied, rotation-particle coupling[7] is found to affect the level spacings of the band and the alpha transition probabilities to its members very significantly. In cases where Coriolis interaction is not significant, Poggenburg's[8] calculations of alpha transition probabilities are fairly helpful in the choice of the intrinsic state.

II. EXPERIMENTAL PROCEDURE

During the course of this work great progress has been made in the improvement of gamma-ray and electron resolution. As these changes have been gradual, various detectors and instrumental techniques have been employed. The choice of the instrument depended mainly on its availability at the time of the experiment and the nature of information required. In the following sections a brief description of these instruments and methods of preparation and purification of sources is given.

A. Alpha Spectroscopy

Except for the measurements of the Bk^{249} α-particle spectrum, all measurements have been made with 6 mm diameter Au-Si surface-barrier detectors. These detectors have been used at 1% and 5% geometries and under good conditions resolutions of 16 keV have been obtained. For γ-α coincidence measurements where α-particles were used as gates, 1 cm diameter detectors which gave resolution of 25 keV at 10% geometry have been used. Attempts were also made to improve the resolution of these detectors by cooling, but with little success. The detector used in the new coincidence chamber will be described in Section D.

For high resolution work a double-focussing magnetic spectrograph has been used. The details of the instrument have been described by Pilger[9] and Ruiz.[10] It is essentially a Siegbahn-Svartholm double-focussing spectrograph, with the modification that the source and the receiver are located outside the magnetic field. After passing through the magnetic field, the alpha particles are recorded on photographic plates. The developed plates were scanned under a microscope every 1/4 mm along the width. The total number of alpha events (which corresponds to alpha intensity) in each of these scans was plotted as a function of the microscope setting (which is proportional to α-particle energy). The energy difference between any two peaks is given by the relation

$$\Delta E(\text{keV}) = \frac{B^2}{4} \cdot F.D_0(1 + c\,x) \cdot \Delta x \cdot 10^{-2} \quad , \qquad (1)$$

where x_1 and x_2 are the positions of the two peaks on the plate in mm, $\Delta x = |x_1 - x_2|$ is the spacing between them, and B is the magnetic field in megacycles (measured by the nuclear magnetic resonance frequency of Li^7). The constants D_0 and c are evaluated by using α-particle energy standards, and are found to be 2.815 and 1.79×10^{-3} respectively. The factor F which is the correction factor for the magnetic field, is almost unity; its value as a function of field B has been determined by Gunter and Asaro.[11] The spectrograph gave a resolution of 8 keV at 0.05% transmission.

B. Electron Spectroscopy

For the measurement of conversion-electron spectra, a 5 mm diameter and 3 mm deep lithium-drifted silicon detector has been used. For the study of Pu^{239} e-α coincidences, the cooled detector was coupled to an EC 1000 preamplifier and gave a resolution of 6 keV at 10% geometry for 200-keV electron lines. For the measurement of the Cf^{249} electron spectrum, a similar detector was coupled to an internal field-effect transistor (FET) preamplifier[12] and gave a resolution of 3.5 keV under the same conditions. It should be pointed out that these devices detect alpha particles also and that electron intensities, in terms of electrons per alpha particle, presumably could be measured directly. It has also been observed, however, that only about 70% of the electrons striking the detector are registered in the peak; the rest are partly scattered away from the detector and appear as the tail of the peak. It was therefore necessary to use electrons of known intensity to calibrate the instrument. A Cm^{243} source was used for the calibration of electron energies and intensities.

C. Gamma-ray Spectroscopy

A 3-in. by 3-in. thallium activated sodium iodide crystal mounted on a Dumont 6363 photomultiplier tube was used for γ-γ and α-γ coincidence experiments. For gamma-singles measurements as well as for γ-α coincidences, lithium-drifted germanium detectors were used. The historic development of these detectors is given elsewhere.[5] As these detectors were being developed at the same time this work was in progress, detectors of various sizes and resolutions have been used. For γ-singles studies of all nuclides except where otherwise mentioned, a $3 \times 1 \times 0.3$ cm Ge(Li) detector made by an LRL-Livermore group was used. This detector was coupled to an internal FET preamplifier and has a resolution of 1.3 keV at 100 keV and 3.2 keV at 1 MeV, when operated at a bias voltage of -2.2 kV. The γ-ray spectrum measured with this detector was found to have false peaks. By calibrating with monoenergetic γ-ray standards, the energies and intensities of these peaks were determined. It was found that each real peak in the spectrum gave rise to a false peak whose energy was 81% of the energy of the real peak. The intensity of the false peak relative to that of the true peak was a function of γ-ray energy. The ratio was 4% for energies up to 100 keV and then started decreasing and became 1% at 500 keV. The false peak in the spectrum will be denoted by $F_{\text{real peak}}$ (for example the false peak caused by a 42.4-keV γ-ray will be shown as $F_{42.4}$).

For L x-ray spectrum measurements, a 5×3 mm Si(Li) detector coupled to an internal FET preamplifier was used. This detector gave a resolution of 0.9 keV at 20 keV, but due to its very low efficiency at higher energies it could not be used for γ-rays above 50 keV. For γ-α coincidence measurements, $3 \times 2 \times 0.8$ cm Ge(Li) detectors were used. The γ-ray detector used in the new coincidence chamber will be described in Section D.

D. Coincidence Apparatus

For most α-γ coincidence experiments a vacuum chamber already available[13] has been used with only slight modifications. Because of a 1/8 in. thick chamber wall, this unit could not be used for coincidences with low-energy γ-rays. Also this chamber has too low geometry for the low efficiency Ge(Li) detectors, when used with activity levels generally available. In order to improve the over-all efficiency of the coincidence system it was necessary to improve the geometries for α-particle and γ-ray detection. This implied the use of larger Ge(Li) and α-particle detectors.

The new coincidence unit required a special design because the alpha detector was to be cooled with liquid nitrogen. The cross-sectional view of the unit is shown in Fig. 1, and its photograph in Fig. 2. It consists of a vacuum chamber which houses an α-particle detector, the source, and the γ-ray detector. The source, sandwiched between two aluminum plates, is placed at a fixed position in the chamber, and hence has a reproducible geometry. The alpha detector mounted on an aluminum clamp is connected to a liquid nitrogen cold finger. To warm the detector quickly or to control its temperature and to maximize resolution versus temperature, a heater plate is fixed close to the detector holder. The clamp holding the detector has a thermocouple connected to it in order to read its temperature. The wire leads from the detector are connected to a BNC connector outside the housing. The alpha detector, along with the heater plate and the cold finger, could be moved close to or away from the source with the help of a driving motor. There is a machine slide connected to the whole unit to indicate the position of the detector and thus insure reproducible geometry. In order not to let the detector down to air while changing sources, there is a valve between the source chamber and the metal bellows.

For γ-ray detection a Ge(Li) detector or 3-in. $\times$ 3-in. NaI(Tl) crystal could be used. The Ge(Li) detector was mounted in a special housing which could fit in the chamber. The detector cap consisted of a 0.01-in. beryllium window and could be placed in contact with the source. The holder

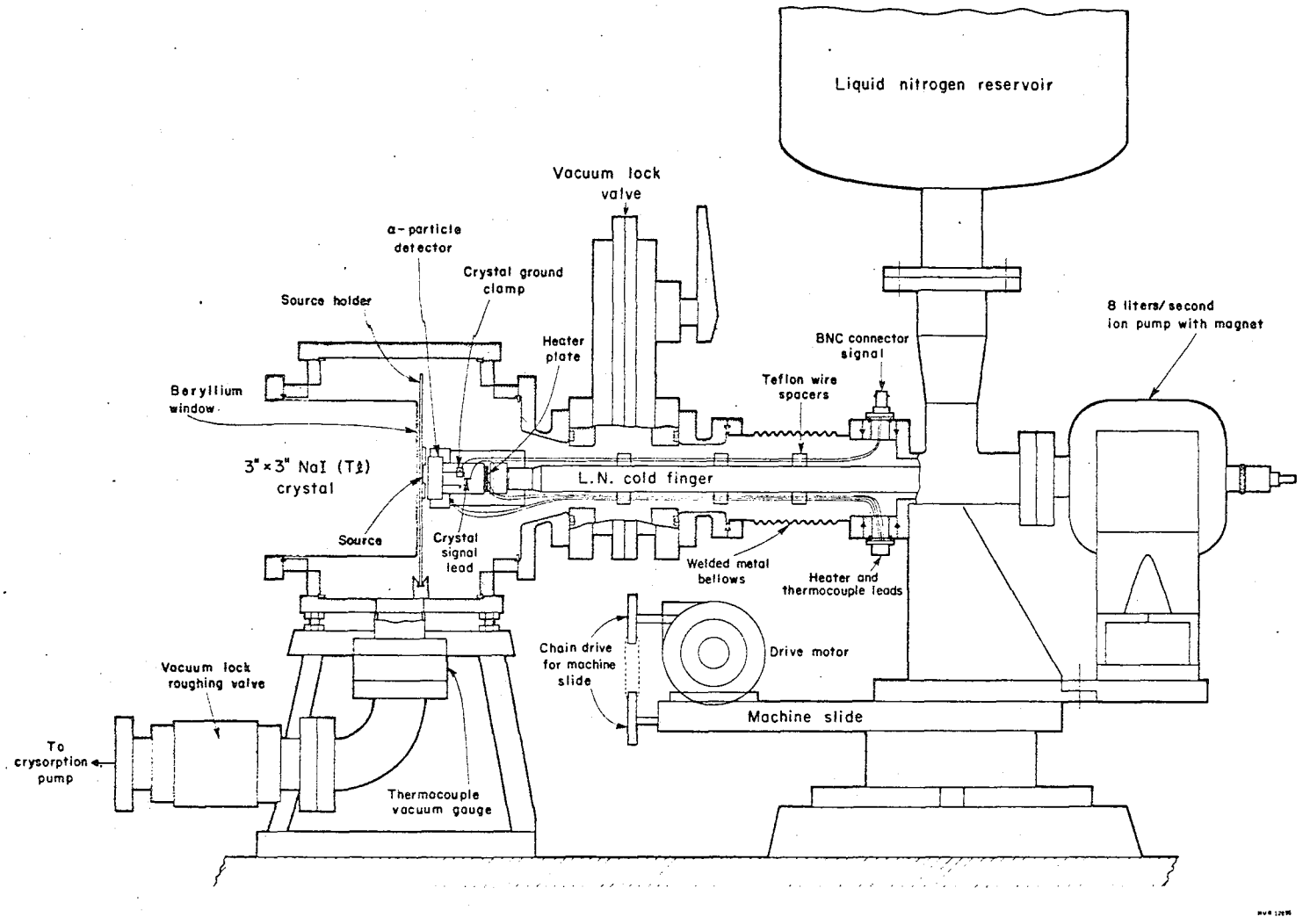

Fig. 1. Cross-sectional view of the new coincidence apparatus.

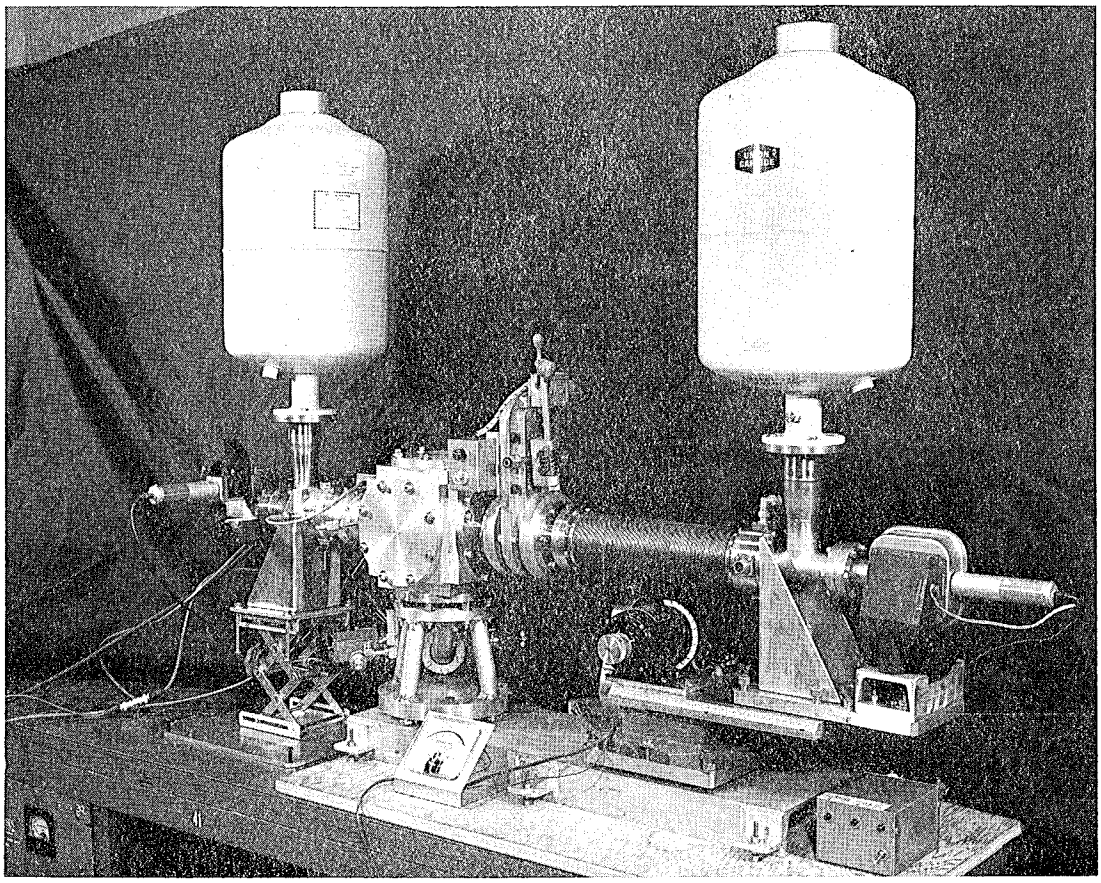

ZN-5935

Fig. 2. Photograph of the α-γ coincidence apparatus, showing the Ge(Li) detector and cooled 4.5-cm diameter semiconductor detector in position for experimental run.

passed through a stainless steel ring which could be bolted to the chamber. Through this arrangement the necessity of a wall between the γ-ray detector and the source was avoided. This increased the γ-ray detection efficiency over the old coincidence unit. Besides, any other detector with the same type of hoursing could be used with the system and also α-L x-ray coincidence measurements could be performed.

To use a NaI(Tl) detector, an aluminum can with a 1 mm thick beryllium window was bolted to the chamber. The scintillation detector could be placed inside the can and could be held in position with the help of lucite rings.

In these γ-α coincidence measurements, the alpha detector was a 4.5 cm diameter semiconductor detector supplied by ORTEC, Oak Ridge, and the γ-ray detector was a 2.7 x 3.0 cm Ge(Li) detector fabricated in this laboratory. The alpha detector was coupled to an EC 1000 preamplifier and the Ge(Li) detector was coupled to an internal FET preamplifier. After placing the source and the detectors in position, the chamber was pumped down with a liquid nitrogen cryosorption pump. A cryosorption pump was used instead of an oil pump in order to insure cleanliness in the system. When the pressure fell below 10^{-3} mm of mercury, an ion pump with 8 liters per second capacity was turned on. When the pressure reached about 5×10^{-4} mm of mercury, liquid nitrogen was poured into the cold finger. In order to avoid abrupt cooling which might cause strain in the crystal-face window, the heater was turned on to control the cooling rate. The resolutions of a pulser and a thin Cm^{244} source were measured as a function of temperature and the time-constants of the amplifier. Best performance was obtained with a long decay time-constant and at a temperature between -30°C and -50°C. As this instrument was built at the end of this work it could not be used as extensively as originally planned.

E. Electronic Components

The alpha particle and γ-ray resolutions depend mainly on the detector-preamplifier system. In order to achieve good resolution a very low-noise preamplifier is required, in addition to a detector with very small leakage current. The preamplifier used with most detectors was designed and built in this laboratory. It was a charge-sensitve type preamplifier, using an EC 1000 tube in the input stage. During the course of this work a preamplifier using a cooled field-effect transistor in the input stage was developed.[12] This type of preamplifier, commonly known as an "internal FET preamp", gives extremely good resolution with detectors having low capacitance and low leakage current. This preamplifier was used in conjection with the $3 \times 1 \times 0.3$ cm LRL-Livermore type Ge(Li) detector and also with the electron detector.

All the electronic components except the multi-channel pulse-height analyzers were designed and built in this laboratory. The linear amplifier, the single-channel analyzer, the delay amplifier, the biased amplifier, and the coincidence unit were all built in separate units and as such were very versatile. The linear amplifier had networks to produce single-delay-line, double-delay-line, or RC pulse shaping, and of various time-constants. In most of the cases, the best resolution was obtained by using pulses with a single-delay-line differentiation time-constant of 0.8 μsec and an integration time-constant of 1.0 μsec. The fast coincidence unit had a variable resolving time and whenever chance coincidences were to be minimized, a resolving time of 40 nsec was used. The slow coincidence unit had a resolving time of 0.8 μsec.

In order to conduct experiments over a long period of time, it was necessary to utilize a system with maximum stability; that is there should be as small a drift in the over-all amplification gain as possible. The Ge(Li) detectors were found to be very stable and could perform very satisfactorily for days with a drift in amplification gain of less than 0.05%. But alpha detectors and the NaI(Tl) γ-ray detectors are not so stable. For

these systems a digital gain stabilizer was extremely useful. The stabilizer, when connected between the preamplifier and the linear amplifier, made the system stable enough for periods of weeks.

For all the experiments RIDL 400-channel analyzers were used. In situations where singles and coincidences were to be measured simultaneously, external routing was employed. To use the external router, some external delay adjustments were necessary. The block diagram of the fast-slow coincidence system is shown in Fig. 3. For γ-α coincidence experiments the NaI(Tl) detector was replaced by a Ge(Li) detector and the α-particle pulses were passed through the single-channel analyzer. In the diagram the external routing is shown only for the alpha side; similar arrangements were made for the gamma side when required.

F. Source Preparation

All source materials used in this work were purified by the usual ion-exchange techniques in which a series of columns were employed to obtain essentially mass-free samples. Elements above americium, in 0.05 M HCl, were loaded on the cation-exchange column (Dowex 50, 12% cross-linked) and eluted with α-hydroxy isobutyric acid[14] at pH 4. This procedure of separation will be referred to as "But column" in the rest of this section. The rare earth elements were removed by loading the material on a Dowex 50 (12% cross-linked) resin column and eluting the actinides as a group with a solution of 20% alcohol saturated with HCl. Plutonium in the samples was removed on an anion-exchange column. Plutonium was first oxidized to the (IV) state with H_2O_2 in 10 M HCl solution and loaded on a column of Dowex A1 (8% cross-linked) anion-exchange resin. The transplutonium elements are not oxidized and hence pass through. Finally the sample was purified from the extraneous mass on a "clean up" column.[15] The activity, in 0.1 M HCl solution, was loaded on a column packed with Dowex 50 (4% cross-linked) cation-exchange resin. The common elements (like Na^{+}, Ca^{2+}, Al^{3+} Ni^{2+}, etc.) were removed by eluting the adsorbed material with 2 M HCl solution. The activity was then stripped off the column with 6 M HCl solution.

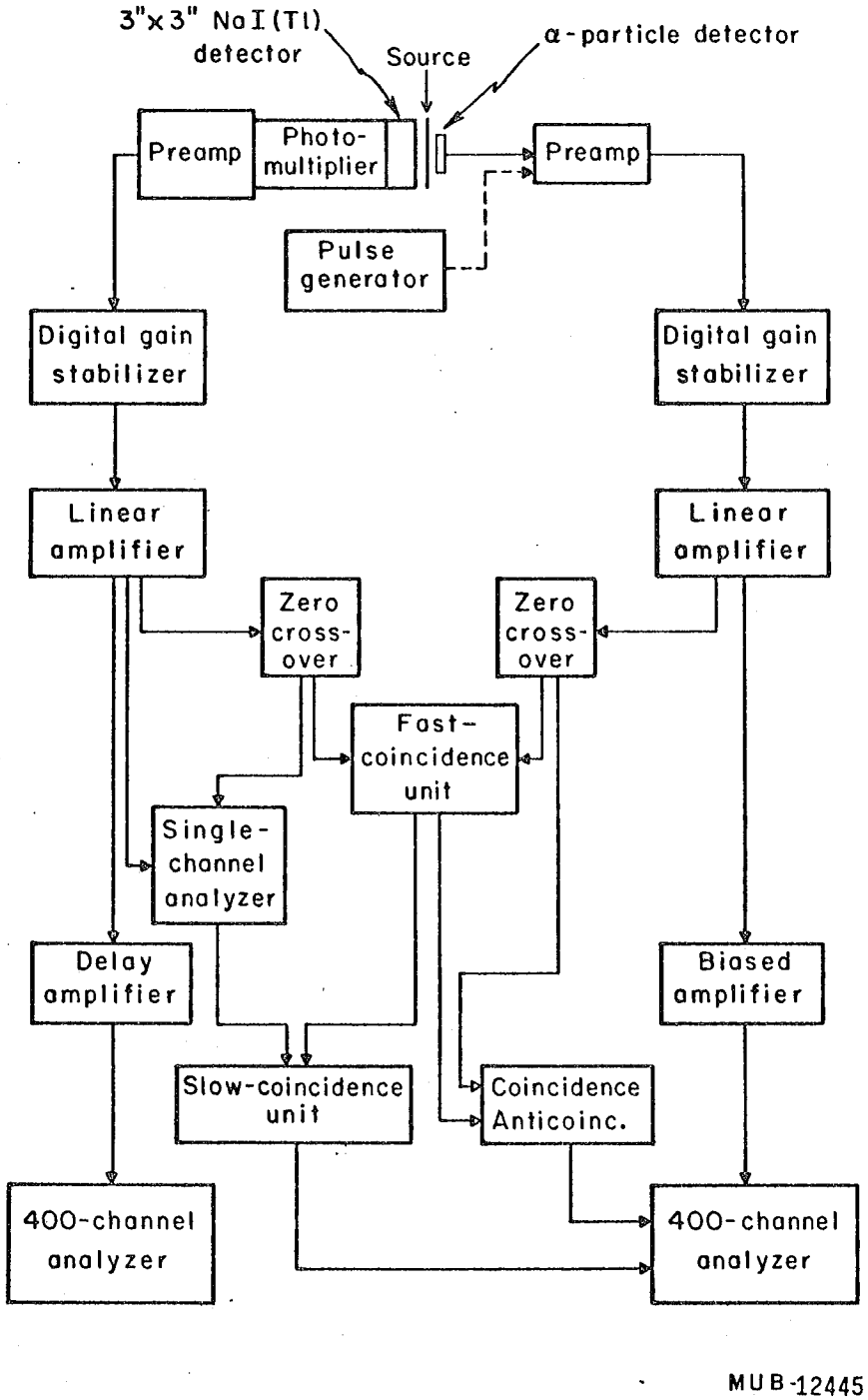

Fig. 3. Block diagram of the fast-slow coincidence circuit.

Thin sources for alpha-particle measurements were prepared either by vacuum-sublimation or by electroplating. Elements which were available in sufficient quantities were vaporized as oxides or chlorides from a hot tungsten filament onto a cold Mylar film or nickel foil. Activities which were available only in limited amounts were electroplated[16] as hydroxide from a 0.004 M HNO_3 solution.

Adequate quantities of U^{233} and Pu^{239} were available in the laboratory. The uranium sample contained 1.5% of U^{232} and 0.5% ^{234} by alpha activity and was purified before each experiment on an anion-exchange column. The chemical purification was required because of the growth of U^{232} daughters. The Pu^{239} was chemically pure and did not require any further separation. Sources for γ-ray measurements were made by evaporating solutions of the active materials on Mylar films, and sources for alpha-particle spectra were prepared by vacuum-sublimation.

Light berkelium[17] isotopes were prepared by bombarding an Am^{243} target with 40- or 33-MeV alpha particles at the 88-inch cyclotron. The Am^{243} (containing 40% Cm^{244} and 17% Am^{241} by alpha activity) was available in the laboratory. Americium was separated from curium on a But column and purified on a clean up column. About 5 mg of the purified material was electrodeposited from a 6 M NH_4Cl solution at 0.6 A/cm^2 of cathode area for 1 1/2 hr. The electrodeposition cell[17] used in the experiment is shown in Fig. 4. The activity, which deposited at the cathode as hydroxide, was washed with water and acetone. It was then dried under a heat lamp, covered with a 0.001-in. platinum plate, and welded vacuum tight. The target was bombarded at a beam intensity of 20 μA for a period of 6 hr. for Bk^{243} and 20 hr. for Bk^{245}. After the bombardment, berkelium was isolated and purified by using the ion-exchange columns described earlier. The source for the alpha-particle spectra was prepared by electroplating.

The nuclides Bk^{249} and Fm^{255} were prepared by prolonged neutron irradiation of curium by the Berkeley and Livermore heavy-element production divisions of this laboratory. The Bk^{249} fraction was isolated from the

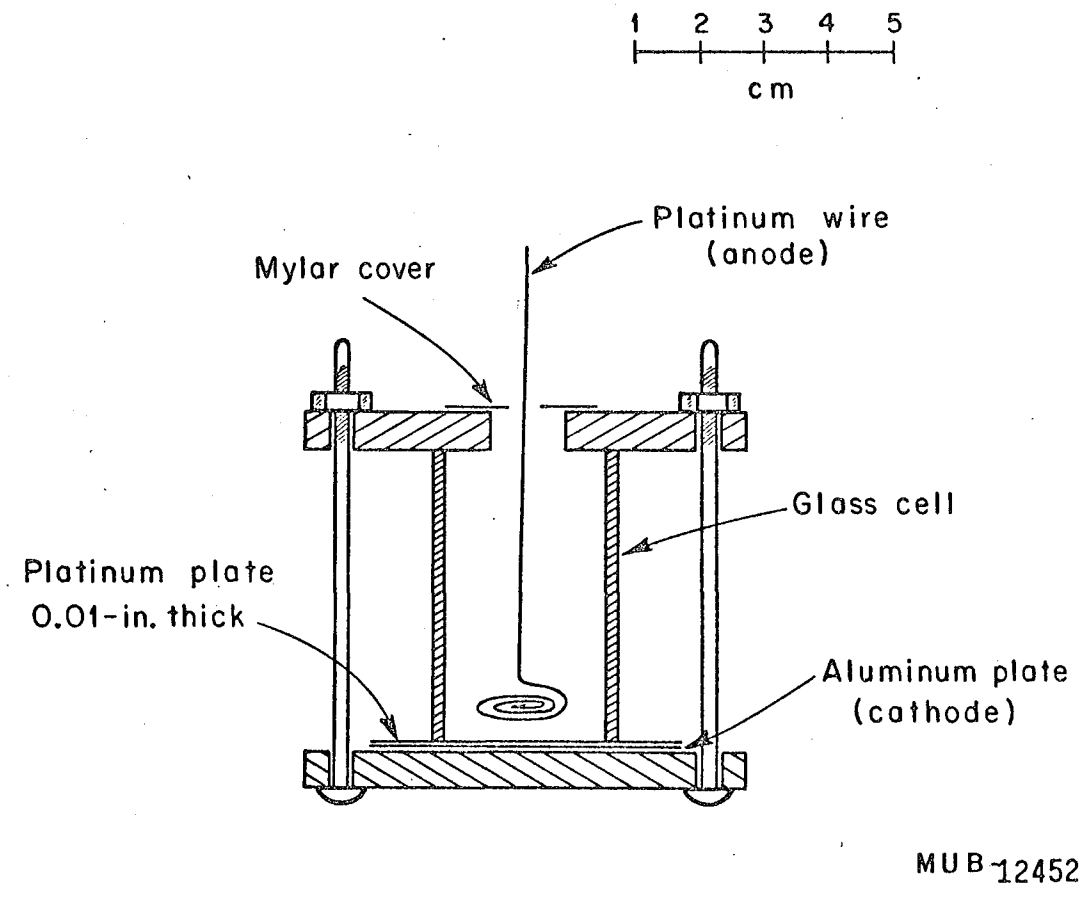

Fig. 4. Electrodeposition unit for the preparation of Am^{243} target.

associated activities by the Berkeley group.[18] The sample was further purified before each experimental run to remove the daughter, Cf^{249}. The Cf^{249} was milked out of the Bk^{249} after 6 months of growth and was purified on ion-exchange columns. Sources for α-particle spectrograph and alpha-gamma coincidence experiments were prepared by vacuum-sublimation.

The nuclide Fm^{255}, along with other Cf, Es, and Fm isotopes, was separated from fission products and lower transuranium elements by the Livermore heavy-element production group.[19] Californium and einsteinium were then removed on a But column. The fermium fraction thus obtained consisted mainly of Fm^{255} (20 hr) and Fm^{254} (3.2 hr). In order to remove the alpha groups of Fm^{254} and its daughter from the spectrum, the sample was allowed to decay for about 16 hr and run through another But column. It was then purified on a clean up column and electroplated on a 0.002-in. nickel foil for coincidence measurements.

III. CALIBRATION PROCEDURES

Gamma-ray singles spectra were measured with Ge(Li) detectors. Gamma-ray energy calibrations were made with standard sources and their energies were taken from the "Table of Isotopes".[20] The absolute photopeak efficiency of the detector was determined with γ-ray standards of known disintegration rates, supplied by the International Atomic Energy Agency, Vienna. The efficiency curve of the $3 \times 1 \times 0.3$ cm detector, used for most of the measurements, is shown in Fig. 5.

The α-particle energy calibration was done with the help of a mercury relay pulser and the main alpha group of the isotope under investigation. The pulser was found to be precisely linear and hence a constant ratio could be assumed between the α-particle energy and the pulser energy. In cases where the α-particle energy of the main alpha group was not known, standard sources of similar α-particle energies and intensities were used. The α-particle energies used for the calibrations were taken from Ref. 21.

Low-intensity alpha groups were usually observed by measuring the alpha spectrum in coincidence with gamma rays. The delays for the maximum fast-slow coincidence rate were adjusted with a Cm^{243} source. At the best setting the coincidence efficiency (the ratio of the fast-slow coincidence rate to the slow coincidence rate) was usually 0.95 or better. In these experiments a 3 in. $\times$ 3 in. NaI(Tl) crystal was used for γ-ray detection; its photopeak efficiency and total efficiency were determined with calibrated gamma-ray sources. The intensity of a particular alpha group, α_i, was calculated from the coincidence measurements by using the formula

$$\alpha_i = \frac{N_i}{N_\alpha \times \epsilon_{coin.} \times \epsilon_\gamma} \qquad (2)$$

where N_i is the total number of coincidences observed in the particular alpha peak, N_α is the total number of α-particles accumulated, $\epsilon_{coin.}$ is the coincidence efficiency, and ϵ_γ is the γ-ray efficiency.

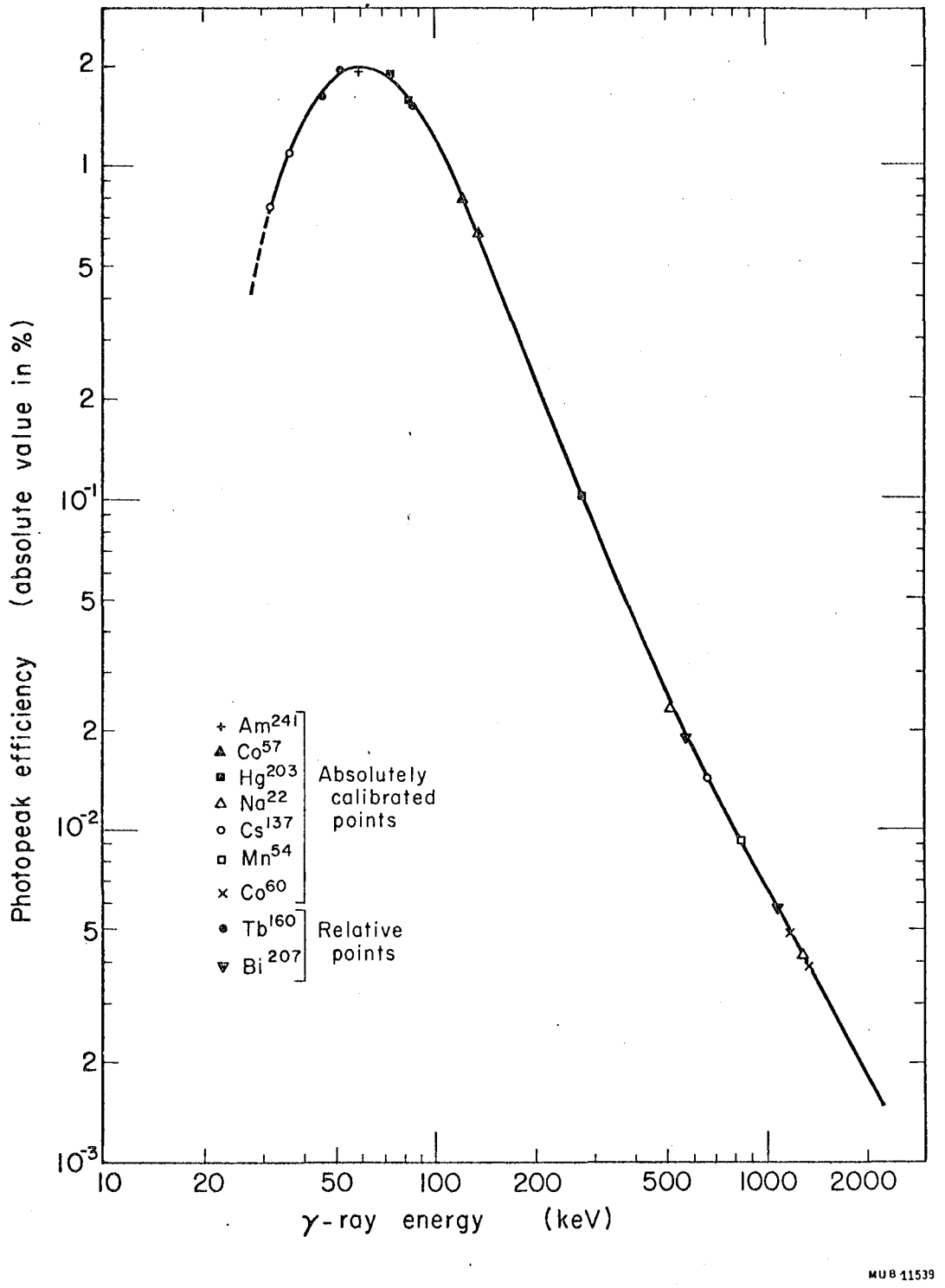

Fig. 5. Photopeak efficiency of the 3 × 1 × 0.3 cm Ge(Li) detector.

Since each level populated by alpha particles de-excites through different γ-ray transitions (sometimes through several transitions in cascade), ϵ_γ has to be weighted. In order to get an accurate value of ϵ_γ one has to know precisely the decay scheme, the γ-ray intensities, and the conversion coefficients of these transitions. It is difficult to know these quantities with good precision in cases of complicated decay schemes and hence the alpha intensities should be expected to have significant errors. The errors quoted in the intensities contain an estimate of the errors in the weighted γ-ray efficiencies. The hindrance factors of the alpha transitions were calculated by Mrs. H. V. Michel,[22] using Preston's equations.[23] In Chapter IV the experimental alpha intensities are compared with the theoretical values calculated with the formula of Bohr, Fröman, and Mottelson.[24] For some nuclei the alpha transition probabilities calculated by Poggenburg[8] are also included in the tables for comparison.

The multipolarities of the internal transitions were determined by the comparison of the experimental and theoretical values[25] of conversion coefficients. The electron intensities, for this purpose, were obtained either from the present measurements or from some other references. In nuclides where only a few significant transitions occur, K x-ray intensities were used as a measure of the K-conversion electron intensities.

IV. RESULTS

A. Alpha Decay of U^{233}

The radiations accompanying the alpha decay of U^{233} have been investigated by various groups.[20,26] The data so far available indicate a rather high nuclear level density in the daughter. The low-intensity alpha groups of U^{233} are difficult to study because of its low specific activity. The "singles" and coincidence measurements of Ruiz[10] reveal a complex structure in the alpha and gamma spectra. Dzhelepov et al.[27] investigated the alpha spectra with a magnetic spectrograph and identified 12 fine-structure alpha groups. Conversion-electron studies of Tret'yakov et al.[28] indicate that the high-lying states of Th^{229} have positive parity. Because of the lack of detailed information, only partial decay schemes have been postulated by these authors. The present study was undertaken with a view to supplement the above measurements with new data and thus formulate a more complete decay scheme.

1. Gamma Rays

Gamma-ray spectra of U^{233} were examined with a variety of detectors. The source for the prominent radiations was a 10-mg sample evaporated on a 0.002-in nickel plate. For the study of weak γ-rays, 6 grams of U^{233} in HCl solution were used. The sample contained about 1.5% of U^{232} and about 0.5% of U^{234} by alpha activity. In order to eliminate the radiations due to the daughters of U^{232} from the spectra, the sample was purified before each experiment. Corrections for U^{232} and U^{234} were made by measuring pure samples of these substances, the spectral lines of which are listed in Table I. The U^{233} γ-rays obtained as a result of the present measurements are given in Table II.

In Fig. 6 the spectrum (a) was taken with a high-resolution Si(Li) detector and the rest were measured with the $3 \times 1 \times 0.3$ cm Ge(Li) detector. In spectrum (b) the 60- to 80-keV region is complex because the false peaks

Table I. U^{232} and U^{234} γ-rays.

A. γ-rays of U^{232}

Energy (keV)		Relative intensity
57.6 ± 0.2		100 (norm)
90.0 ± 0.2	(Th K_{α_2})	2.9 ± 0.4
93.4 ± 0.2	(Th K_{α_1})	4.7 ± 0.6
129.0 ± 0.2		39 ± 4
270.5 ± 0.3		1.8 ± 0.3
327.8 ± 0.3		1.6 ± 0.3

B. γ-rays of U^{234}

Energy (keV)		Relative intensity
53.3 ± 0.2		100 (norm)
90.0 ± 0.2	(Th K_{α_2})	2.8 ± 0.4
93.3 ± 0.2	(Th K_{α_1})	4.2 ± 0.6
120.9 ± 0.2		34 ± 4

Table II. Gamma-ray transitions in Th^{229}.

E_γ^a(keV)	$I_\gamma^a(\%) \times 10^3$	$I_e^b(\%) \times 10^3$	Conversion shell	Multipolarity[c] and remarks
11.1 ± 0.1	130 ± 40			Th L_ℓ
12.9 ± 0.1	2400 ± 400			Th L_α
16.1 ± 0.1	3300 ± 500			Th L_β
19.0 ± 0.1	900 ± 150			Th L_γ
25.2 ± 0.1	2 ± 0.5			
29.0 ± 0.1	10 ± 2	540	partly L_I	M1 ?
		270	M	
		150	N	
32.0 ± 0.2	≈ 1			
42.4 ± 0.1	77 ± 7	2300	L_I	M1-E2
		4500	L_{II}	
		4300	L_{III}	
		400	M	
54.6 ± 0.1	14 ± 2	600	$L_I + L_{II}$	M1-E2
		320	M	
66.0 ± 0.2	1.1 ± 0.2	10	M	
68.0 ± 0.2	0.5 ± 0.1			
71.7 ± 0.2	3.6 ± 0.6	80	L_{III}	E2
		70	M	
74.4 ± 0.2	1.9 ± 0.4			
90.0 ± 0.2	9.6 ± 1.0			Th K_{α_2}
93.3 ± 0.2	14 ± 1.4			Th K_{α_1}
97.1 ± 0.2	29 ± 3	250	L_{II}	E2
		180	L_{III}	
		120	M	

Table II. (cont.)

E_γ(keV)	I_γ(%) × 10^3	I_e(%) × 10^3	Conversion Shell	Multipolarity and remarks
105.1 + 0.3	5.8 ± 0.6			Th $K_{\beta_1'}$
108.7 ± 0.3	1.5 ± 0.3			Th $K_{\beta_2'}$
117.1 ± 0.2	3.8 ± 0.6			
118.9 ± 0.2	4.7 ± 0.8			
120.7 ± 0.2	3.2 ± 0.5	12	L_{II}	E2
		10	L_{III}	
		7	M	
124.0 ± 0.2	0.8 ± 0.15			
135.3 ± 0.2	2.9 ± 0.3			
144.8 ± 0.4	2 ± 0.5			
146.4 ± 0.3	8 ± 1.5			
164.5 ± 0.2	7.8 ± 0.8			
175.3 ± 0.5 ?	≈ 0.2			
187.9 ± 0.2	2.3 ± 0.3			
208.1 ± 0.2	2.7 ± 0.3			
212.5 ± 0.5 ?	≈ 0.1			
217.0 ± 0.2	4.5 ± 0.5			
230.3 ± 0.5 ?	≈ 0.1			
245.4 ± 0.2	4.2 ± 0.5	10	K	M1
		3	L	
248.4 ± 0.2	1.7 ± 0.3	4	K	M1
260.0 ± 0.5	0.4 ± 0.1			
261.5 ± 0.5	0.4 ± 0.1			
268.1 ± 0.4	0.3 ± 0.08			
274.5 ± 0.3	0.6 ± 0.1			

Table II. (cont.)

E_γ(keV)	I_γ(%) × 10^3	I_e(%) × 10^3	Conversion Shell	Multipolarity and remarks
277.9 ± 0.3	1.7 ± 0.3	2	K	M1
288.0 ± 0.3	1.4 ± 0.3			
291.2 ± 0.2	6.7 ± 0.7	8	K	M1
		2	L	
294.0 ± 0.7	≈ 0.2			
302.6 ± 0.7	≈ 0.1			
316.8 ± 0.2	9 ± 1	12	K	M1
		3	L	
320.2 ± 0.2	3.2 ± 0.5	4	K	M1
323.1 ± 0.3	0.9 ± 0.15			
328.2 ± 0.4	0.04± 0.01			
336.4 ± 0.3	0.7 ± 0.1			
353.9 ± 0.3	0.07± 0.01			
365.5 ± 0.3	0.9 ± 0.1	1.5	K	?
		< 1	L	
383.0 ± 0.3	0.12± 0.03			
393.3 ± 0.3	≈ 0.02			

[a] γ-ray energies and intensities are obtained from our measurements.

[b] Electron intensities are taken from Ref. 28.

[c] For conversion coefficient determination, the electron intensities were reduced to 60% of the given values.

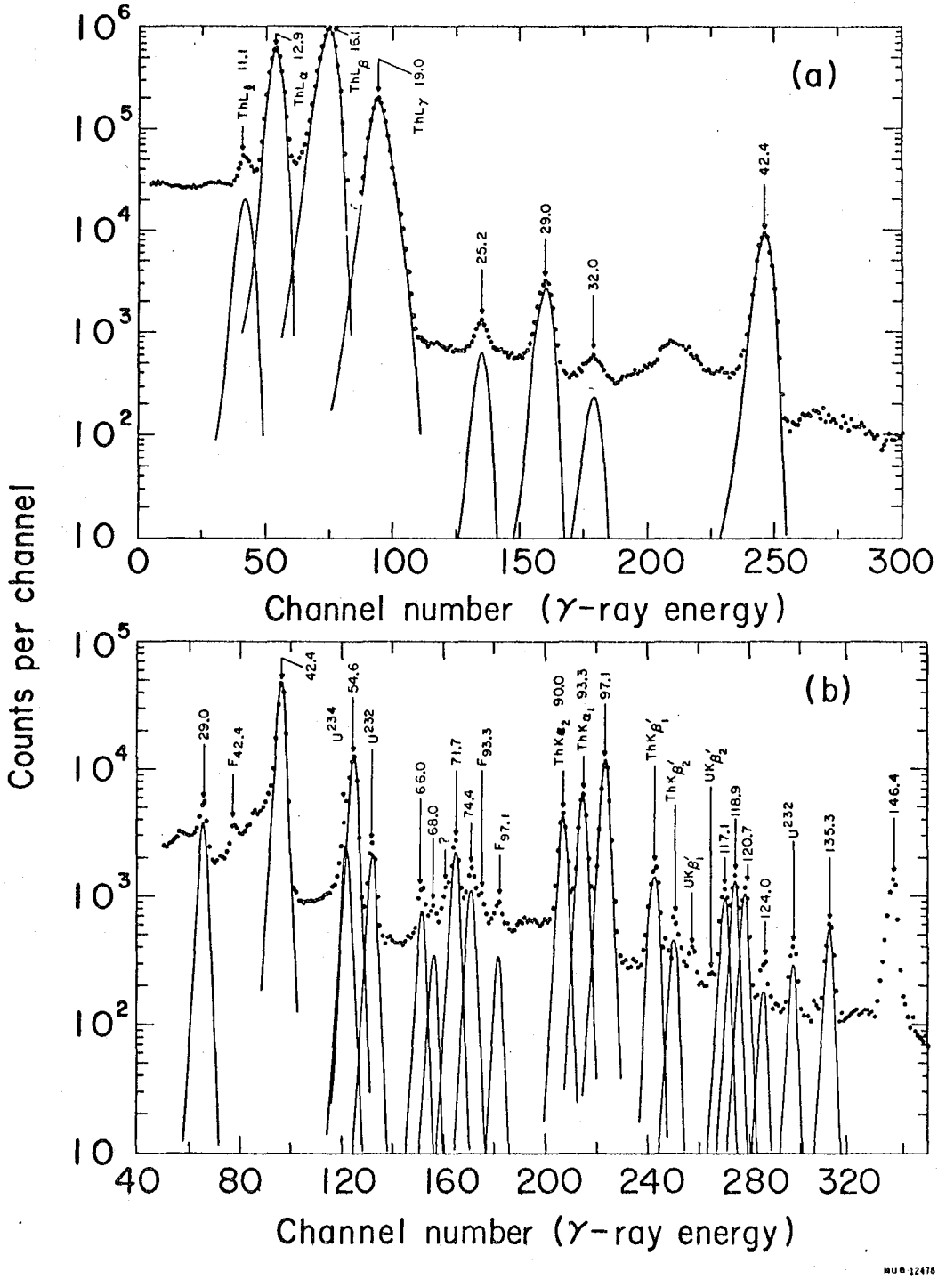

Fig. 6a,b. U^{233} γ-ray spectra.
(a) L x-ray and low-energy γ-ray spectrum, measured with a 0.5 × 0.3 cm Si(Li) detector.
(b) γ-ray spectrum taken with the 3 × 1 × 0.3 cm Ge(Li) detector.

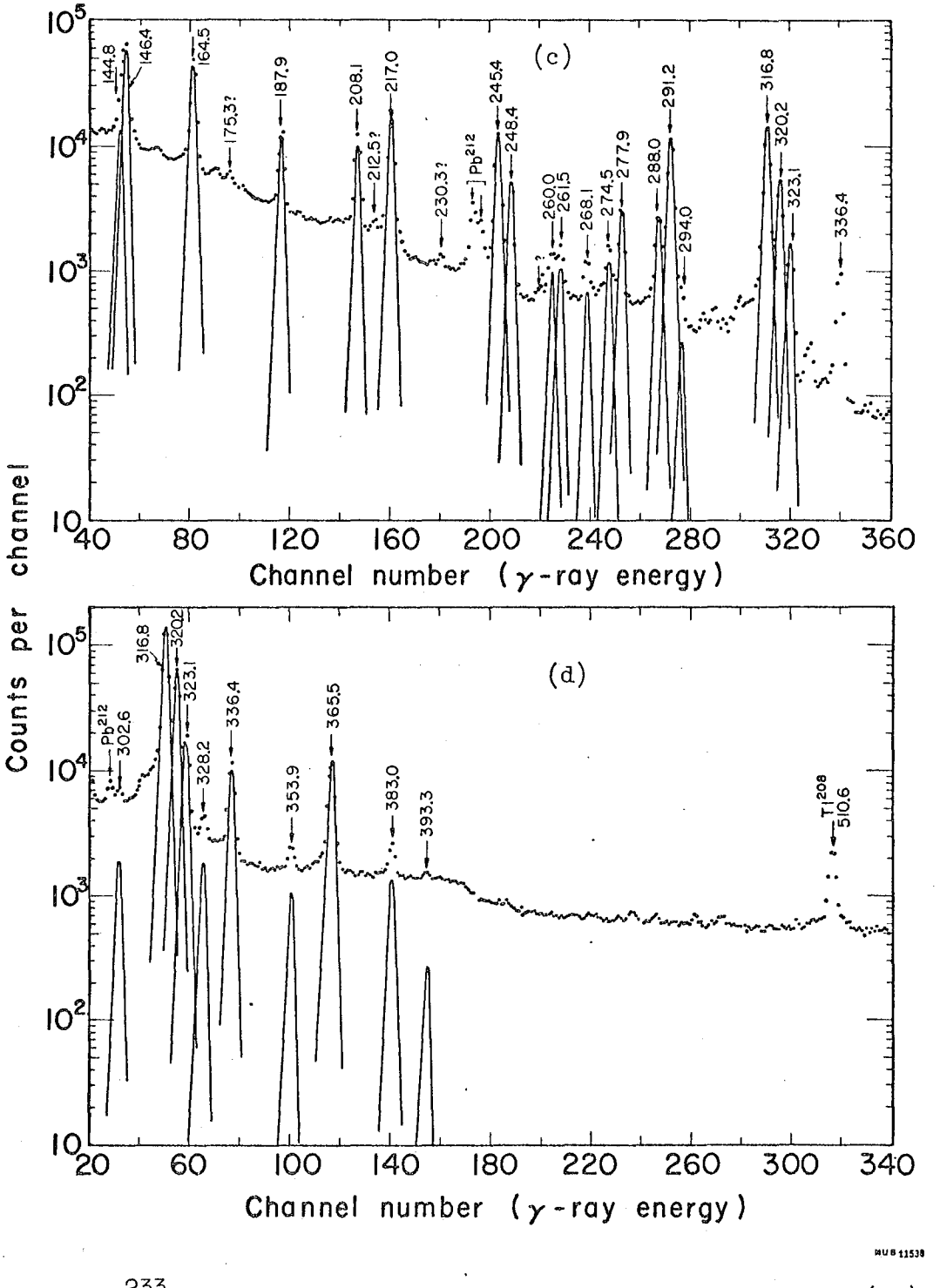

Fig. 6c,d. U^{233} γ-ray spectra measured with the 3 × 1 × 0.3 cm Ge(Li) detector.

of the 90.0-, 93.3-, and 97.1-keV radiations and the Pb and Bi K x-ray energies fall in this region. The existence of the 71.7- and 74.4-keV γ-rays was verified by using a different detector. But as this other detector did not have as good resolution as the 3 × 1 × 0.3 cm detector, the existence of other weaker transitions could not be confirmed. The intensities (in photons per 100 α-particles) of the 42.4-, 54.6-, and 97.1-keV γ-rays were determined from γ-singles and γ-α coincidence measurements. The intensities of the γ-rays below the 54.6-keV line are normalized to that of the 42.4-keV γ-ray and those of higher energy γ-rays are normalized to the value of the 97.1-keV γ-ray.

2. Conversion Electrons

No measurement on the conversion electrons of U^{233} decay was made in the present studies but these were investigated by Tret'yakov et al. with a β spectrometer. The conversion coefficients, calculated from their intensities (given in Table II) were found about a factor of 2 higher than the theoretical values. The 97.1-keV transition, which is pure E2, was used to obtain the normalization factor for the electron intensities, which was found to be 60%. The multipolarities listed in the last column of the table were determined from the corrected electron intensities.

3. α-γ Coincidence Measurements

The α-γ coincidence experiments were performed by using a scintallation detector for the γ-rays and a semiconductor detector for α-particle analysis. The alpha spectra were measured in coincidence with (i) all γ-rays, and (ii) γ-rays > 100 keV. The purpose of the latter experiment was to cut down the intensities of the favored α groups in the spectrum (Fig. 7). This decreased the background, and thus the low-intensity alpha groups populating the levels of the unfavored bands could be identified. In the spectrum 3 complex peaks should be observed. Because of the γ gates setting, one can say almost definitely that the intensity of the α_{166} group

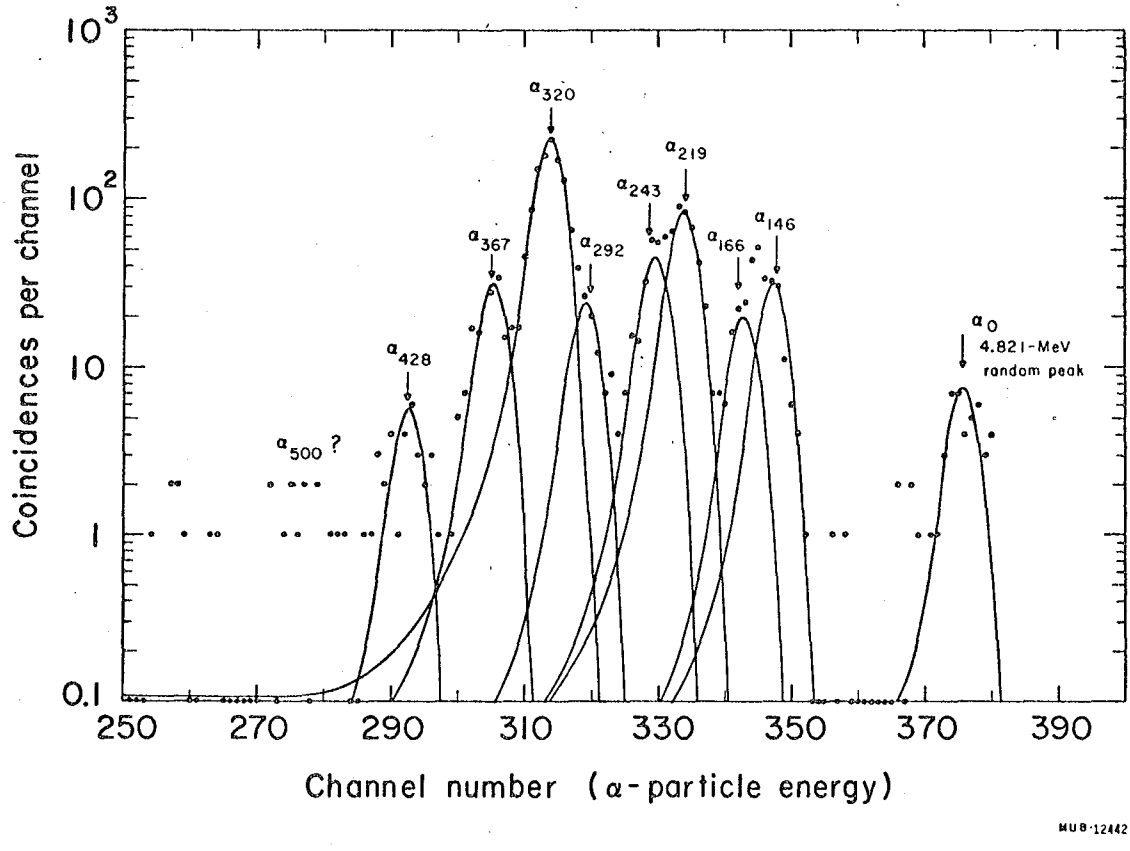

Fig. 7. U^{233} α-particle spectrum measured in coincidence with γ-rays > 100 keV. Zero events are plotted at 0.1.

is mainly due to the alpha population to the 164.5-keV state. The resolution of the complex peaks was aided by the previous information. The results of the present α-γ coincidence measurements are given in Table III.

4. Decay Scheme

The decay scheme, postulated on the basis of the previsou measurements as well as the present work is shown in Fig. 8. The spins and parities of the levels in Th^{229} are determined from the mode of their de-excitations. The Nilsson quantum number assignments are based on the alpha intensity pattern to these levels and should be considered only tentative. In the following paragraphs the reasons for these assignments are discussed.

The ground state spin of U^{233} has been measured[29] and found to be 5/2. The most reasonable state for the 141st neutron in the Nilsson diagram (Fig. 9) is 5/2 + (633↓). The favored alpha group of U^{233} populates the ground state of Th^{229}, and hence the Th^{229} ground state must be 5/2 + (633↓). This is consistent with the measured spin[30] of Th^{229} ground state. The energies of the levels at 42.4, 97.1, 163.1, and 242 keV fit well with the values, calculated from the equation,[4]

$$(\Delta E)_I = \frac{\hbar^2}{2\Im}\left[I(I+1) - K(K+1) + a\{(-)^{I+1/2}(I+1/2) - (-)^{K+1/2}(K+1/2)\}\delta_{K,\,1/2}\right] \qquad (3)$$

and with a rotational constant $(\hbar^2/2\Im)$ of 6.06 keV. In Eq. (3), $\Im$ is the effective moment of inertia of the nucleus, I, is the nuclear angular momentum for a given state, K is the projection of I on the nuclear symmetry axis, and $(\Delta E)_I$ is the energy difference between the state with spin I and the base member of the band (spin = K). The second term in the equation has a non-vanishing value only for K = 1/2 bands.

Table III. U^{233} alpha groups measured in the present work.

α-particle energy (MeV)	Excited state (keV)	Intensity (%)	Hindrance factor
4.677 ± 0.004	146	$(6 \pm 3) \times 10^{-3}$	1.6×10^{3}
4.658 ± 0.004	166	$(4 + 2) \times 10^{-3}$	1.8×10^{3}
4.606 ± 0.004	219	$(1.4 \pm 0.3) \times 10^{-2}$	200
4.582 ± 0.004	243	$(6 \pm 2) \times 10^{-3}$	300
4.534 ± 0.004	292	$(5 \pm 2) \times 10^{-3}$	150
4.507 ± 0.004	320	$(3.5 \pm 1) \times 10^{-2}$	17
4.460 ± 0.004	367	$(5 \pm 2) \times 10^{-3}$	50
4.400 ± 0.005	428	$\approx 8 \times 10^{-4}$	90
≈ 4.330	≈ 500	$\approx 1 \times 10^{-4}$	150

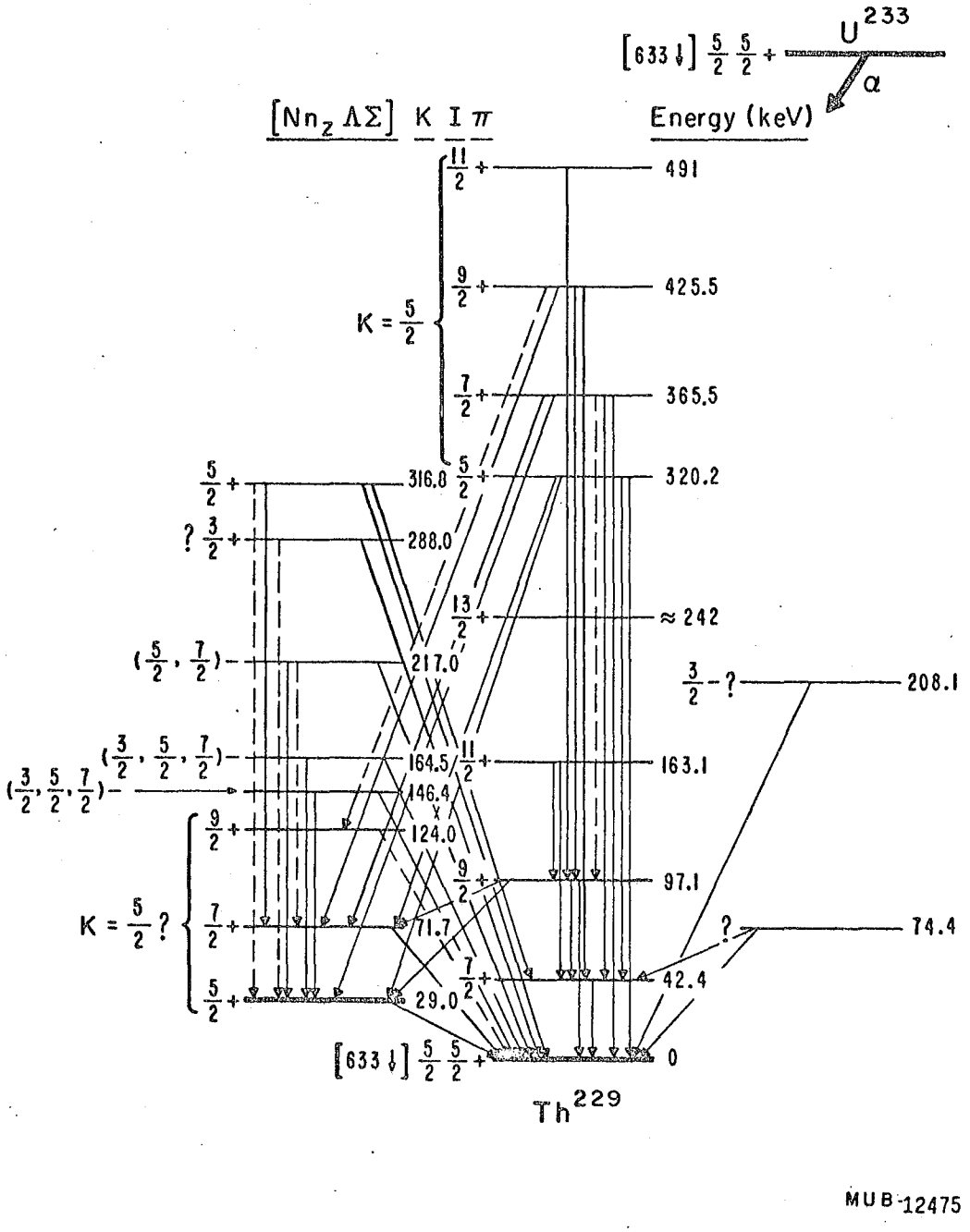

Fig. 8. Decay scheme of U^{233}.

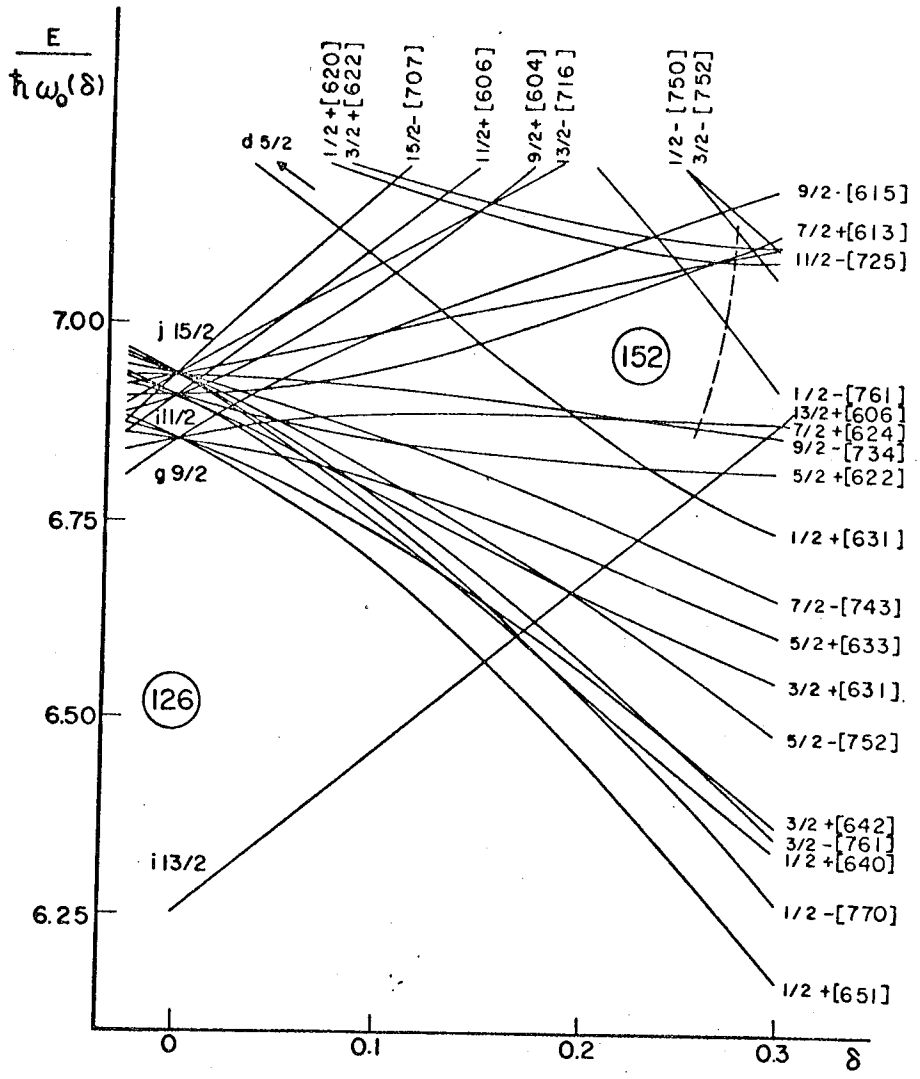

MU-15744

Fig. 9. Nilsson diagram for neutrons in the region $126 \leq N \leq 160$. The abscissa represents the nuclear deformation and the ordinate shows the excitation energy of the various levels. The dashed line indicates very roughly the deformations of the nuclei in this region. The quantum numbers shown in the figure are explained in Chapter V.

The alpha transition probabilities to these levels are also in good agreement with the theoretical values obtained from the equation,[24,58]

$$P = P_0(Z,E) \sum_L C_L |\langle I_i\ L\ K_i(K_f-K_i)|I_i\ L\ I_f\ K_f\rangle + b_L(-)^{I_f+K_f}\langle I_i\ L\ K_i(-K_f-K_i)|$$

$$I_i\ L\ I_f\ -K_f\rangle|^2 \qquad (4)$$

as shown by Ruiz. In Eq. (4), $P_0(Z,E)$ is the transition probability calculated from simple spin-independent alpha-decay theory,[23] the subscript i and f refer to the parent and the daughter respectively, and the terms in the brackets are the vector-addition coefficients. The parameter C_L is determined empirically from the known alpha intensities and is inversely proportional to the hindrance factor of the alpha wave of angular momentum L. The second term is used only when $L \geq K_i + K_f$.

The total intensity of the alpha groups (unresolved) populating the 316.8- and 320.2-keV levels is found to be 3.5×10^{-2}%. From the γ-ray intensities it appears that the two states receive almost equal alpha population. This gives a hindrance factor of ≈ 35 for each of the alpha groups. The low hindrance factors indicate that two states should have some admixture of the favored band. This means that one of the states is probably member of a vibrational band built on the ground state and the other has K=3/2 or 7/2 with strong Coriolis interaction with the 5/2+(633↓) state. The comparison of the experimental and theoretical values of the conversion coefficients of the transitions from these states give the multipolarity M1. Thus both of the levels must have positive parity. The γ-ray intensity pattern indicates that the spin of the 316.8-keV level should be 5/2. In order to have a non-vanishing Coriolis matrix element the value of the K quantum number should be 3/2. The most reasonable Kπ=3/2+ Nilsson state in this energy region is 3/2+(631↑).

The de-excitation of the 320.2- and 365.5-keV levels (see the decay scheme) indicates that the two states should have spins 5/2 and 7/2 respectively. The spin and parity assignments of the 320.2-keV level rule

out any possibility of its being octupole vibrational band ($K I\pi = 01-$) or gamma vibrational band ($K I\pi = 22+$). Thus it is most likely the β vibrational band ($K I\pi = 00+$) built on the ground state. The 365.5-, 425.5-, and 491-keV levels fit well as the rotational members of this band. The alpha intensities to the member of the $K = 5/2$ band are calculated with Eq. (4), and are compared with the observed values in Table IV. The similarity between the alpha intensity patterns for this band and the ground state band is in favor of the above assignment. As the electron intensities of the transitions de-exciting these levels are not accurately known, it is difficult to determine the E0 and E2 contributions in these transitions.

As seen in Table V, the reduced transition probabilities of the γ-rays from the high-lying states do not agree with the theoretical values for M1 transitions, calculated on the basis of the above assignments. This, we think, is due to the Coriolis interaction of these bands with the other even-parity states in this energy region. For the lack of sufficient information, detailed calculations are not possible.

The levels at 29.0 and 71.7 keV have been observed in the U^{233} alpha spectrum.[27] The fact that the transitions connecting the high-lying states to the 29.0- and 71.7-keV levels are M1, fixes the parity of the two levels as even. Also the multipolarities of the 29.0- and 71.7-keV γ-rays, determined from the comparison of the experimental and theoretical values of conversion coefficients, are most probably M1. The intensity pattern of the γ-rays from the 320.2- and 365.5-keV levels indicates that the two states are the $I = 5/2$ and $I = 7/2$ members of a $K = 5/2$ band. The level at 124 keV is most likely the $I = 9/2$ member of this band. The energy spacings between these levels are consistent with the K quantum number assignment. In the Nilsson diagram there is no $K\pi = 5/2+$ state available in this energy region. One could think of constructing an octupole vibrational band on the 5/2-(752↑) state, but in that case one would expect to observe an intense alpha group to the octupole vibrational band built on the ground state. The absence of such an alpha group invalidates the above assumption.

Table IV. Relative alpha intensities to the members of K = 5/2 band.

Level (keV)	Spin	Observed intensity (%) × 10^3	Theoretical value[a] of relative intensity (%) × 10^3			
			L=0	L=2	L=4	Σ
320.2	5/2	17[b]	8.2	8.4	0.1	16.7
365.5	7/2	5	-	4.8	0.3	5.1(norm)
425.5	9/2	1	-	0.7	0.3	1.0(norm)
491	11/2	0.1	-	-	0.06	0.06

[a] Hindrance factors for L=0, L=2, and L=4 alpha waves are 71, 25, and 126 respectively.

[b] This intensity was obtained by dividing the total intensity of α_{320}, measured in this work into $\alpha_{316.8}$ and $\alpha_{320.2}$ on the basis of γ-ray intensities de-exciting 316.8- and 320.2-keV levels.

Table V. Reduced transition probabilities of γ-rays (assuming them to be M1 transitions).

Level (keV)	Transition $K_i I_i \rightarrow K_f I_f$	γ-rays	$(B_1/B_2)_{exp.}$	$(B_1/B_2)_{theo.}$
320.2	5/2 5/2→ 5/2 5/2	320.2	1.3	2.5
	5/2 7/2	277.9		
	→ 5/2 5/2	291.2		
	5/2 7/2	248.4	2.5	2.5
365.5	5/2 7/2→ 5/2 5/2	365.5	0.68	0.54
	→ 5/2 7/2	323.1		
	5/2 7/2→ 5/2 5/2	336.3		
	→ 5/2 7/2	294.0	≈ 2	0.54

The levels at 146.4, 164.5, 208.1, and 217.0 keV have been identified in the α-γ coincidence spectra. In the spectrum $\alpha_{208.1}$ and $\alpha_{217.0}$ could not be resolved. The level at 208.1 keV has been postulated because the 208.1-keV transition does not seem to originate from any other level and also the intensity of the α_{219} is about twice the intensity of the γ-rays depopulating the 217.0-keV level. As the K- and L-conversion electrons of the 135.3-, 146.4-, 164.5-, 187.8-, 208.1-, and 217.0-keV transitions are not observed, one would expect them to be E1. Hence the levels originating these radiation should have odd parity. The possible single-particle states in this region are 5/2-(752↑) and 7/2-(743↑). The negative-parity levels, shown in the decay scheme, seem to be the rotational members of these bands. The lack of sufficient information prevents us from making specific assignment.

The apparent occurrence of three K=5/2 bands within 330 keV poses a serious question for the Nilsson model and may be a result of the fact that Th^{229} is close to the transition region for stable deformed shapes. Also, some further work is necessary to make definite spin and parity assignments of the Th^{229} low-lying states.

B. Alpha Decay of Pu^{239}

The radiations associated with the alpha decay of Pu^{239} have been the subject of various investigations.[20,26] In recent yeats attempst have been made to resolve the complex structure of the alpha groups and the internal transitions of the daughter. Murri and Clines[31] examined the gamma rays with NaI(Tl) detector and observed a complex structure between the 300- and 500-keV region. Baranov et al.[32] measured the alpha spectra with a magnetic spectrograph and identified 20 alpha groups. It is apparent from these studies that the energy-level diagram of U^{235} is fairly complex. The availability of high-resolution Ge(Li) detectors and an efficient α-γ coincidence system induced us to study the Pu^{239} decay scheme in further detail.

1. Gamma Rays

In the present work, Pu^{239} γ-rays upto 500 keV have been thoroughly investigated. The spectra were taken with a Si(Li) detector [Fig. 10(a)], a 3 × 1 × 0.3 cm Ge(Li) detector [Fig. 10(b),(c),(d)] and a 3 × 2 × 0.8 detector [Fig. 10(e)]. The source for the first three measurements was about 10 mg of Pu^{239} evaporated on a thin Mylar film. The absence of the Am^{241} 208-keV γ-ray in the spectrum indicates the purity of the sample. For spectra (d) and (e), 2 grams of Pu^{239} metal foils, placed in an iron pipe, were used. The absolute intensities of the 38.7-, 51.6-, and 129.3-keV γ-rays were determined from γ-singles and γ-α coincidence measurements. The intensities of other γ-rays are normalized to that of 129.3-keV γ-ray. The results of all these measurements are given in Table VI.

2. Conversion Electrons

The conversion electrons accompanying the alpha decay of Pu^{239} were investigated by electron-alpha coincidence experiments, using semiconductor detectors. The intensities of the K-conversion electrons of the 413.7-, 393.4-, 375.2-, and 345.1-keV transitions were determined, and these are listed in Table VII. Electron resolution and the source thickness limited the investigation of the weaker transitions. During the course of this work, a careful investigation of the conversion electrons was carried out by Tret'yakov and Kondrat'ev,[33] using a double iron-free β spectrometer. The intensities of the electron lines measured by these authors are included in Table VI. Their electron intensities are somewhat lower than our values, as can be seen in Table VI and VII. Also the conversion coefficients of the transitions, determined from these intensities, are found to be consistently lower than the theoretical values. In order to get correct conversion coefficients we increased their electron intensities by 50%. The multipolarities listed in the last column of the table were obtained on the basis of the corrected intensities.

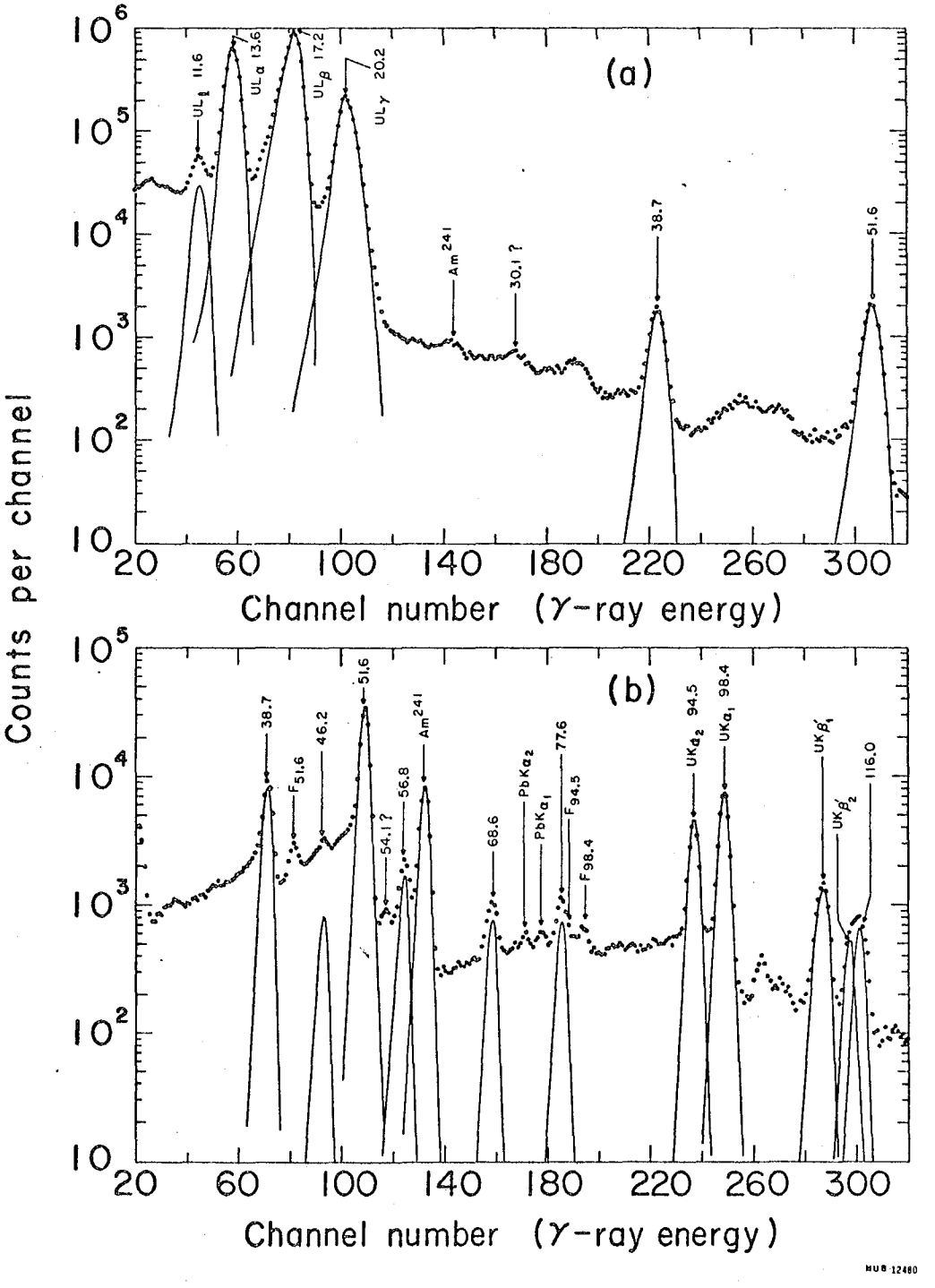

Fig. 10a,b. Pu^{239} γ-ray spectra.
(a) L x-ray and low-energy γ-ray spectrum, measured with a 0.5 × 0.3 cm Si(Li) detector.
(b) γ-ray spectrum taken with the 3 × 1 × 0.3 cm Ge(Li) detector.

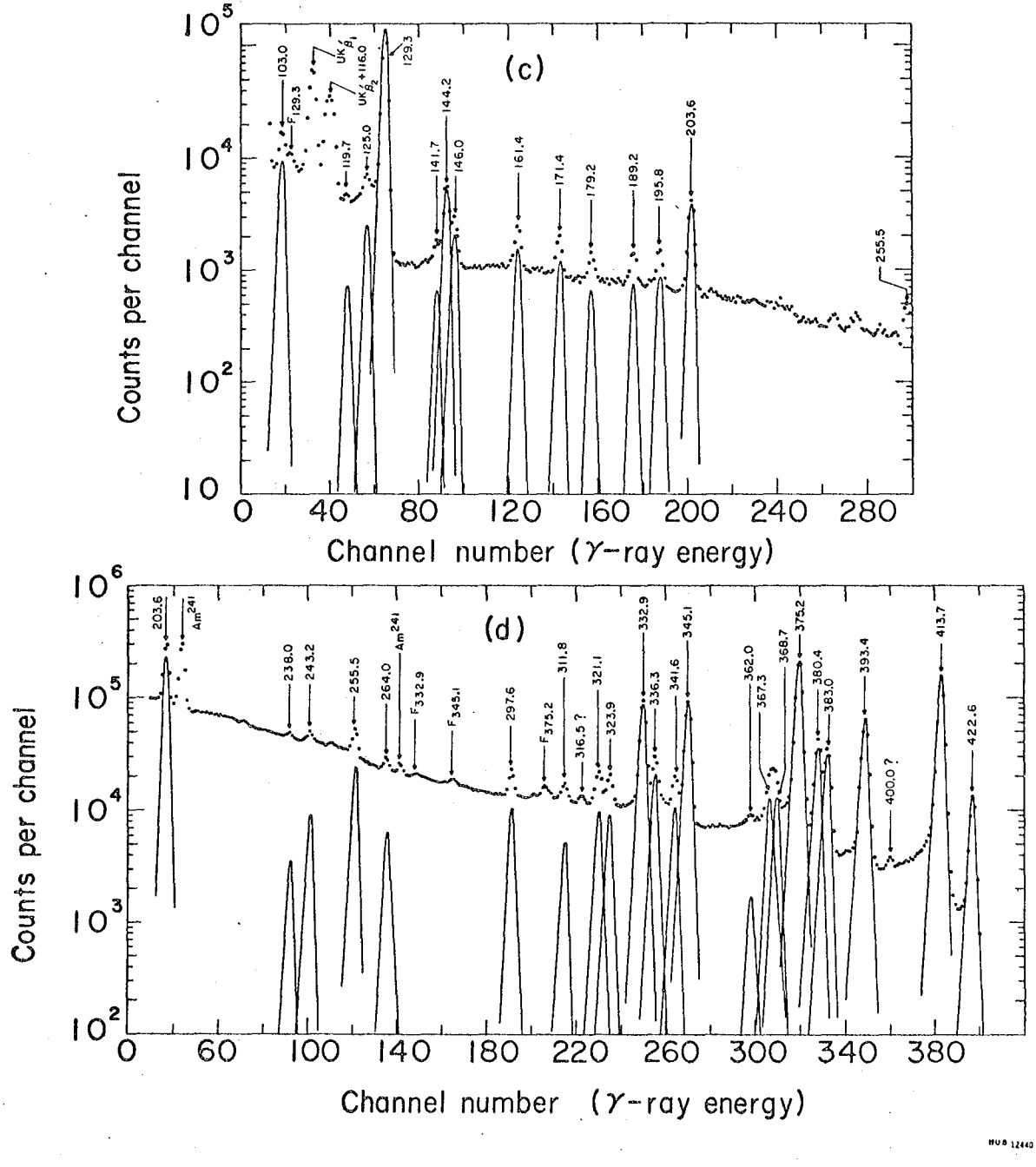

Fig. 10c,d. Pu^{239} γ-ray spectra taken with the 3 × 1 × 0.3 cm Ge(Li) detector.

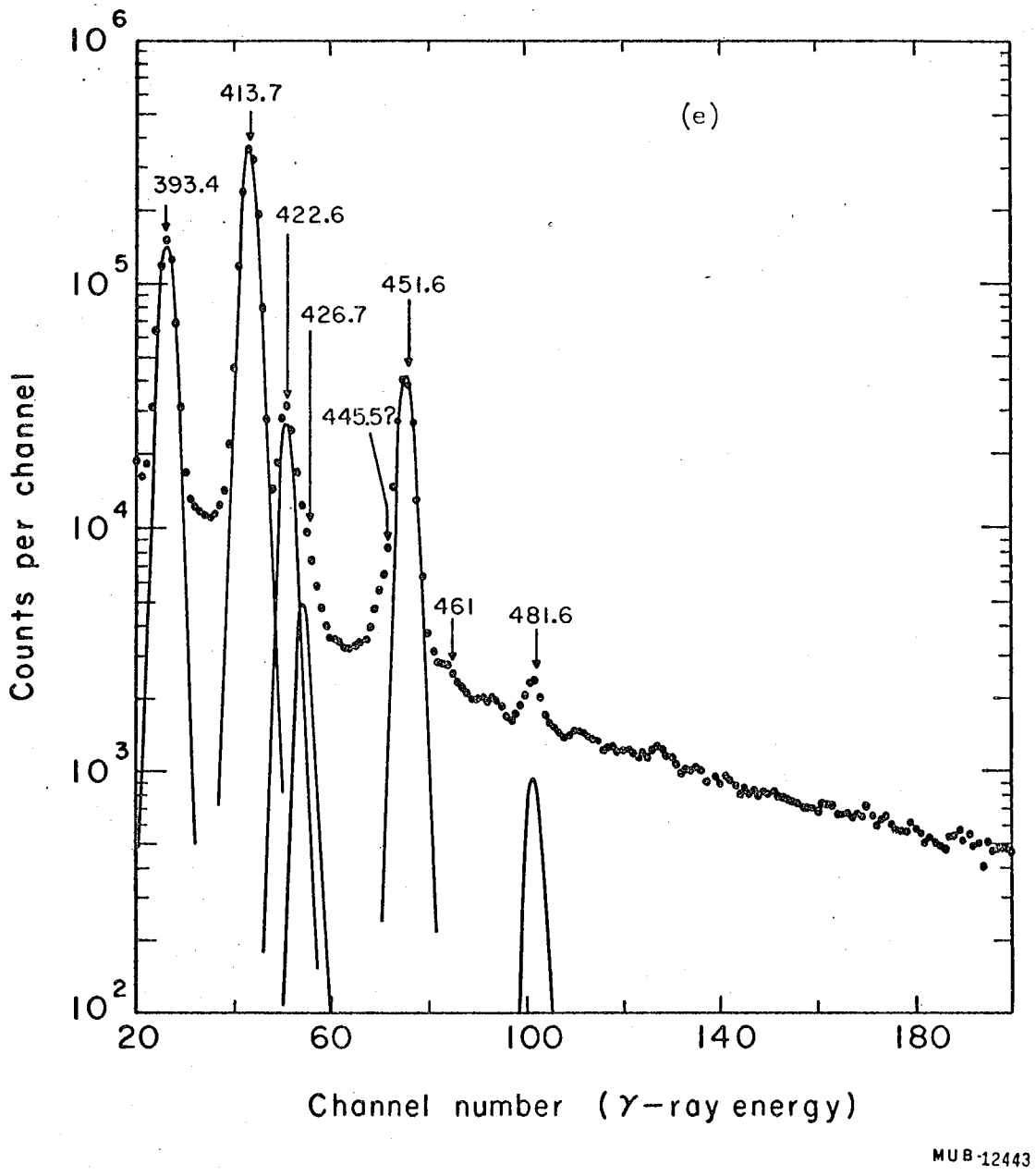

Fig. 10e. Pu^{239} γ-ray spectrum measured with a 3 × 2 × 0.8 cm Ge(Li) detector.

Table VI. Internal transitions of U^{235}.

E_γ^a(keV)	I_γ^a(%) × 10^4	I_e^b(%) × 10^4	Conversion shell	Multipolarity[c] and remarks
11.6 ± 0.1	(13 ± 4) × 10^2			U L_ℓ
13.6 ± 0.1	(24 ± 4) × 10^3			U L_α
17.2 ± 0.1	(33 ± 5) × 10^3			U L_β
20.2 ± 0.1	(9 ± 1.5) × 10^3			U L_γ
30.1 ± 0.2 ?	≈ 5			
38.7 ± 0.1	83 ± 10	8 × 10^3	L_I	M1 + E2
		9 × 10^3	L_{II}	
		10 × 10^3	L_{III}	
46.2 ± 0.1	8 ± 1	not observed		
51.6 ± 0.1	230 ± 20	2.9 × 10^4	L_{II}	E2
		2.7 × 10^4	L_{III}	
56.8 ± 0.2	9 ± 1	150	L_I	M1 + E2
		50	L_{II}	
68.6 ± 0.2	8 ± 1	21	M_{II}	
		16	M_{III}	
77.6 ± 0.2	6 ± 1	7	L_I	
94.5 ± 0.2	40 ± 5			U K_{α_2}
98.4 ± 0.2	70 ± 8			U K_{α_1}
103.0 ± 0.3	2.2 ± 0.5	4	L_{III}	E2
111.0 ± 0.3	30 ± 6			U $K_{\beta'_1}$
114.6 ± 0.3	≈ 10			U $K_{\beta'_2}$
116.0 ± 0.4	≈ 10			mixture of 115.6 and 116.3-keV γ-rays.
119.7 ± 0.3	0.3 ± 0.1	not observed		
125.0 ± 0.3	1.0 ± 0.2	3	L_I + L_{II}	Two γ-rays (124.3 + 125.0) keV.
129.3 ± 0.2	55 ± 5	2	L_I	E1
141.7 ± 0.3	0.33 ± 0.06	not observed		
144.2 ± 0.2	2.6 ± 0.3	4	L_{II}	E2
		2.3	L_{III}	

Table VI. (cont.)

E_γ(keV)	I_γ(%) × 10^4	I_e(%) × 10^4	Conversion shell	Multipolarity and remarks
146.0 ± 0.3	1.1 ± 0.2	not observed		
161.4 ± 0.2	1.3 ± 0.2	0.15	M	M1 ?
		0.1	N	
171.4 ± 0.2	1.0 ± 0.2	1.0 ?	K	
179.2 ± 0.2	0.7 ± 0.1	not observed		
189.2 ± 0.2	0.8 ± 0.1	< 1.0 ?	K	
		0.3 ?	L	
195.8 ± 0.2	1.0 ± 0.1	not observed		
203.6 ± 0.2	5.0 ± 0.6	8	K	M1
		1.3	L_I	
238.5 ± 0.4	0.1 ± 0.03	≤ 1.5 ?	K	
243.2 ± 0.4	0.3 ± 0.08	~ 0.3 ?	L	
255.5 ± 0.3	0.7 ± 0.1	masked		
264.0 ± 0.3	0.22± 0.04	0.2	K	M1
297.6 ± 0.3	0.42± 0.05	masked		
311.9 ± 0.3	0.24± 0.04	not observed		
321.0 ± 0.3	0.52± 0.07	not observed		
324.0 ± 0.3	0.46± 0.06	0.2	K	M1
332.9 ± 0.2	4.6 ± 0.5	0.1	K	E1 or E2
336.2 ± 0.3	1.0 ± 0.2	0.6	K	
		0.1	L	M1
341.5 ± 0.3	0.56± 0.07	0.3	K	M1 ?
345.1 ± 0.3	4.8 ± 0.5	1.4	K	M1
		0.4	L	
362.0 ± 0.4	0.12± 0.03	0.3 ?	K	
367.3 ± 0.4	0.8 ± 0.2	not observed		
368.7 ± 0.4	0.9 ± 0.2	not observed		
375.2 ± 0.2	14 ± 1.5	2.6	K	M1
		0.7	L_I	
380.4 ± 0.3	2.6 ± 0.4	0.9	K	M1

Table VI. (cont.)

E_γ(keV)	I_γ(%) × 10^4	I_e(%) × 10^4	Conversion shell	Multipolarity and remarks
383.0 ± 0.3	2.4 ± 0.4	1.0	K	M1
393.4 ± 0.3	5.3 ± 0.6	1.5	K	M1
399.8 ± 0.5 ?	≈ 0.1	not observed		
413.7 ± 0.2	13 ± 1.3	1.7	K	M1
		0.3	L_I	
422.6 ± 0.3	1.2 ± 0.2	0.2	K	M1
426.7 ± 0.3	≈ 0.17	not observed		
451.6 ± 0.3	1.9 ± 0.3	0.3	K	M1
461.0 ± 0.5	≈ 0.02	not observed		
481.6 ± 0.3	0.05± 0.02	not observed		

[a] The energies and intensities are obtained from our measurements.

[b] The electron intensities are those of Tret'yakov and Kondrat'ev.[33]

[c] For conversion coefficient determination, the electron intensities were increased by 50%.

Table VII. Pu^{239} conversion electrons measured by e-α coincidence experiment.

Transition energy (keV)	Electron intensity (%) $\times 10^4$
413.7	2.7 ± 0.7
393.4	1.5 ± 0.4
375.2	3.5 ± 0.8
345.1	2.5 ± 0.7

3. α-γ Coincidence Measurements

Alpha-particle spectra in coincidence with various regions of γ-rays have been measured. The alpha spectrum in coincidence with γ-rays > 50 keV is shown in Fig. 11(a). In the spectrum all alpha groups populating the high-lying states of U^{235} except $\alpha_{393.4}$ and $\alpha_{414.5}$ are well resolved. The alpha abundance listed in Table VIII are calculated with weighted γ-ray efficiencies determined on the basis of the decay scheme (Fig. 12). The α-particle energies are measured relative to the Pu^{239} α_0 group which is taken as 5.155 MeV.[21]

The levels at 393.4 and 414.5 keV were first postulated in the level scheme in order to account for all the gamma transitions. As shown in the decay scheme and Table VI, the 393.4-keV state de-excites mostly by a 393.4-keV γ-ray, whereas the 414.5-keV level decays by the 189.2-keV γ-ray and the intraband transitions. It is thus possible to identify the $\alpha_{393.4}$ group if the γ-ray gates are selected to include only the 393.4-keV photopeak. The alpha spectrum in coincidence with 375- to 415-keV γ-rays was measured for 16 days and is shown in Fig. 11(b). The existence of the 393.4-keV level in U^{235} is established and the estimated alpha intensity is included in Table VIII.

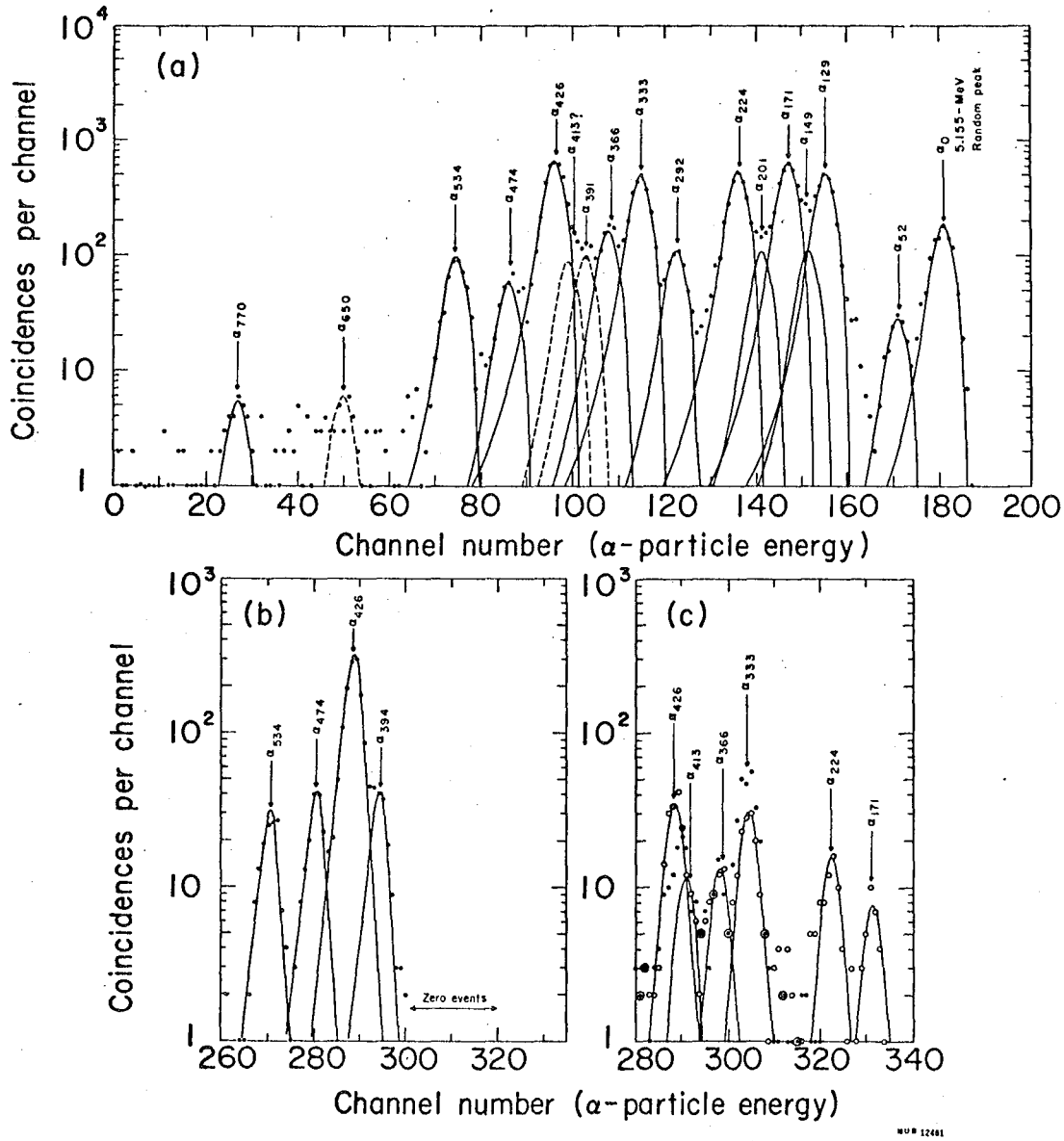

Fig. 11a,b,c. Pu^{239} α-γ coincidence spectra.
(a) α-particles in coincidence with γ-rays > 50 keV.
(b) α-particles in coincidence with 375- to 415-keV γ-rays.
(c) α-particles in coincidence with i) 200- to 230-keV γ-rays (·) and ii) 175- to 200-keV γ-rays (o).

Table VIII. Pu^{239} alpha groups measured in the present work.

α-particle energy (MeV)	Excited state (keV)	Intensity (%) × 10^3	Hindrance factor[22]
5.028 ± 0.003	129	5 ± 1	6.5×10^3
4.987 ± 0.003	171	7 ± 2	2.5×10^3
4.935 ± 0.003	224	3 ± 0.8	2.5×10^3
4.911 ± 0.005	248	≈ 0.2	7×10^4
4.868 ± 0.004	292	≈ 0.8	3×10^3
4.828 ± 0.003	333	2.4 ± 0.6	5.9×10^2
4.795 ± 0.004	366	0.7 ± 0.2	1.2×10^3
4.769 ± 0.005	394	0.8 ± 0.3	7×10^2
4.749 ± 0.005	413	≈ 0.6	6×10^2
4.736 ± 0.003	426	4.5 ± 1.0	69
4.689 ± 0.003	474	0.5 ± 0.15	2.9×10^2
4.630 ± 0.003	534	0.7 ± 0.15	75

Attempts were also made to identify the $\alpha_{414.5}$ group. According to the decay scheme the 414.5-keV level decays mostly through intraband transitions. Thus the alpha group populating the 414.5-keV level should be expected to be in coincidence with a 203.6-keV γ-ray. Alpha spectra, measured in coincidence with i) 200- to 230-keV γ-rays and ii) 175- to 200-keV γ-rays, are shown in Fig. 11(c). It should be noted in the figure that a peak appears, presumably $\alpha_{414.5}$, in the first spectrum, which has higher alpha intensity than the $\alpha_{426.7}$ group. As the amplifier gain was stabilized and the positions of the $\alpha_{332.9}$ and $\alpha_{367.5}$ groups are identical in the two spectra, the possibility of a shift in the peak positions should be ruled out. But, because of poor statistics, this result should not be considered considered conclusive. It is also worth pointing out that a 415-keV level has been identified in the $U^{234}(d,p)U^{235}$ reaction,[34] and spin of 9/2 has been assigned to this state.

4. Decay Scheme

The measured spin[35] of Pu^{239} is 1/2 and from the alpha decay of Cm^{243} this state has been identified as the 1/2+(631↓) Nilsson state.[26] The favored alpha group of Pu^{239} will thus populate the levels of 1/2+(631↓) band in the daughter. The position of an I=K=1/2 state has been established at ≈ 80 keV above the ground state by Asaro and Perlman[36] and also by Huizenga et al.[37] The energy spacings between various members of the band fit well with the values calculated from Eq. (3) and give the value of the rotational constant as 6.1 keV and that of the decoupling parameter as -0.267. A better fit between the experimental and theoretical values of the rotational energies has been obtained by using more parameters in the equation (see Chapter V). The alpha intensities to these levels are in good agreement with the theoretical values.[8] The level at 294.6 keV is identified as the I=13/2 member of this band. The assignment is based on the direct observation of the $\alpha_{294.6}$ group and the de-excitation of this level.

The ground state spin of U^{235} is known to be 7/2 from direct measurement.[29] The state is assigned as 7/2-(743↑) on the basis of Coulombic excitation of U^{235} by Newton.[38] Recently members of this band up to I=19/2 have been identified[39] in the Coulombic excitation of U^{235} with heavy ions. The rotational constant of the band is found to be 5.13 keV, which is smaller than the usual value of ≈ 6 keV for other states in this region. This contraction between the levels of the band is due to the Coriolis interaction of the band with other odd-parity levels, especially with the 5/2-(752↑) and the 9/2-(734↑). The interaction of these bands is also observed[26] in the alpha decay of U^{235}. An alpha group populating a 248-keV level has been observed by Baranov et al.[32] and also in the present measurements. The energy of the level fits well for the I=15/2 member of the 7/2- band. The I=13/2 member is expected at 170 keV above the ground state, and the theoretical value[8] of alpha abundance to this state is ≈ 1×10^{-3}% (obtained by comparing Poggenburg's values of alpha intensities to the member of K=7/2 band). The alpha group to this level and the gamma transitions de-exciting it are masked by radiations from another 171.4-keV level, the I=7/2 member of the 5/2+(622↑) band. The alpha population to the 13/2 state could also be estimated from the γ-ray and the electron intensities. This is possible because the 13/2- state decays to the 9/2- level by an E2 transition, whereas the 125-keV γ-ray de-exciting the 171.4-keV state is expected to be E1. Thus the L-conversion electrons of 124.3-keV transition observed by Tret'yakov and Kondrat'ev[33] are almost entirely due to the de-excitation of the 13/2- state. The alpha intensity estimated on this basis is about the same as estimated from the alpha-decay theory.[8] The mode of de-excitation of the 170-keV state also indicates that the 4.998-MeV alpha group in Fig. 11(a) contains only a small fraction (≈ 5%) of the α_{170} group.

The rotational band built on the 129.3-keV state is based on the fact that the alpha groups to the 129.3-, 171.4-, and 225.3-keV levels are in coincidence with the 129.3-keV γ-ray. The value of the K quantum number,

calculated from the spacings of these levels, comes out to be 5/2. The K-conversion coefficient of the 203.6-keV γ-ray (the transition 332.9→ 129.3) is found to be in agreement with the theoretical value for an M1 transition. Hence the 129.3-keV state must have the same parity as the 332.9-keV level, namely even. The most reasonable Kπ=5/2+ Nilsson state in this energy region if 5/2+(622↑), which is also observed[26] in the Pu^{239} nucleus, but at somewhat higher energy relative to the 1/2+(631↓) state. The multipolarities of the transitions de-exciting these states (see Table VI) are consistent with the spin and parity assignment.

The 332.9-keV level decays predominantly to the 5/2+ and to the 7/2- states, but no transition to the 9/2- state is observed. The multipolarity of the 332.9-keV γ-ray, determined by comparison of the experimental and the theoretical values of K-conversion coefficients is found to be E1 (although the possibility of its being E2 cannot be ruled out). The only spin and parity assignment of the 332.9-keV state consistent with the above observations is 5/2+. The states at 367.3 and 414.7 keV appear to be the rotational members of this band. The observed gamma transitions de-exciting these states follow the spin and parity assignments. The only Kπ=5/2+ single-particle state, available in the Nilsson diagram is 5/2+ (633↓), the ground state of U^{233}. The theoretical values[8] of the alpha abundances to these levels are also in fair agreement with the observed values.

From the de-excitation of the 393.4-keV level to the members of the 1/2+(631↓) and the 5/2+(622↑) bands, one concludes that the spin of the state is 3/2. The energies of the 426.8-, 474.2-, and 533.3-keV states fit well for the rotational members of the K=3/2 band. The γ-rays from these states are consistent with the above spin assignments. The K-conversion coefficients of these radiations give the multipolarities of these transitions as M1 (with very little E2 admixture). Hence the parity of the 393.4-keV state and its associated rotational members must be even.

The single-particle orbitals with $K\pi=3/2+$, available in the Nilsson diagram are $3/2+(631\uparrow)$ and $3/2+(642\downarrow)$. From the excitation-energy point of view the former is a better choice. Also, if these levels were the members of the $3/2+(642\downarrow)$ band, one would expect a strong Coriolis interaction with the $5/2+(633\downarrow)$ band. This would have resulted in stronger distortions of the level spacings in the two bands than those experimentally observed.

In our experiments, the 426.8- and 533.3-keV levels are observed to receive higher alpha population than the 393.4- and 474.2-keV states. The theoretical calculations made on the assumption that these states are the members of the $3/2+(631\uparrow)$ band show that the $I=3/2$ and the $I=7/2$ levels should be the more-populated states. The observed pattern of the alpha intensities would be expected if one assumes Coriolis mixing of this band with the favored band and the β-vibrational band built on it. But because of the smallness of the Coriolis matrix element between the $1/2+(631\downarrow)$ and the $3/2+(631\uparrow)$ states the interaction will not be significant enough to explain the deviation from theory. The assignment of the 393.4-keV level as $3/2+(631\uparrow)$ seems very reasonable despite the above disagreement.

The slightly low value of the rotational constant for the $5/2+(633\downarrow)$ band and somewhat higher value for the $3/2+(631\uparrow)$ band (the usual value of $\hbar^2/2\Im \approx 6$ keV) are explained in terms of the Coriolis interaction of these bands with the other positive-parity bands in this region. Calculations can be made by taking all such bands into account, as has been done for the Am^{245} energy levels. But for the sake of simplicity only the strongly interacting band for each case has been used in the calculations. As the two interacting states lie across the Fermi surface, the Coriolis matrix element was reduced[40] to 43% of the theoretical[41] value. The excitation energies of the states were taken from the decay scheme, except for the energy of the $7/2+(624\downarrow)$ state, which was assumed to be 523 keV. This assumption is based on the fact that this state has been observed in the Pu^{239} nucleus at a similar energy.[1] The results of these calculations are given in Table IX. The good agreement between the observed and calculated values further support the single-particle state assignments.

Table IX. Effect of the Coriolis interaction on the level spacings.

A. Interaction between 5/2+(633↓) and 7/2+(624↓) states.[a]

Spin I	energy of the state (keV)	
	Experimental	Calculated[b]
5/2	332.9	332.9
7/2	367.3	367.4
9/2	414.5	414.0

[a] The 7/2+(624↓) level was assumed to be 190 keV above the 5/2+(633↓) state.
[b] $A_{5/2,\ 7/2}$ (used) = 0.43 $A_{5/2,\ 7/2}$ (calculated) = 12.9 keV.

B. Interaction between 3/2+(631↑) and 5/2+(622↑) states.

Spin I	energy of the state (keV)	
	Experimental	Calculated[a]
3/2	393.4	393.4
5/2	426.8	426.5
7/2	474.2	473.7
9/2	533.4	533.2

[a] $A_{3/2,\ 5/2}$ (used) = 0.43 $A_{3/2,\ 5/2}$ (calculated) = 14 keV

The decay scheme constructed on the basis of the present measurements is shown in Fig. 12. The reduced transition probabilities of the prominent γ-rays are compared with the theoretical values,[42] calculated on the basis of the decay scheme, in Table X. The agreement between the two values is very good except for the transitions de-exciting the levels of the K=3/2 band. This disagreement may be due to small E2 admixtures in these transitions. In Table XI. the experimental values of b_L for L=2 and L=4 alpha waves are compared with the theoretical values. The experimental values of b_L were calculated with Eq. (4) using the observed alpha intensities. The theoretical values of b_L were obtained from Ref. 8. In Ref. 8, the quantity b_L is the ratio of the matrix elements $H(L, K_i + K_f)$ and $H(L, K_i - K_f)$ divided by the ratio of the respective vector-addition coefficients. It will be observed that the agreement between the two values is not good.

C. Alpha Decay of Bk^{243} and Bk^{245} and Electron-Capture Decay of Bk^{244} and Bk^{246}

The light isotopes of berkelium were first prepared[26] by the bombardment of americium and curium with deutrons and alpha particles. The excitation functions for the reactions, $Am^{243}(\alpha, xn)$ and $Cm^{244}(\alpha, xn)$, were obtained by Chetham-Strode.[17] The radiations of the resulting nuclides were also investigated and several alpha groups of Bk^{243} and Bk^{245} were identified. The levels in Am^{239} and Am^{241}, populated by the alpha groups, have been classified[1,2] in terms of Nilsson single-particle orbitals. As the rotational members of the bands were not observed, there was not sufficient experimental support for the assignments. It was the purpose of this work to analyze the radiations in the alpha decay of Bk^{243} and Bk^{245} with high-resolution detectors and to study their decay schemes.

The berkelium isotopes for the present experiments were prepared by the bombardment of an Am^{243} target with 40- and 33-MeV alpha particles from the 88-inch cyclotron. The product after chemical purification was a

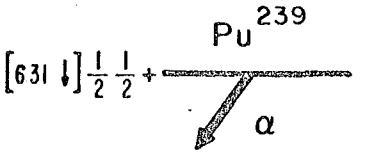

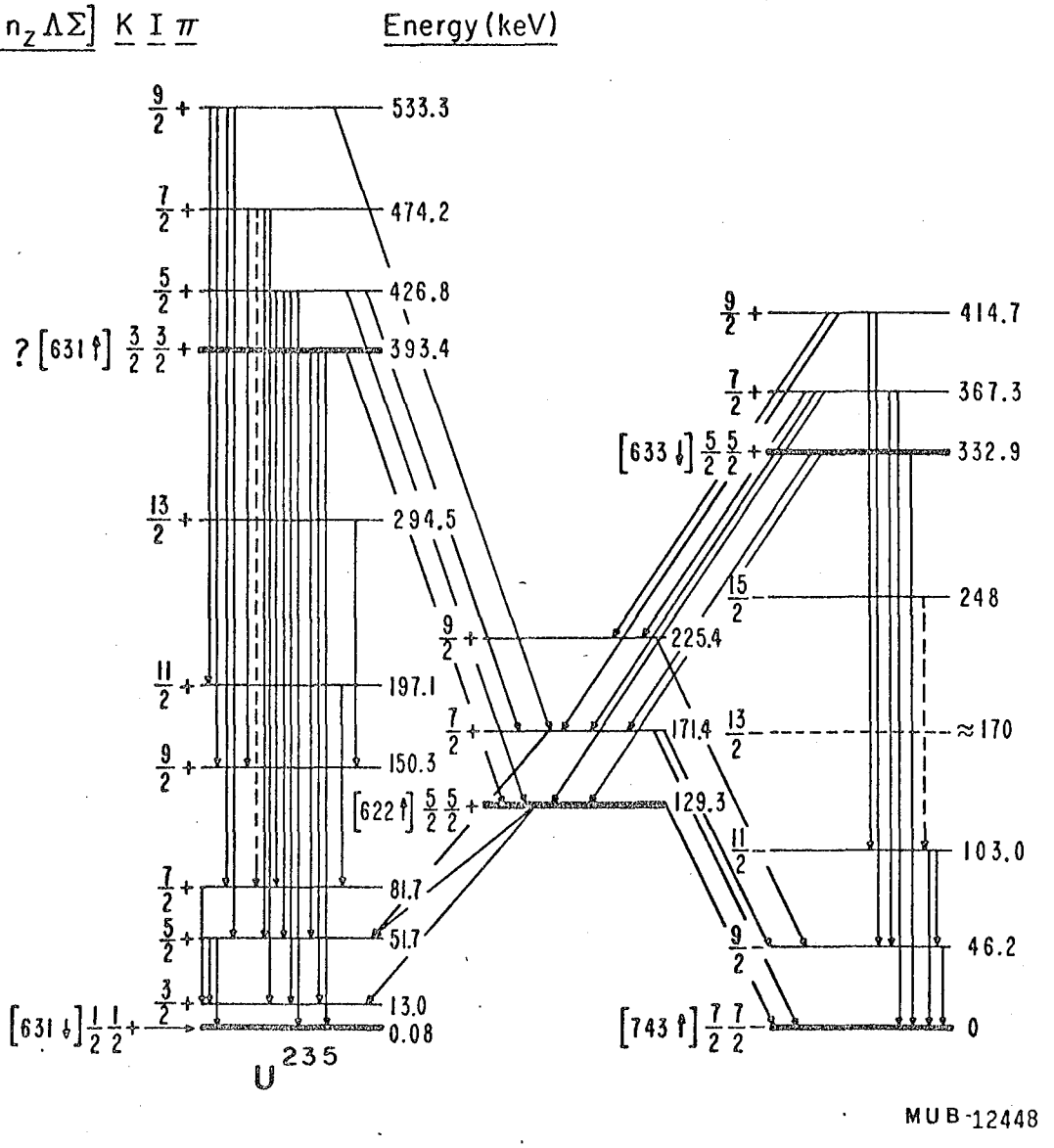

Fig. 12. Decay scheme of Pu^{239}.

Table X. Reduced transition probabilities of γ-rays (assuming them to be M1 transitions).

Level (keV)	Transition $K_i I_i \rightarrow K_f I_f$	E_γ (keV)	Relative value of reduced transition probabilities	
			Experimental	Theoretical[42]
332.9	5/2 5/2 → 5/2 5/2	203.6	2.4	2.5
	5/2 7/2	161.4	1.0	1.0
393.4	3/2 3/2 → 1/2 3/2	380.4	3.4	4
	1/2 5/2	341.5	1.0	1.0
4.26.8	3/2 5/2 → 1/2 3/2	413.7	2.0	2.7
	1/2 5/2	375.2	2.8	3.2
	1/2 7/2	345.1	1.0	1.0
	→ 5/2 5/2	297.6	0.38	0.4
	5/2 7/2	255.5	1.0	1.0
474.2	3/2 7/2 → 1/2 5/2	422.6	1.2	2.1
	1/2 9/2	324.0	1.0	1.0
533.3	3/2 9/2 → 1/2 7/2	451.6	1.2	1.8
	1/2 9/2	383.0	1.7	2.7
	1/2 11/2	336.2	1.0	1.0

Table XI. Determination of the coefficient b_L in Eq. (4)

Excited state of the band (keV)	Kπ	Value of L	Value of b_L	
			Exp.	Theo.
393.4	3/2+	2	+0.20	+8.4
			+0.90	
		4	+0.15	
			+1.8	+100
129.3	5/2+	4	+0.36	
			-1.8	-3.0
332.9	5/2+	4	+0.2	-0.03
			-2.4	

mixture of Bk^{243}(4.5 hr), Bk^{244}(4.4 hr), Bk^{245}(4.95 days), and Bk^{246}(1.8 days). The alpha particles and the gamma rays were investigated immediately after the chemical separation. The radiations were ascribed to a certain isotope on the basis of their decay rates. Several bombardments were made in order to collect enough information to postulate the decay schemes.

1. Alpha Groups

Alpha-particle spectra of Bk^{243} and Bk^{245}, taken with a Au-Si surface-barrier detector, are shown in Fig. 13. The Bk^{245} spectrum was measured 3 days after the cyclotron bombardment so that Bk^{243} could die out. The decay of each peak was followed for a few days in order to ascertain its assignment to a particular nuclide. As seen in Fig. 13(a) the 6.666-MeV alpha group, composed in part of Bk^{243} α_{94}, has a much higher intensity than the corresponding Bk^{245} α_{95}. Also there is a 6.624-MeV alpha peak in the spectrum that does not seem to belong to Bk^{243}. The half lives for the 6.666- and 6.624-MeV groups indicate that they belong to either Bk^{243} or Bk^{244}. In order to identify the Bk^{244} alpha groups, an Am^{243} target was bombarded with 33-MeV α-particles, which would increase the relative yield[17] of Bk^{244}. In the resulting spectrum the intensities of the 6.666- and 6.624-MeV alpha particles increased relative to the Bk^{243} groups, confirming that they belong to the isotope Bk^{244}. However, because of low statistics the alpha abundances of these groups could not be determined accurately. For that reason the intensities of the Bk^{243} α_{94} and α_{156} groups are only approximate. The α-particle energies and intensities are given in Tables XII, XIII, and XIV.A. along with the hindrance factors calculated by Mrs. H. V. Michel.[22] The α-particle energies were measured relative to Cm^{244} α_0 and Th^{226} α_0 groups which were taken as 5.805 and 6.334 MeV[21] respectively.

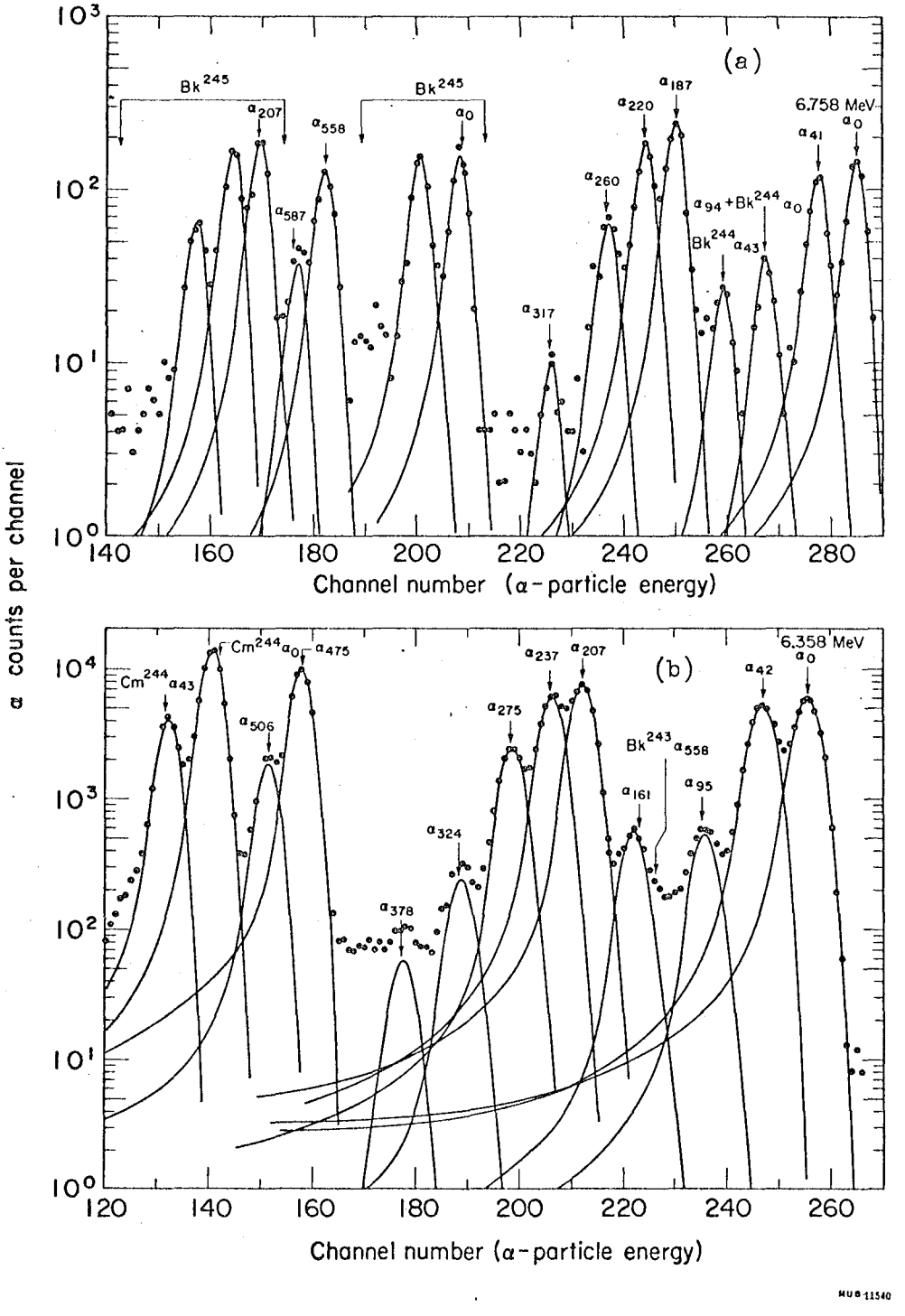

Fig. 13a,b. α-particle spectra of light berkelium isotopes.
(a) α-particle spectrum of Bk^{243} and Bk^{244}.
(b) α-particle spectrum of Bk^{245}, taken after the decay of Bk^{243} and Bk^{244}.

Table XII. Alpha groups of Bk^{243}.

α-particle energy (MeV)	Excited state energy (keV)	Intensity (%)	Hindrance factor[22]
6.758 ± 0.004	0	15.4 ± 1.0	1.1×10^3
6.718 ± 0.004	41	12.5 ± 0.9	9.5×10^2
6.666 ± 0.004	94	≈ 1.2	5.8×10^3
6.605 ± 0.005	156	≈ 0.7	5.4×10^3
6.574 ± 0.004	187	25.6 ± 1.6	1.1×10^2
6.542 ± 0.004	220	19.4 ± 1.3	1.0×10^2
6.502 ± 0.004	260	6.9 ± 0.7	1.9×10^2
6.446 ± 0.005	317	0.7 ± 0.2	1.0×10^3
≈ 6.394	≈ 370	≈ 0.2	2.1×10^3
6.210 ± 0.004	558	13.6 ± 0.9	3.8
6.182 ± 0.004	587	3.9 ± 0.5	9.7

Table XIII. Alpha groups of Bk^{245}.

α-particle energy (MeV)	Excited state energy (keV)	Intensity (%)	Hindrance factor[22]
6.358 ± 0.004	0	16.5 ± 0.5	7.2×10^2
6.317 ± 0.004	42	15.0 ± 0.5	5.0×10^2
6.265 ± 0.004	95	1.4 ± 0.1	3.0×10^3
6.200 ± 0.004	161	1.0 ± 0.2	2.0×10^3
6.153 ± 0.004	207	19.0 ± 0.5	64
6.124 ± 0.004	237	14.8 ± 0.5	59
6.087 ± 0.004	275	5.6 ± 0.3	1.0×10^2
6.038 ± 0.004	324	0.6 ± 0.1	5.3×10^2
5.985 ± 0.006	378	0.12 ± 0.04	1.7×10^3
5.889 ± 0.004	475	21.9 ± 0.5	2.4
5.858 ± 0.004	506	4.0 ± 0.2	9.3

Table XIV. A. Alpha groups of Bk^{244}.

α-particle energy (MeV)	Intensity (%)	Hindrance factor[22]
6.666 ± 0.004	≈ 50	4.4×10^3
6.624 ± 0.004	≈ 50	2.8×10^3

B. Gamma rays in the electron-capture decay of Bk^{243}

Energy (keV)	Relative intensity
755 ± 2	1.0 (norm)
946 ± 2	≈ 0.8

C. Gamma rays in the electron-capture decay of Bk^{245}

Energy (keV)	Relative intensity
252.7 ± 0.3	100 (norm)
380.5 ± 0.4	7.5 ± 0.8

2. Gamma Rays

Gamma rays following the alpha and the electron-capture decay of these nuclides were investigated by γ-singles and γ-α coincidence experiments. The low-energy γ spectrum taken immediately after the chemical purification, with a $2 \times 1 \times 0.6$ cm Ge(Li) detector, is shown in Fig. 14(b). The high-energy γ-rays of the shorter-lived isotopes were measured with the $3 \times 1 \times 0.3$ cm detector and are shown in Fig. 15(a). The Bk^{246} spectrum [shown in Fig. 15(b)] was taken after 2 days of the bombardment in order to allow for the decay of Bk^{244}. The γ-rays in these spectra are all due to the electron-capture decay of these isotopes. These radiations are assigned to the different isotopes on the basis of their decay rates, and their energies and intensities are given in Tables XIV.B, XIV.C, XV, and XVI. The assignment of the γ-rays to the electron-capture decay of Bk^{243} is based on the previous measurements.[17] In Table XV. the relative intensities of the γ-rays > 491.5 keV are normalized to the intensity of the 491.5-keV γ-ray, measured from the low-energy spectrum. The K x-ray intensities are obtained after subtracting the contribution due to Bk^{245} and Bk^{246}.

The γ-rays in the alpha decay of Bk^{243} and Bk^{245} were observed in γ-α coincidence experiments with a $3 \times 2 \times 0.8$ cm Ge(Li) detector. The electromagnetic radiations in coincidence with all α-particles and in coincidence with specific alpha groups have been investigated. The α spectrum in coincidence with all Bk^{245} α groups is shown in Fig. 14(a) and the results of all γ-α coincidence measurements are given in Table XVII. The large errors in the intensities are mainly due to poor statistics. γ-rays de-exciting the $K\pi=3/2-$ band of Am^{239} could not be examined because of the low efficiency of the Ge(Li) detector at higher energies. The results of the present investigations, although more accurate because of higher resolution, are consistent with the previous values.[17]

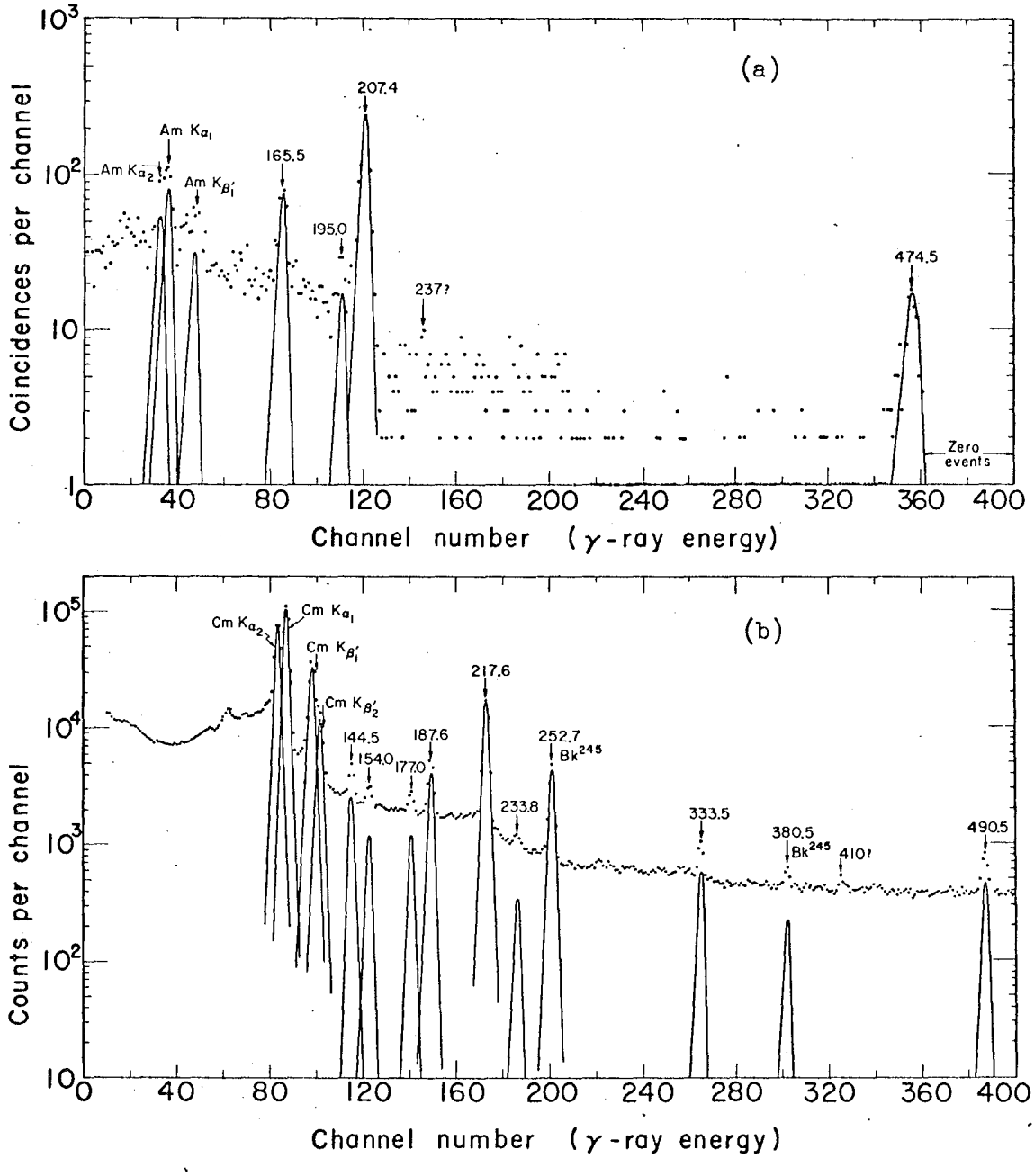

Fig. 14a,b. γ-ray spectra of light berkelium isotopes.
(a) γ-rays in coincidence with all Bk^{245} α-particles.
(b) Bk^{244} and Bk^{245} γ-ray spectrum.

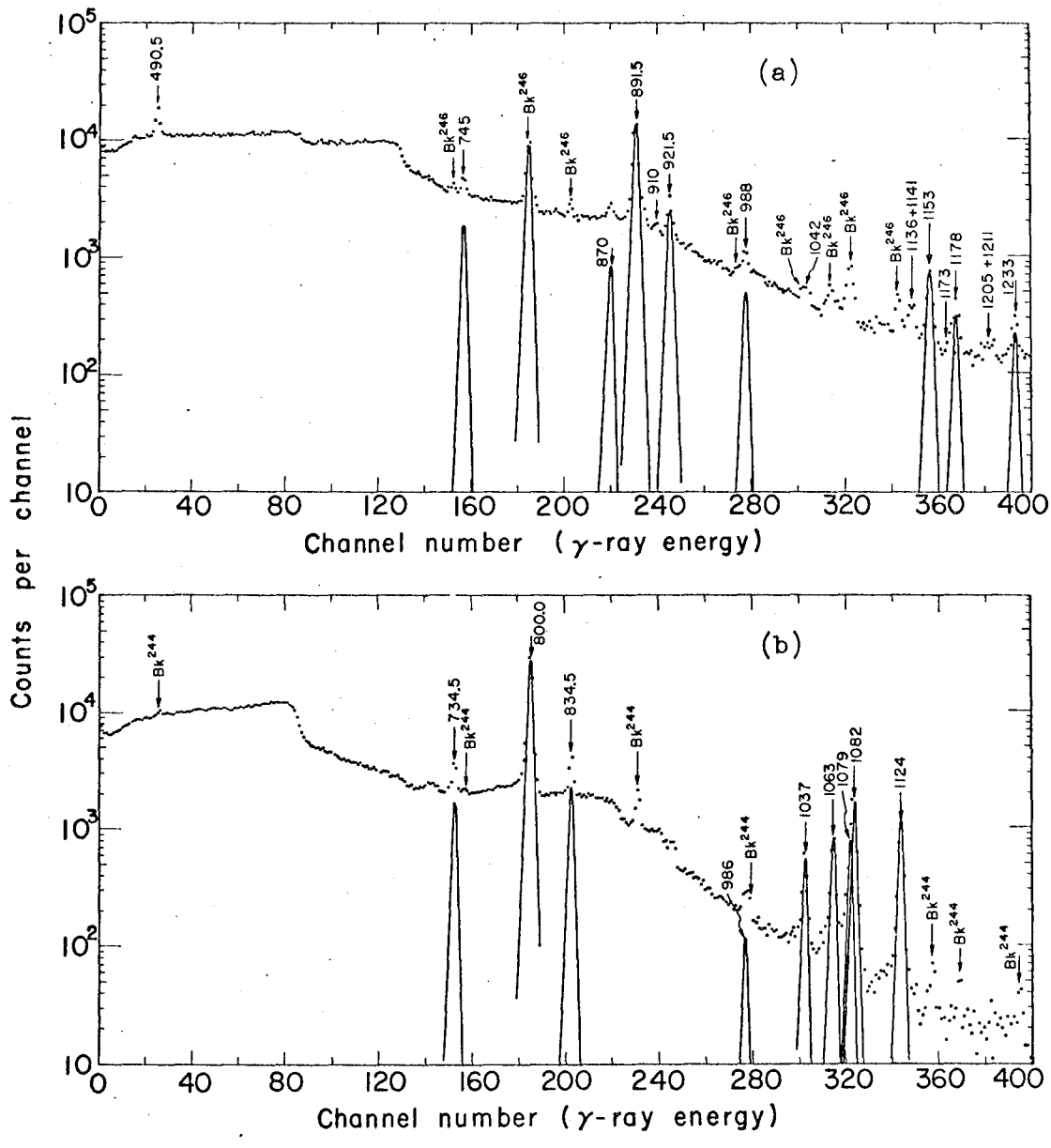

Fig. 15a,b. γ-ray spectra of Bk^{244} and Bk^{246}.
(a) γ-ray spectrum of Bk^{244} and Bk^{246}.
(b) γ-ray spectrum of Bk^{246}, measured after the decay of Bk^{244}.

Table XV. Gamma rays in the electron-capture decay ob Bk^{244}.

Energy (keV)		Relative intensity
104.5 ± 0.2	(Cm K_{α_2})	85 ± 10
109.3 ± 0.2	(Cm K_{α_1})	130 ± 15
123.2 ± 0.3	(Cm $K_{\beta_1'}$)	48 ± 6
127.1 ± 0.3	(Cm $K_{\beta_2'}$)	20 ± 4
144.5 ± 0.3		7.4 ± 0.7
154.0 ± 0.3		3.7 ± 0.4
177.0 ± 0.3		4.2 ± 0.5
187.6 ± 0.3		16.5 ± 1.5
217.6 ± 0.3		100 (norm)
233.8 ± 0.4		2.9 ± 0.4
333.5 ± 0.5		10.0 ± 1.5
490.5 ± 0.5		18 ± 2
745 ± 1		8 ± 1
870 ± 1		7 ± 1
891.5 ± 1.0		114 ± 12
910 ± 1		3.0 ± 0.5
921.5 ± 1.0		22 ± 3
988 ± 1		5 ± 1
1042 ± 2		≈ 3
1136 ± 2		≈ 1.5
1141 ± 2		≈ 2
1153 ± 1		9.5 ± 1.4
1173 ± 2		≈ 0.7
1178 ± 1		5.0 ± 0.8
1205 ± 2		≈ 1
1211 ± 2		≈ 1.3
1233 ± 1		4.0 ± 0.8
1252 ± 1		3.0 ± 0.6
1333 ± 1		1.2 ± 0.4
1505 ± 5		≈ 3

Table XVI. Gamma rays in the electron-capture decay of Bk^{246}.

Energy (keV)	Relative intensity
734.5 ± 0.5	4.6 ± 0.7
800.0 ± 0.5	100 (norm)
834.5 ± 0.5	8.0 ± 0.9
986 ± 1	≈ 0.5
1037 ± 1	2.8 ± 0.4
1063 ± 1	5.2 ± 0.6
1079 ± 1	5.0 ± 0.8
1082 ± 1	10.0 ± 1.4
1124 ± 1	7.5 ± 0.9

Table XVII.A. Bk^{245} γ-rays observed in γ-α coincidence experiment

(i) γ-rays in coincidence with 6.00- to 6.18-MeV α-particles.

Energy (keV)	Intensity (photons per α-particle)
K x-rays	0.04 ± 0.01
165.5 ± 0.5	0.07 ± 0.015
195 ± 1	≈ 0.01
207.4 ± 0.5	0.33 ± 0.05

(ii) γ-rays in coincidence with 5.84- to 5.92-MeV α-particles.

Energy (keV)	Intensity (photons per α-particle)
K x-rays	0.04 ± 0.01
474.5 ± 1.5	0.20 ± 0.03

Table XVII.B. Bk^{243} γ-rays in coincidence with 6.44- to 6.59-MeV α-particles.

Energy (keV)	Intensity (photons per α-particle)
K x-rays	0.08 ± 0.03
146.4 ± 0.5	0.08 ± 0.03
187.1 ± 0.5	0.4 ± 0.1

3. Decay Scheme

The spin and parity assignments of the levels of Am^{239} and Am^{241} have been discussed by Stephens, Asaro, and Perlman[1] and also by Mottelson and Nilsson,[2] on the basis of the previous measurements. In the following paragraphs some of their arguments are given along with our new results.

The nuclide Am^{241} has a measured spin[43] of 5/2. From the studies of its alpha decay to Np^{237}, it was concluded that this state must be 5/2-(523↓). The next three Am^{241} levels, observed in the present work, fit well with the expected energies for the rotational members of this band. The rotational constants calculated from Eq. (3) have values of 5.96 keV for Am^{241} and 5.81 keV for Am^{239}.

The ground state of Bk^{245} has been assigned 3/2-(521↑) on the basis of its electron-capture decay to Cm^{245}. The very low hindrance factor of the alpha transition to the 475-keV level indicates that this state must be the same as the ground state of the parent, 3/2-(521↑). The K x-ray intensity of the transition de-exciting this level to the ground state is in agreement with the theoretical value for an M1 (with ≈ 40% E2) transition (see Table XVIII.A). The 475-keV level and a 600-keV level [the 1/2-(530↑) Nilsson state] have also been observed[44] in the electron-capture decay of Cm^{241}. The E2 admixture in the 475-keV transition is, most likely, due to the Coriolis mixing of the 1/2-(530↑) band in the 475-keV state. The energy as well as the alpha intensity of the next rotational member of this band is consistent with the assignment.

The level at 207.4 keV de-excites to the ground state and to the 41.7-keV level. As seen in Table XVIII.A a comparison of the K x-ray and the γ-ray intensities with the values obtained from the theoretical K-conversion coefficients indicates that these transitions are either E1 or E2. From their energy spacings, the levels at 207.4, 237, 275, 324, and 378 keV appear to constitute a rotational band with the spin of the lowest state being 3/2 or 5/2. The only reasonable Nilsson state (see Fig. 16) in this region cosistent with the above results has the assignment 5/2+(624↑),

Table XVIII.A. Multipolarity determinations.

Energy (keV)	Relative intensity				
	Exper.	Theor. K x-ray intensities			Multi-polarity
		E1	E2	M1	
Bk^{243} α-decay					
187.1	5.0	5.0	5.0	5.0	E1 or E2
146.4	1.0	1.0	1.0	1.0	
K x-rays	1.0	0.7	1.0	40	
Bk^{245} α-decay					
207.4	4.7	4.7	4.7	4.7	E1 or E2
165.5	1.0	1.0	1.0	1.0	
K x-rays	0.6	0.5	0.8	18	
Bk^{245} α-decay					
474.5	1.0	1.0	1.0	1.0	M1 + ≈ 40%E2
K x-rays	0.2	0.013	0.035	0.3	

Table XVIII.B. Relative γ-ray intensities depopulating the Kπ = 5/2+ levels in Am^{239} and Am^{241}.

		Multipolarity	$(B_1/B_2)_{exp.}$	$(B_1/B_2)_{theo.}$[42]
Bk^{243}	$\frac{B_{187.1}}{B_{146.4}}$	E_1	2.4	2.5
		E_2	1.4	0.75
Bk^{245}	$\frac{B_{207.4}}{B_{165.5}}$	E_1	2.3	2.5
		E_2	1.5	0.75

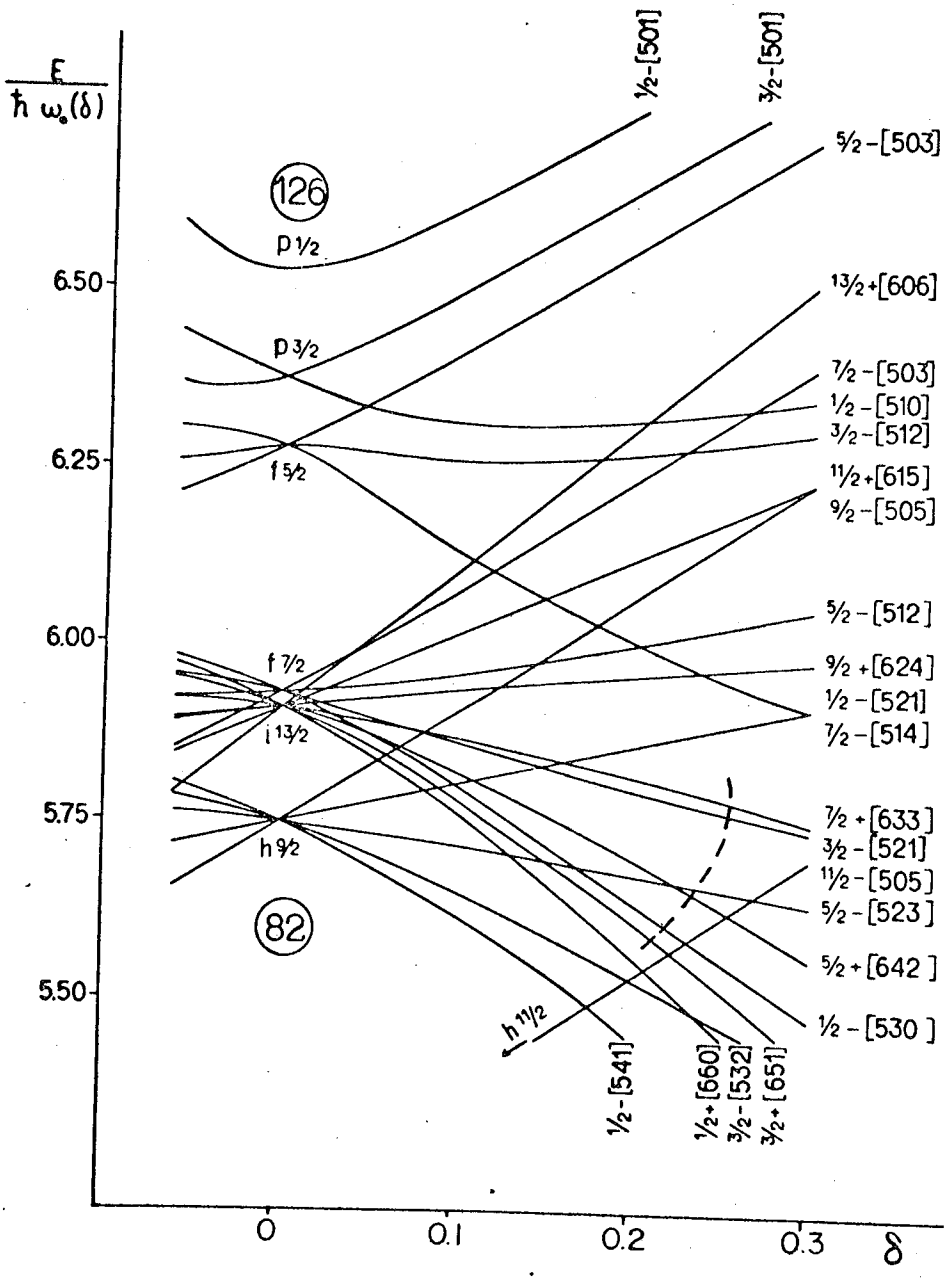

MU-15745

Fig. 16. Nilsson diagram for protons in the region $82 \leq Z \leq 126$. The abscissa represents the nuclear deformation and the ordinate shows the excitation energy of the various levels. The dashed line indicates very roughly the deformations of the nuclei in this region. The quantum numbers shown in the figure are explained in Chapter V.

the ground state of Np^{237}. The relative intensities of the 165.5- and the 207.4-keV γ-rays agree well with the theoretical expectations[42] of fast E1 transitions between K=5/2 rotational bands, as shown in Table XVIII.B. The spacing between the base member and the first rotational member of this band is 29.6 keV, which is much smaller than the usual value of 42 keV for other K=5/2 bands in this region. The disturbed spacings between various members of the band are due to the Coriolis interaction of this band with the other positive-parity states associated with the $i_{13/2}$ shell-model state. As the position of none of the other even-parity intrinsic states is known, it is not yet possible to calculate the effect of this interaction.

The spectra associated with Bk^{243} alpha decay are similar to those associated with Bk^{245}, as can be seen by comparison of the two decay schemes (Figs. 17 and 18). The quantum number assignments for Am^{239} levels are based on arguments which are nearly identical with those for Am^{241} levels and hence will not be repeated. The alpha transition probabilities to the levels of the two nuclides are compared with the theoretical values in Tables XIX.A and XIX.B. In the calculations the L=4 and L=5 alpha waves are not included because it is difficult to make a correct estimate of the parameter b_L required in Eq. (4). The hindrance factors for L=0 and L=2 alpha waves of the favored decay were obtained from the adjacent even-even nuclides. It should be observed that the agreement between the experimental and calculated values is not good.

In the present investigations no new information has been obtained about the electron-capture decay of Bk^{243} and Bk^{245}. In the case of Bk^{244} electron-capture decay, 26 γ-rays have been identified (Table XV). However, this information is not sufficient to postulate a decay scheme. The Bk^{246} γ-rays are consistent with the energy-level diagram of Cm^{246}, constructed by Stephens, Asaro, Fried, and Perlman,[45] from the β decay of Am^{246}. The spins and parities of the levels were assigned on the basis of two quasi-particle excited states of even-even nuclei[46] and the superfluid model.

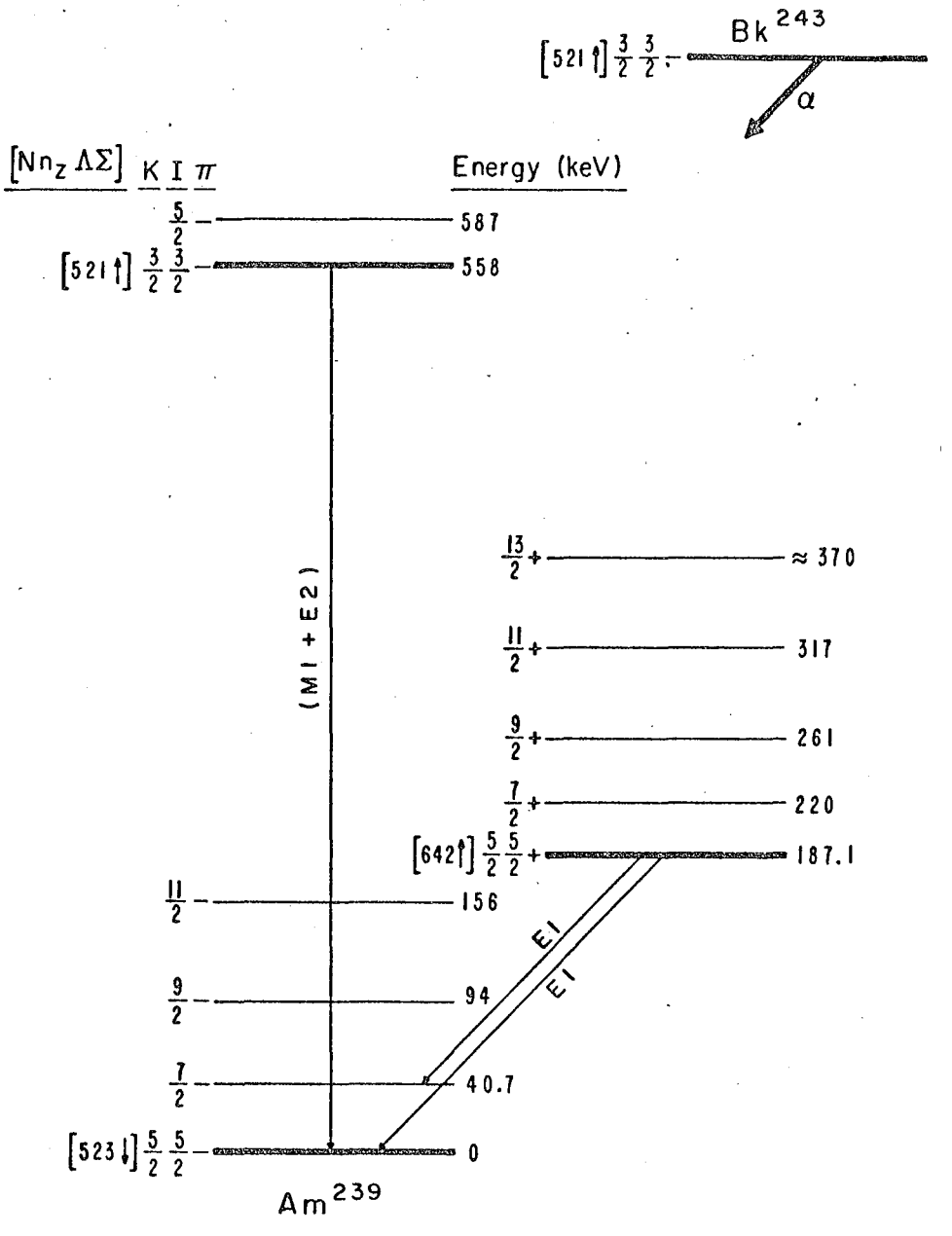

Fig. 17. Alpha decay scheme of Bk^{243}.

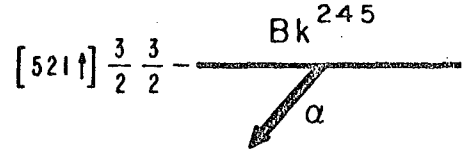

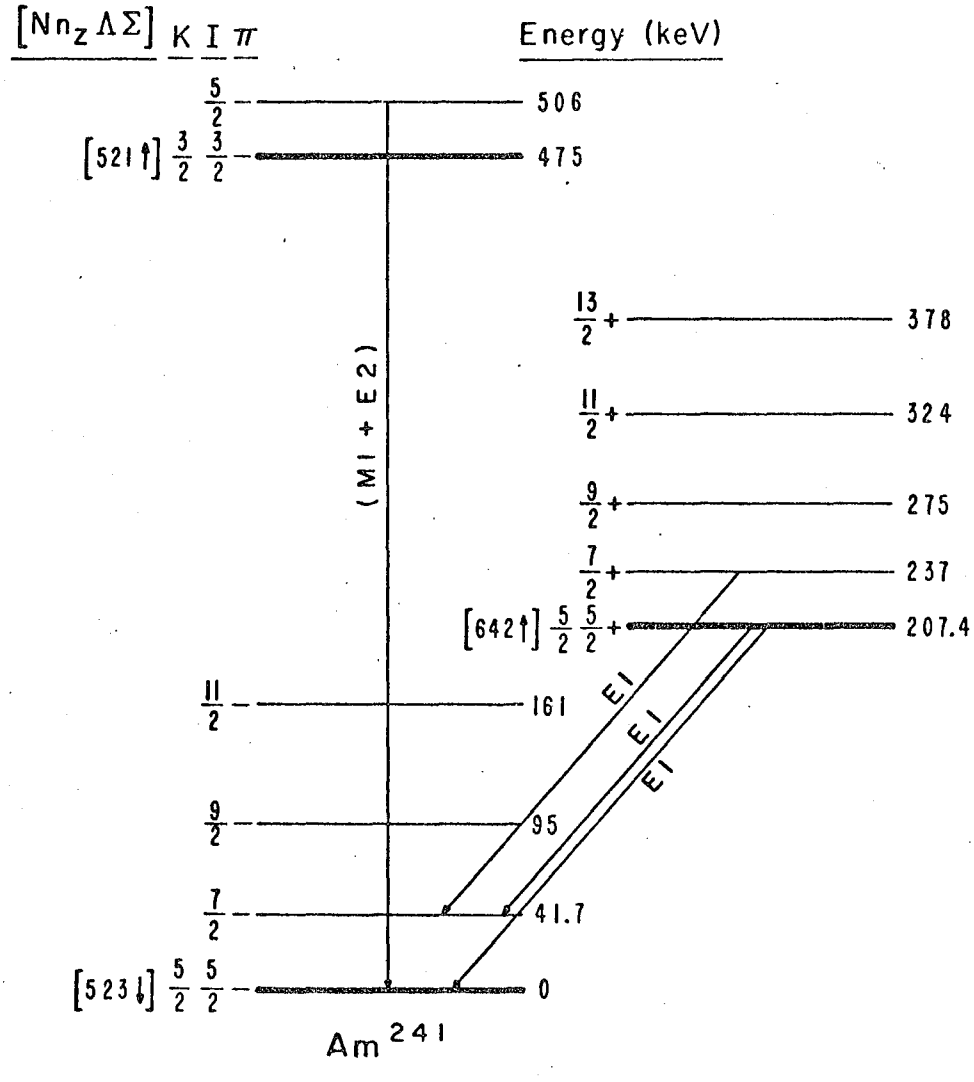

MUB-12449

Fig. 18. Alpha decay scheme of Bk^{245}.

Table XIX.A. Alpha population to the levels of Am^{239}

(i) Final state = 5/2-(523↓).

Level (keV)	Iπ	Observed intensity (%)	Theoretical value[a] of relative intensity (%) L=2	Poggenburg's value (%)
0	5/2-	15.4	14.5	14.3
40.7	7/2-	12.5	13.5	14.9
94	9/2-	≈ 1.2	-	2.8
156	11/2-	≈ 0.7	-	2.0

[a]The hindrance factor for L=2 alpha wave = 500

(ii) Final state = 5/2+(642↑).

Level (keV)	Iπ	Observed intensity (%)	Theoretical value[a] of relative intensity (%) L=1	L=3	Σ	Poggenburg's value (%)
187.1	5/2+	25.6	21.1	4.5	25.6	21.1
220	7/2+	19.4	-	13.9	13.9	15.3
260	9/2+	6.9	-	8.0	8.0	8.7
317	11/2+	0.7	-	-	-	0.5
≈ 370	13/2+	≈ 0.2	-	-	-	0.1

[a]The hindrance factors for L=1 and L=3 alpha waves are 133 and 67 respectively.

(iii) Final state = 3/2-(521↑).

Level (keV)	Iπ	Observed intensity (%)	Theoretical value[a] of relative intensity (%) L=0	L=2	Σ	Poggenburg's value (%)
558	3/2-	13.6	12.4	1.2	13.6	17.2
587	5/2-	3.9	-	2.4	2.4	2.9

[a]The abundances are calculated from Eq. (4) with hindrance factors for L=0 and L=2 alpha waves as 1 and 2 respectively.

Table XIX.B. Alpha population to the levels of Am^{241}.

(i) Final state = 5/2-(523↓).

Level (keV)	Iπ	Observed intensity (%)	Theoretical value[a] of relative intensity (%) L=2	Poggenburg's value (%)
0	5/2-	16.5	16.4	15.5
41.7	7/2-	15.0	13.7	14.5
95	9/2-	1.4	-	2.7
161	11/2-	1.0	-	1.7

[a]The hindrance factor for L=2 alpha wave = 310.

(ii) Final state = 5/2+(642↑).

Level (keV)	Iπ	Observed intensity (%)	Theoretical value[a] of relative intensity (%) L=1	L=3	Σ	Poggenburg's value (%)
207.4	5/2+	19.0	15.1	3.9	19.0	14.4
237	7/2+	14.8	-	12.5	12.5	10.3
275	9/2+	5.6	-	7.0	7.0	5.9
324	11/2+	0.6	-	-	-	0.3
378	13/2+	0.12	-	-	-	0.1

[a]The hindrance factors for L=1 and L=3 alpha waves are 81 and 33 respectively.

(iii) Final state = 3/2-(521↑).

Level (keV)	Iπ	Observed intensity (%)	Theoretical value[a] of relative intensity (%) L=0	L=2	Σ	Poggenburg's value (%)
475	3/2-	21.9	20.1	1.8	21.9	30
506	5/2-	4.0	-	3.3	3.3	4.6

[a]The abundances are calculated from Eq. (4) with hindrance factors for L=0 and L=2 alpha waves as 1.0 and 2.2 respectively.

The level at 1125 keV (see Fig. 19) was not observed in the beta decay of Am^{246}. The strong intensities of the transitions de-exciting this state to the ground state and the 43-keV level suggest collective nature of this state. In a recent work[47] on the decay of Bk^{246}, the multipolarities of these transitions have been determined and are found to be E2. The relative intensities of the two γ-rays are also in fair agreement with the theoretical values.[42]

D. Alpha Decay of Bk^{249}

The nuclide Bk^{249} was first isolated[48] from the debris of the thermonuclear explosion "Mike". It was later prepared[26] by prolonged neutron irradiation of plutonium, americium, or curium. The half life, the alpha branching ratio, and the radiations of Bk^{249} have been investigated by various groups.[26] The best balues of half life and alpha branching ratio are 314 days and 2.2×10^{-3}% respectively. The fine structure of the alpha spectrum has been noted by Milsted and Friedman,[49] but for the lack of sufficient information no decay scheme could be postulated. In the present work the radiations accompanying the α decay of Bk^{249} have been examined and a decay scheme has been constructed.

1. Alpha Groups

The alpha spectra of Bk^{249} have been measured with a double-focusing magnetic spectrograph and these are given in Fig. 20. The source for these measurements was 1/2 in. long by 1/16 in. wide and was prepared by vacuum-sublimation of about 1 μg of purified Bk^{249} onto a cold platinum plate. The exposure time for spectrum (a) was 30 hr, whereas for spectrum (b) it was 8 days. The comparatively high background in the spectra is due to the growth of the daughter, Cf^{249}. The α-particle energies were measured relative to Pu^{238} and Pu^{240} alpha groups which were present in the sample. The two α groups of each standard were used to verify the constants D_0 and

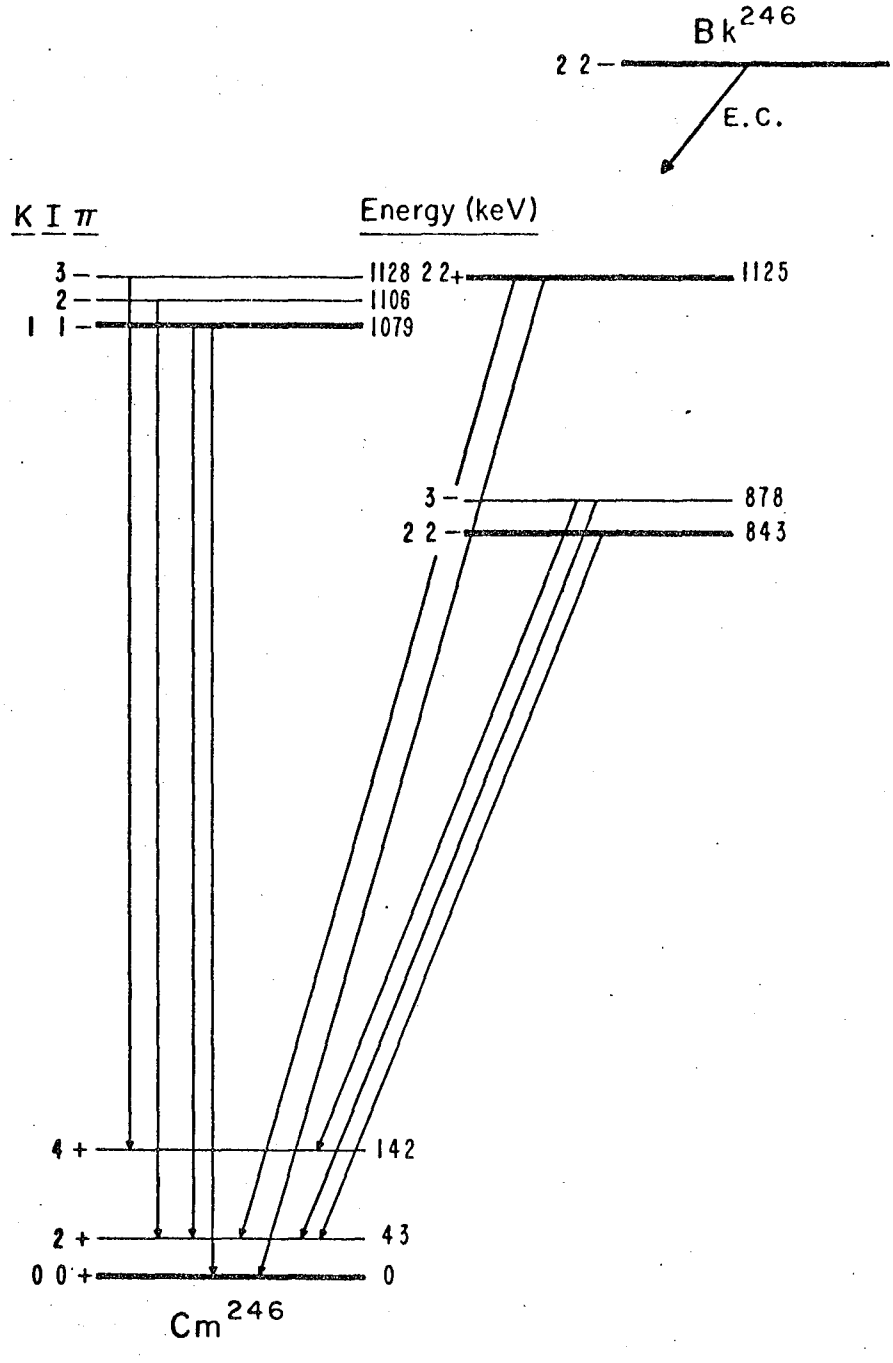

Fig. 19. Electron-capture decay scheme of Bk^{246}.

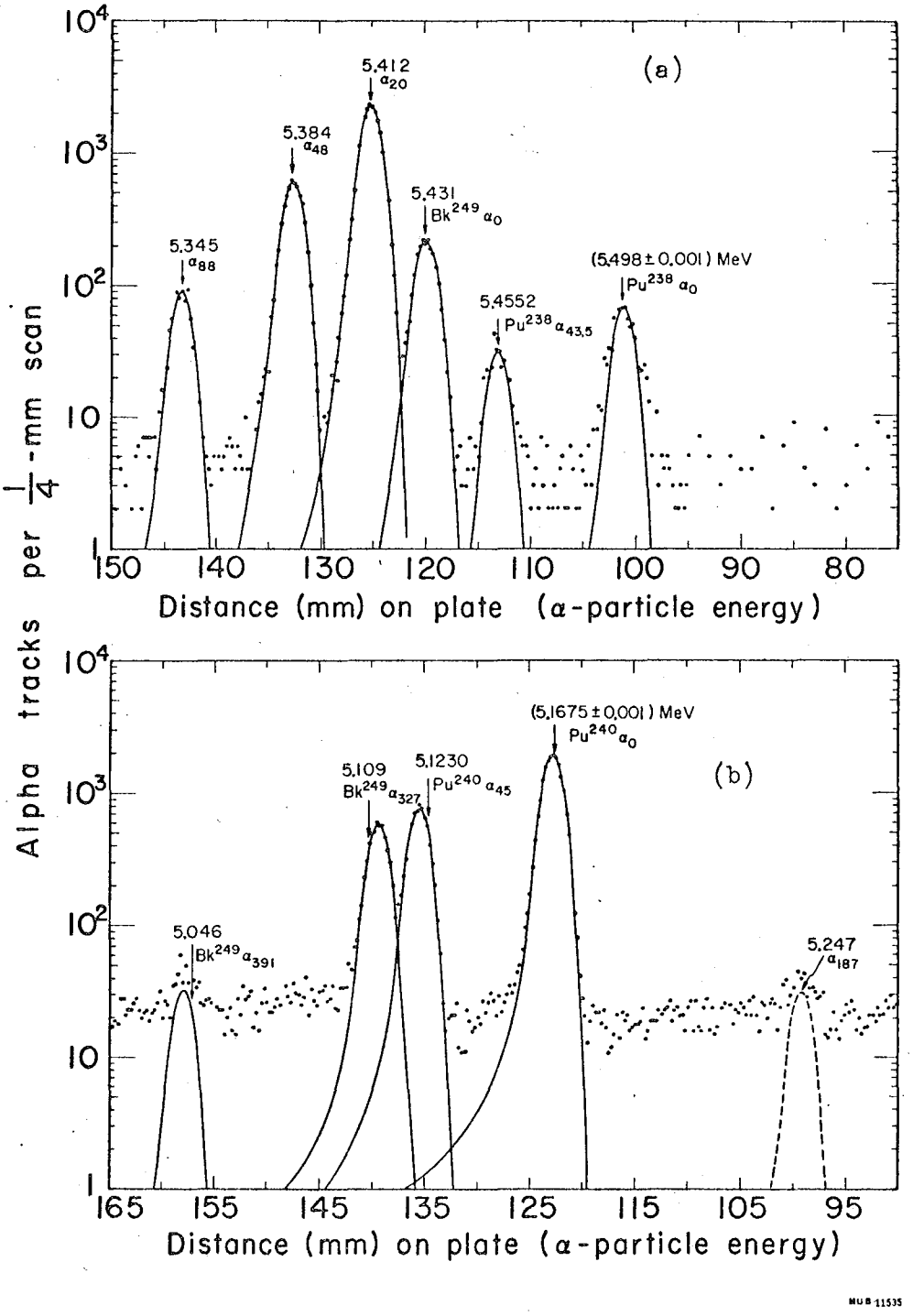

Fig. 20a,b. α-particle spectra of Bk^{249}, measured with the double-focusing magnetic spectrograph. The background in the spectra is due to the growth of the daughter, Cf^{249}.

and c of Eq. (1). The energies of Pu^{238} $\alpha_{43.5}$ and Pu^{240} α_{45} groups were obtained on the basis of the transition energies of 43.5- and 45-keV levels of U^{234} and U^{236} respectively, which are known accurately.[26] The energies and abundances of the alpha groups measured from these spectra are given in Table XX.

Attempts were made to use Au-Si surface-barrier detectors for α-γ coincidence measurements. But the intense β particles of Bk^{249} broadened the peaks on the high-energy side and hence no worthwhile information could be obtained from α-γ coincidence experiments.

2. Gamma Rays

Gamma rays of chemically purified Bk^{249} were investigated by γ-singles and γ-α coincidence experiments. In the singles spectrum a 327.2-keV γ-ray was identified. In the γ-α coincidence spectrum (shown in Fig. 21) the same γ-ray along with another γ-ray of energy 307.5 keV was observed. The K-conversion coeffcients of this radiation, determined from the K x-ray intensity, is in good agreement with the theoretical value expected for M1 transition. The energies and intensities of the γ-rays and K x-rays are tabulated on page 78.

3. Decay Scheme

The ground state of Bk^{249} has been assigned 7/2+(633↑) on the basis of alpha decay[50] of Es^{253}. The low hindrance factor of the 5.109-MeV alpha group indicates favored alpha decay, and hence the 327.2-keV level (shown in Fig. 22) must be identical with the Bk^{249} ground state, 7/2+(633↑). The 391-keV level fits well as the 9/2+ member of this band. The value of the rotational constant is influenced by rotation-particle coupling and will be discussed later.

From the studies of Bk^{245} alpha decay, one should expect the ground state of Am^{245} to be 5/2-(523↓) or 5/2+(642↑). In the present work it has not been proved that the 5.431-MeV alpha group populates the ground state of Am^{245}.

Table XX. Alpha groups of Bk^{249}

α-particle energy (MeV)	Excited state energy (keV)	Intensity (%)	Hindrance factor[22]
5.431 ± 0.002	0 ?	6.7 ± 0.3	60
5.412 ± 0.002	20	69.2 ± 1.5	4.5
5.384 ± 0.002	48	18.4 ± 0.5	11.3
5.345 ± 0.002	88	2.6 ± 0.2	46
5.247 ± 0.006	≈ 187	≈ 0.1	290
5.109 ± 0.002	327	2.7 ± 0.2	1.4
5.046 ± 0.005	391	0.10 ± 0.04	14

Table XXI. Gamma rays in coincidence with all Bk^{249} α-particles

Energy (keV)	Intensity (photons per 10^2 α-particles)
327.2 ± 0.5	1.2 ± 0.2
307.5 ± 1.0	0.22 ± 0.6
K x-rays	1.1 ± 0.2

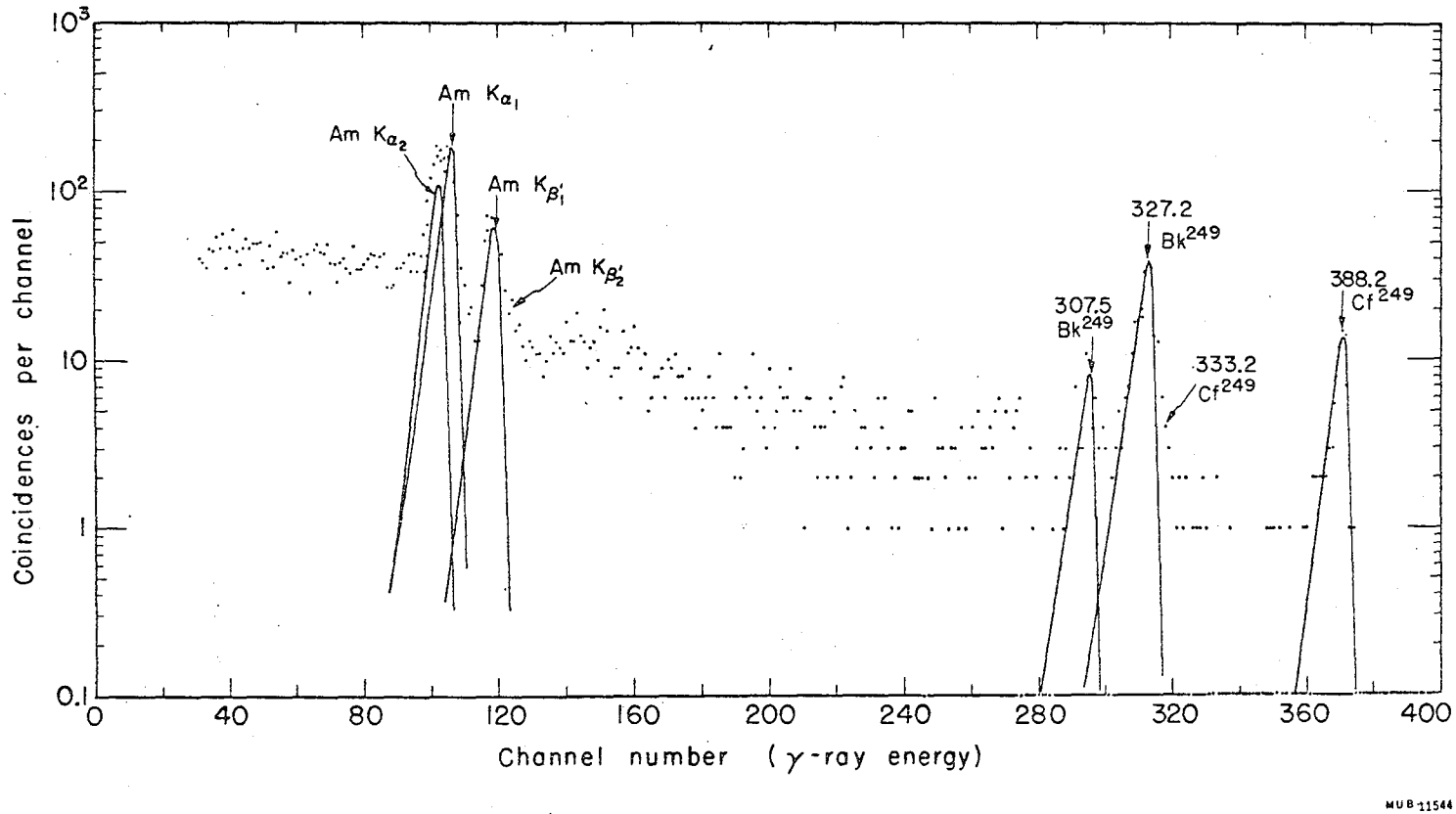

Fig. 21. γ-ray spectrum in coincidence with all Bk^{249} α-particles, taken with a 3 × 2 × 0.8 cm Ge(Li) detector. Zero events are plotted at 0.1.

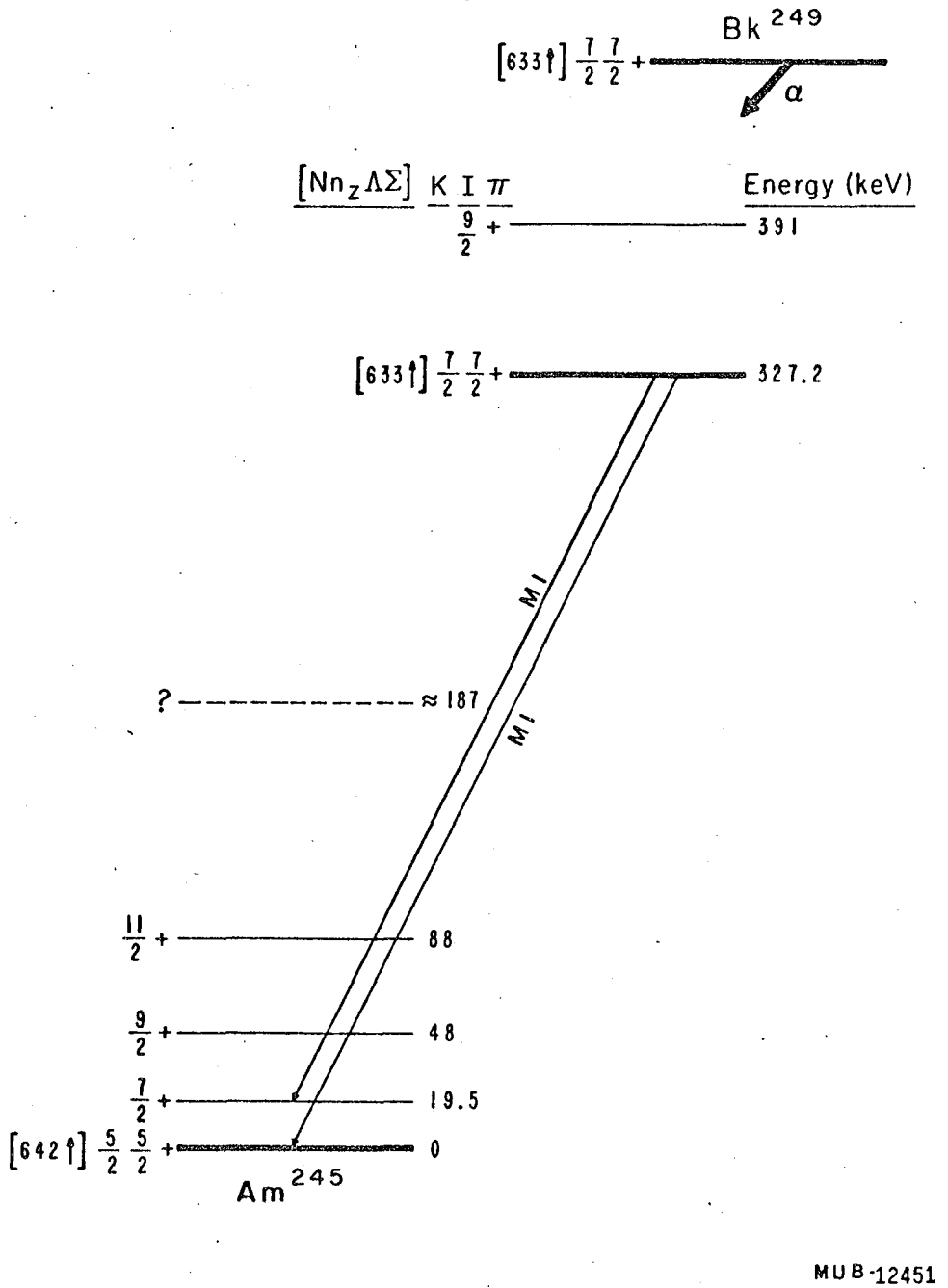

Fig. 22. Alpha decay scheme of Bk^{249}.

But as it is the highest energy alpha group that has been observed, one is justified in tentatively assuming that it populates the ground state. The M1 character of the 327.2-keV transition indicates that the Am^{245} level, populated by the highest energy group, has even parity and spin 5/2, 7/2, or 9/2. It is thus definite that this state is 5/2+(642↑) and not the 5/2-(523↓). The next three levels appear to be the rotational members of this band. The small spacings between various members of the band and the high alpha population to them are due to Coriolis mixing of this band with the favored band.

Some of the states arising from the $i_{13/2}$ shell-model level have strong Coriolis interactions with each other. The states with $\Delta K=\pm 1$ interact strongly whereas other have only a small effect. The level spacings of 7/2+(633↑) and 5/2+(642↑) bands have been claculated by taking all of the states arising from the $i_{13/2}$ shell-model level into account. The excitation energies of most of the states were obtained from Nilsson eigne-value,[3] and the matrix elements $A_{K,K+1}$ were calculated[41] with Nilsson wave functions. In the calculations, $A_{5/2,7/2}$ and the energy of the 7/2+(633↑) state were used as adjustable parameters because they would be strongly influenced by pairing correlation. The two variables were adjusted to get the best agreement with the observed energies of Am^{245} levels. The results, obtained by reducing the matrix element $A_{5/2,7/2}$ to 55% and the energy of the 7/2+(633↑) state to 92% of the calculated values, are given in Table XXII.

From the alpha decay scheme of Es^{253} it was known that the ground state of Bk^{249} has an admixture[51] of 5/2+(642↑), (a=0.164). From our calculations on the Coriolis interactions following Bk^{249} α-decay we have the admixtures of K=7/2 band in each of the members of the 5/2+ ground state band. For the alpha trasnition to the spin 7/2 first excited state, the "reduced transition probability" factor for the L=0 transition should be approximately $(a_{parent} \pm a_{daughter})^2$. Small corrections can be made, as given by Poggenburg, for the difference in the favored L=0 reduced transition probability for the 5/2+(642↑) and the 7/2+(633↑) states. The reciprocal hindrance factor for the intrinsic component of the L=2 alpha wave

Table XXII. Energy spacings and alpha population of the Am^{245} levels.

K	Iπ	Excited state energy (keV)		Alpha reduced transition probabilities[a]					
				Exp.	Calc.				
					$L=0^{b}$		$L=2^{c}$		Σ^{d}
		Exp.	Calc.		(relative phases)				
					+-	++	+-	++	
5/2	5/2+	0	0	0.028	-	-	0.06	0.012	0.012
	7/2+	19.5	19.8	0.36	0.007	0.16	0.001	0.085	0.25
	9/2+	48.0	48.0	0.14	-	-	0.012	0.094	0.094
	11/2+	88.0	87.8	0.035	-	-	0.01	0.031	0.031
7/2	7/2+	327.0	326.6						
	9/2+	391.0	391.5						

[a]These are the reciprocals of the alpha-decay hindrance factors divided by the reciprocal of the hindrance factor for the favored L=0 transition.

[b]The phases refer to the two Coriolis-induced L=0 alpha waves.

[c]The two Coriolis-induced L=2 alpha waves are assumed to be in phase. The choice of the phase refers to the major intrinsic L=2 component between the 7/2+(633↑) and 5/2+(642↑) bands.

[d]The sum in the last column is obtained by taking the two L=0 components of the alpha waves in phase and the three major L=2 components in phase.

was assumed to be the same as found for Es^{253} decay to the 5/2+(642↑) band. The reciprocal hindrance factors for the Coriolis-induced "favored" L=2 transitions were taken the same as for Bk^{249} favored alpha decay. The resulting reduced transition probabilities are given in Table XXII. It should be noted that a fair agreement is reached if one assumes that the various components of the alpha waves are in phase with each other. The agreement is further improved by increasing the alpha-decay matrix element between the 7/2+(633↑) and 5/2+(642↑) states by 30%.

E. Alpha Decay of Cf^{249}

The nuclide Cf^{249} was first identified[48] in the debris of a thermonuclear test explosion. Larger quantities of Cf^{249} are obtained from the β decay ob Bk^{249}, which can be produced in a reactor. The alpha spectrum of Cf^{249} has been measured by Magnusson[52] and also by Stephens et al.[53] The latter group analyzed the spectrum with a magnetic spectrograph and identified 11 α groups. They also examined the γ radiations with a scintillation detector and on the basis of these results constructed a decay scheme. In the present work a more thorough investigation of the Cf^{249} radiations has been carried out and a new band at 644 keV has been identified.

1. Alpha Groups

The Cf^{249} α groups have been examined by α-singles and α-γ coincidence experiments using a cooled 6-mm diameter surface-barrier detector. The source for the measurements was prepared by vaporizing a pure sample ($\approx 5 \times 10^5$ dis/min) of Cf^{249} onto a 0.002-in. nickel plate. In the singles spectrum (Fig. 23) 14 alpha groups have been observed. The α-particle energies have been measured with respect to the Cm^{244} α_0 group, which was taken as 5.805 MeV. The 6.115- and 6.026-MeV α groups in the spectrum belong to Cf^{252} and Cf^{250} respectively. The intensity of Cf^{249} α_{122} group was obtained after subtracting the contribution of Cf^{252} $\alpha_{43.4}$. The α-particle energies and intensities along with the hindrance factors are listed in Table XXIII.

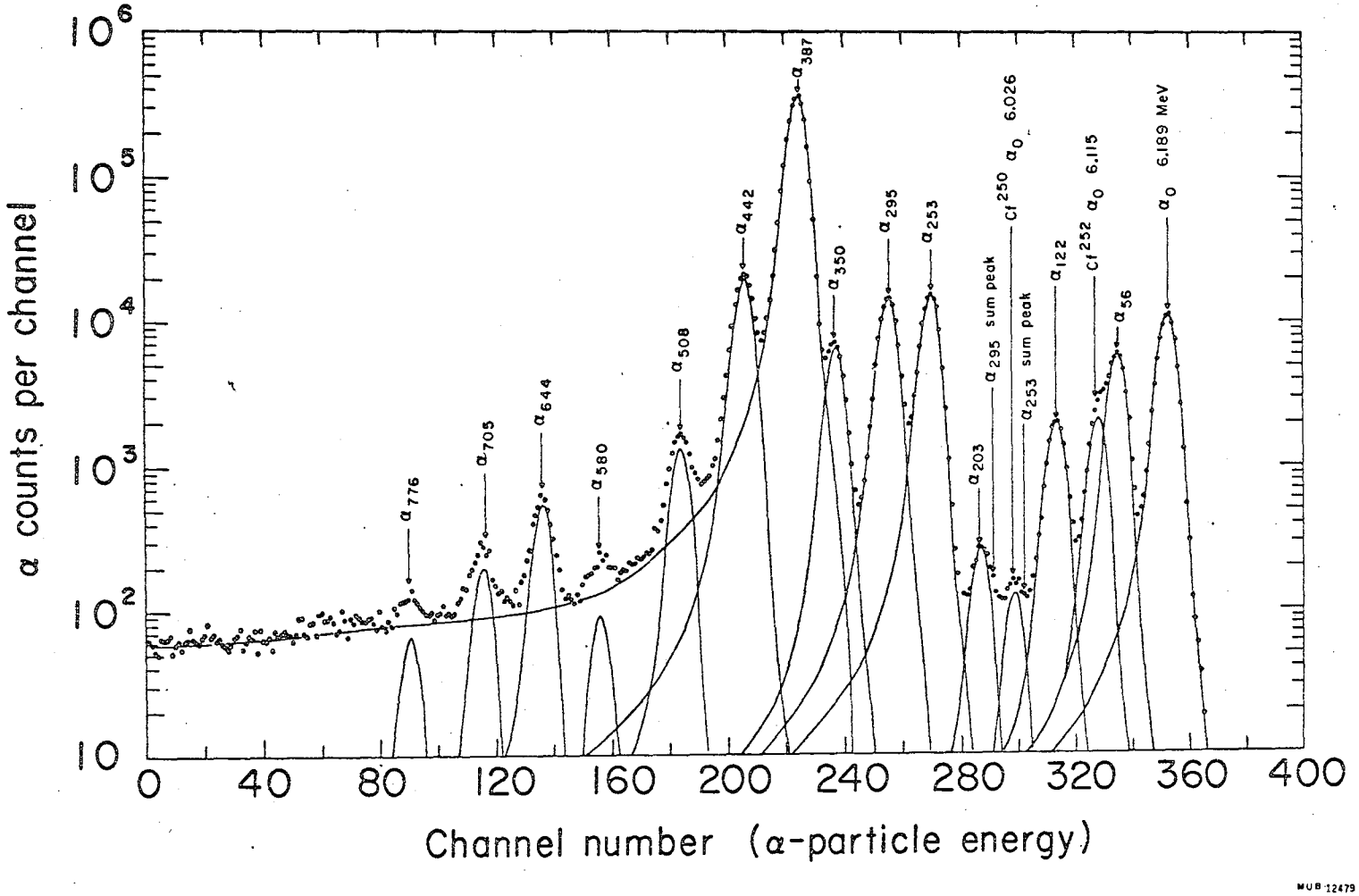

Fig. 23. Cf^{249} alpha spectrum, measured with a cooled 6-mm diameter Au-Si surface-barrier detector.

Table XXIII. Cf^{249} alpha groups.

α-particle energy (MeV)	Excited state energy (keV)	Intensity (%)	Hindrance factor[22]
6.189 ± 0.003	0	2.4 ± 0.1	6.7×10^3
6.134 ± 0.004	56	1.3 ± 0.1	6.6×10^3
6.069 ± 0.004	122	0.4 ± 0.06	1.0×10^4
6.989 ± 0.004	203	0.06± 0.01	2.6×10^4
6.940 ± 0.003	253	3.4 ± 0.1	2.5×10^2
5.899 ± 0.003	295	3.2 ± 0.1	1.6×10^2
5.845 ± 0.004	350	1.4 ± 0.1	1.8×10^2
5.808 ± 0.003	387	82.6 ± 0.3	2.0
5.754 ± 0.003	442	4.8 ± 0.2	17
5.690 ± 0.004	507	0.3 ± 0.05	1.2×10^2
5.618 ± 0.006	580	$\approx 2 \times 10^{-2}$	7×10^2
5.555 ± 0.004	644	0.11± 0.01	53
5.497 ± 0.004	703	$(4.4 \pm 0.4) \times 10^{-2}$	60
5.426 ± 0.005	775	$(1.0 \pm 0.3) \times 10^{-2}$	98
≈ 5.345	857	$\approx 0.2 \times 10^{-2}$	1.5×10^2

2. α-γ and γ-α Coincidence Measurements

The α-γ and γ-α coincidence experiments were performed in order to get information about the de-excitation of the high-lying states. As seen in the decay scheme (Fig. 27), the band built on the 644-keV level can decay to any or all of the lower bands. In order to observe the distribution of the transitions to various bands, α spectra were measured in coincidence with (i) the 252.7-keV photopeak, (ii) the 388.2-keV photopeak, and (iii) γ-rays > 420 keV. Only a small fraction of the α-particles were found to be in coincidence with γ-rays > 420 keV, compared to those in coincidence with the 388.2- and 252.7-keV γ-rays. It was found that only $\approx$ 20% of the de-excitation went to the ground state band. In a γ-α coincidence experiment using a scintillation detector, a 644-keV transition was identified in coincidence with 5.30- to 5.56-MeV α-particles. The α spectrum in coincidence with γ-rays > 420 keV is shown in Fig. 24. In this spectrum α_{443} and α_{508} are observed to rise in relation to $\alpha_{388.2}$. This, perhaps, is due to M2 transitions from the 443- and 508-keV levels to the ground state band, which are included in the γ gates. There seems some complex structure between the α_{508} and α_{644} groups. It appears that there are some levels in this energy region which receive very low alpha population. The groups determined from the coincidence measurements are included in Table XXIII.

3. Gamma Rays

Gamma rays following the α decay of Cf^{249} have been measured with the 3 × 1 × 0.3 cm Ge(Li) detector. The spectra are shown in Fig. 25 and the γ-ray energies and intensities obtained from this run are given in Table XXIV. In spectrum (b) the 321-keV γ-ray is masked by the false peak of the 388.2-keV γ-ray. This γ-ray was identified in a spectrum measured with another detector.

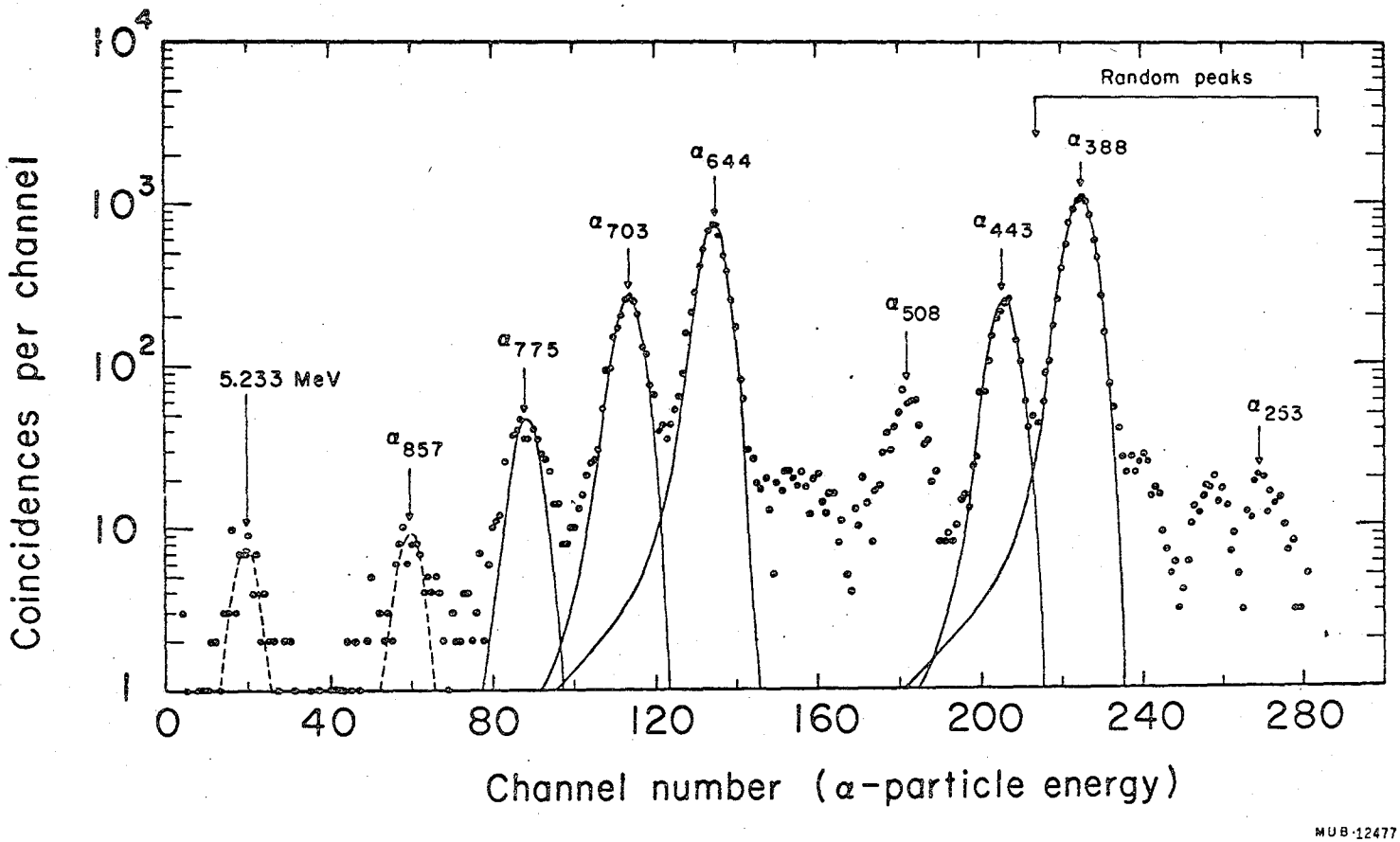

Fig. 24. Cf^{249} α-particle spectrum in coincidence with γ-rays > 420 keV.

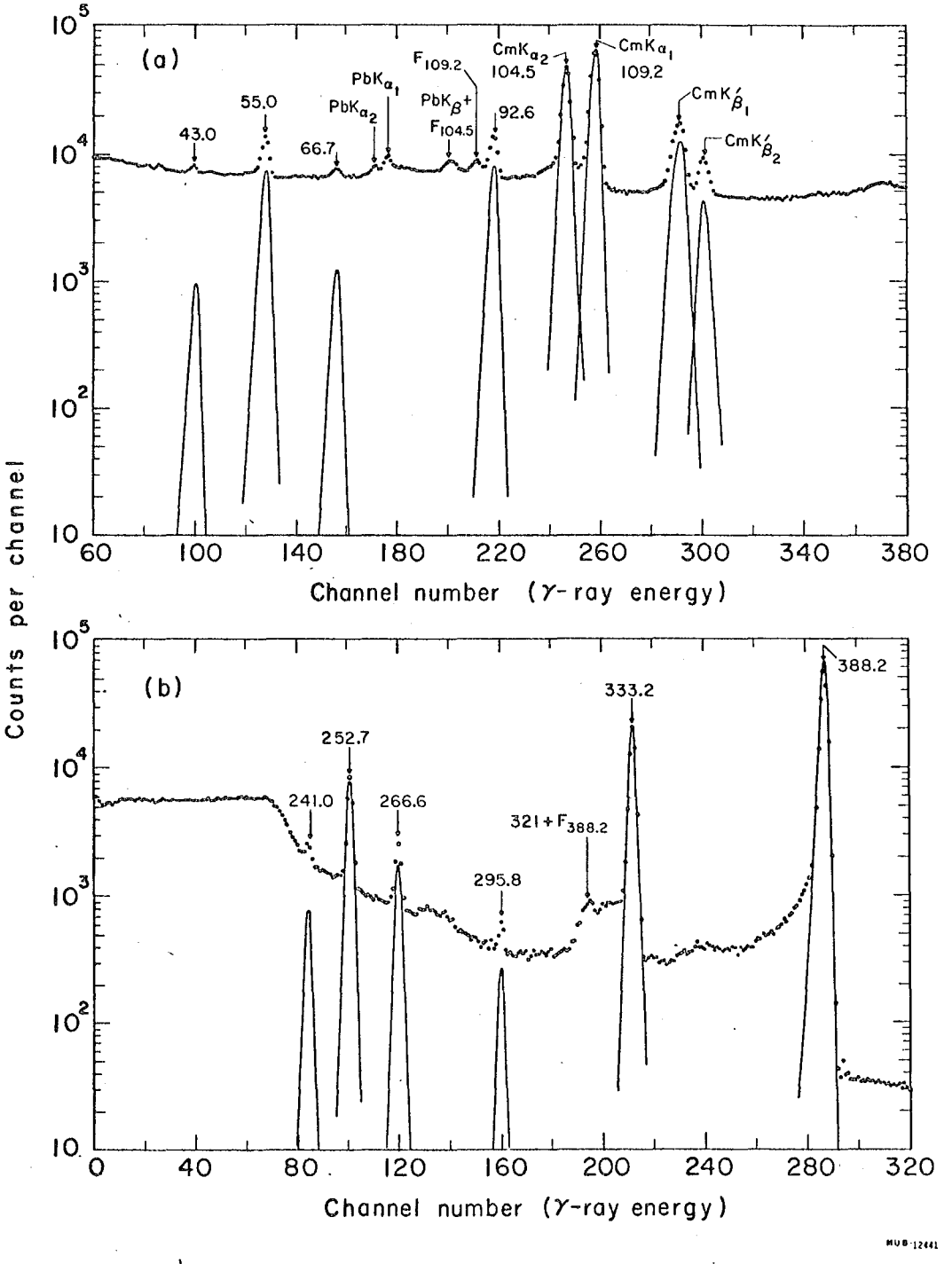

Fig. 25a,b. Cf^{249} γ-ray spectra taken with the 3 × 1 × 0.3 cm Ge(Li) detector.

Table XXIV. Cf^{249} γ-rays.

Energy (keV)		Intensity (photons per 10^2 Cf^{249} α-particles)
43.0 ± 0.2		0.03 ± 0.01
55.0 ± 0.2		0.20 ± 0.05
66.7 ± 0.2		0.04 ± 0.01
92.6 ± 0.2		0.36 ± 0.06
104.5 ± 0.2	(Cm K_{α_2})	2.7 ± 0.3
109.2 ± 0.2	(Cm K_{α_1})	3.7 ± 0.4
122.9 ± 0.3	(Cm $K_{\beta_1'}$)	2.0 ± 0.3
126.8 ± 0.4	(Cm $K_{\beta_2'}$)	0.5 ± 0.08
241.0 ± 0.3		0.29 ± 0.03
252.7 ± 0.3		2.9 ± 0.3
266.6 ± 0.3		0.7 ± 0.1
295.8 ± 0.3		0.17 ± 0.03
321.0 ± 0.8		0.08 ± 0.03
333.2 ± 0.3		16 ± 1.2
388.2 ± 0.3		70 ± 5

4. Conversion Electrons

The conversion electrons associated with the α decay of Cf^{249} have been analyzed with a semiconductor detector and the spectrum is shown in Fig. 26. The source for the measurement was the same as used for α-particle analysis. In the spectrum the low-energy electron lines are not well separated because of the high background. A Cm^{243} source was used as standard for the electron energy and intensity determination. The intensities of the Cm^{243} electron lines (in terms of electrons per α-particle) were obtained by normalizing the γ-ray and electron intensities[54] of the transitions from the 5/2+(622↑) band in Pu^{239} to the total alpha intensity[26] to that band. The efficiency (excluding the geometry), thus determined was (70 ± 10%). The electron intnesities and the conversion coefficients determined from this measurement are given in Table XXV. It should be noticed that the K- and L- conversion coefficients of the 388.2- and 333.2-keV transitions are a factor of 2 higher than the theoretical values[25] for fast El transitions.

5. Decay Scheme

The decay scheme of Cf^{249} formulated by Stephens et al. has been discussed in Ref. 26. The single-particle state assignments to the levels of Cm^{245} have been confirmed in the present work. In the following paragraphs the reasons for these assignments are discussed.

The energies of the levels of the Cm^{245} ground state band indicate the value of the K quantum number is (3.7 ± 0.2). The most reasonable K=7/2 Nilsson state for the neutron number 151 is 7/2+(624↓). This state has also been identified in the α decay of Cm^{245} at 172 keV above the ground state of Pu^{241}. As will be seen later, the assignment is consistent with the de-excitations of the higher-energy bands to the levels of the ground state band.

The levels at 252.7, 295.8, 350, and 418 keV seem to constitute a rotational band. The α group populating the 418-keV level was not observed

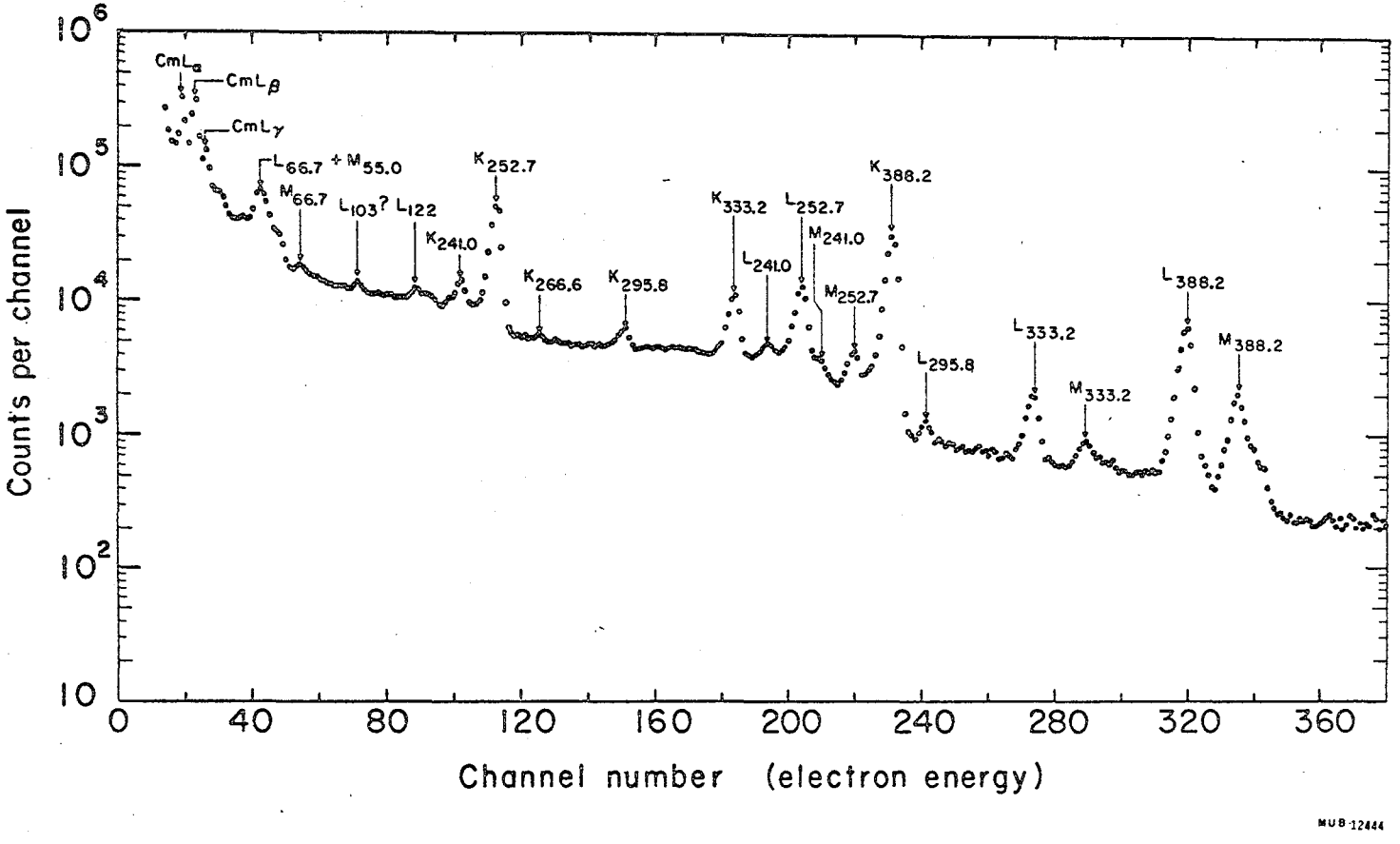

Fig. 26. Cf^{249} conversion-electron spectrum measured with a cooled Si(Li) detector.

Table XXV. Conversion electrons of Cf^{249}.

Transition energy (keV)	Conversion shell	Electron intensity (%)	Conversion coefficient	Multipolarity
241.0	K	0.51 ± 0.08	1.8 ± 0.4	M1
	L	$(1.0 \pm 0.2)\times10^{-2}$	0.33± 0.08	
252.7	K	4.3 ± 0.7	1.5 ± 0.3	M1
	L	1.0 ± 0.2	0.34± 0.07	
	M	0.18 ± 0.04	0.06± 0.02	
266.6	K	$(7.0 \pm 1.3)\times10^{-2}$	0.1 ± 0.02	anomalous E1
295.8	K	0.17 ± 0.03	1.0 ± 0.2	M1
	L	$\approx 3 \times 10^{-2}$	≈ 0.2	
333.2	K	0.7 ± 0.1	$(4.4\pm0.8)\times10^{-2}$	anomalous E1
	L	0.16 ± 0.03	$(1.0\pm0.2)\times10^{-2}$	f ≈ 1
	M+N+O	$(5.5 \pm 1.0)\times10^{-2}$	$(4\pm1)\times10^{-3}$	
388.2	K	2.9 ± 0.4	$(4.0\pm0.7)\times10^{-2}$	anomalous E1
	L	0.7 ± 0.1	$(9\pm2)\times10^{-3}$	f ≈ 1
	M+N+O	0.27 ± 0.05	$(4\pm1)\times10^{-3}$	

in our experiments. The α group was identified by Stephens et al.[53] and the energy of the 418-keV level in our decay scheme was obtained from the energy difference between this level and the 252.7-keV level, measured by these authors. The value of the K quantum number calculated from the level spacings of this band comes out to be (2.8 ± 0.3). The conversion coefficients of the transitions from these levels to the ground state band are found to be in agreement with the theoretical values for M1 transitions. Hence the parity of the band must be positive. The only Nilsson orbital with $K\pi=5/2+$ available in this energy region is $5/2+(622\uparrow)$ state, the ground state of Cm^{243}. This assignment is consistent with the fact that the electron-capture decay of Bk^{245} populates mainly the 252.7-keV state.

The favored α group of Cf^{249} populates the 388.2-keV level of Cm^{245}. The multipolarities of the transitions de-exciting this state are found to be E1 with anomalously high conversion coefficients. This fixes the parity of the level as odd. The level spacings between the members of the band indicate that the value of the K quantum number should be either 7/2 or 9/2. As the 388.2-keV level decays to the I=11/2 member of the ground state band by an E1 transition (determined by the conversion coefficient), the spin of the state must be 9/2. The most reasonable choice of $K\pi=9/2-$ Nilsson state is the $9/2-(734\uparrow)$. The assignment is further supported by the fact that the 388.2-keV level decays to the 7/2+ member but not to the 5/2+ member of the $5/2+(622\uparrow)$ band. The relative alpha abundances calculated with Eq. (4) for the rotational members of the $K\pi=9/2-$ favored band are given in Table XXVI. It should be noticed that the observed intensity of the third member of the band is lower than the calculated value. This pattern has also been observed[58] in the α decay of other odd-mass nuclei, and in the case of U^{233} decay it has been explained[55] in terms of the interaction of the nuclear quadrupole moment with the outgoing alpha wave. The small spacings between the members of this band are attributed to the Coriolis mixing of this band with other odd-parity bands.

Table XXVI. Alpha population to the levels of Cm^{245}.

(i) Final state = 7/2+(624↓).

Level (keV)	Iπ	Observed intensity (%)	Theoretical value[a] of relative intensity (%)			
			L=1	L=3	L=5	Σ
0	7/2+	2.4	0.94	1.45	0.011	2.4
55.0	9/2+	1.3	0.114	1.184	0.029	1.33
121.7	11/2+	0.4	0.005	0.366	0.028	0.4
203	13/2+	0.06	-	0.046	0.011	0.057

[a]The hindrance factors for L=1, L=3, and L=5 alpha waves are found to be 1.4×10^4, 2.8×10^3, and 5.4×10^4 respectively.

(ii) Final state = 5/2+(622↑).

Level (keV)	Iπ	Observed intensity (%)	Theoretical value[a] of relative intensity (%)		
			L=3	L=5	Σ
252.7	5/2+	3.4	3.32	0.15	3.47
295.8	7/2+	3.2	2.66	0.49	3.15
350	9/2+	1.4	0.88	0.52	1.4
418	11/2+	≈ 0.5	0.15	0.28	0.43

[a]The hindrance factors for L=3 and L=5 alpha waves are found to be 70 and 177 respectively.

(iii) Final state = 9/2-(734↑).

Level (keV)	Iπ	Observed intensity (%)	Theoretical value[a] of relative intensity (%)			
			L=0	L=2	L=4	Σ
388.2	9/2-	82.6	69.7	12.7	0.2	82.6
443	11/2-	4.8	-	4.34	0.27	4.6
508	13/2-	0.3	-	0.36	0.13	0.49
580	15/2-	≈ 0.02	-	-	0.023	0.023

[a]The hindrance factors for L=0, L=2, and L=4 alpha waves are 1.0, 3.0, and 47 respectively and are obtained from the adjacent even-even nuclei.

(iv) Final state assumed to be 7/2-(743↑).

Level (keV)	Iπ	Observed intensity (%) × 10^2	Theoretical value[a] of relative intensity (%) × 10^2		
			L=2	L=4	Σ
644	7/2-	11	10.1	0.85	11
703	9/2-	4.4	3.2	1.0	4.2
775	11/2-	1.0	0.36	0.49	0.85
857	13/2-	0.2	0.02	0.08	0.1

[a]The hindrance factors for L=2 and L=4 alpha waves are found to be 29 and 74 respectively.

(v) Final state assumed to be 7/2+(613↑).

Level (keV)	Iπ	Observed intensity (%) × 10^2	Theoretical value[a] of relative intensity (%) × 10^2		
			L=1	L=3	Σ
644	7/2+	11	5.5	5.5	11
703	9/2+	4.4	0.57	3.83	4.4
775	11/2+	1.0	0.02	0.94	0.96
857	13/2+	0.2	-	0.1	0.1

[a]The hindrance factors for L=1 and L=3 alpha waves are found to be 85 and 27 respectively.

The data on the anomalous E1 transitions, available in the heavy-element region have been analyzed by Asaro et al.[56] The authors plotted the logarithms of the anomaly factors "f" [$f = (\alpha_{exp.} - \alpha_{theo.})/\alpha_{theo.}$] against the logarithms of the retardation factors ($t_{exp.}/t_{theo.\ single-particle}$) and found that most of the points for odd-proton nuclei fell on a straight line. A similar correlation might be expected for the odd-neutron nuclei, but because of the lack of sufficient data it could not be verified. For the present calculations, a straight line was drawn parallel to the odd-proton line and passing through the Pu^{239} point. The retardation factor for the 388.2-keV γ-ray was determined from this line and was found to be $\approx 2 \times 10^6$. The half-life of the 388.2-keV level, calculated with the above retardation factor and the theoretical value of single-particle half-life, comes out to be $\approx 1 \times 10^{-9}$ sec.

A new rotational band at 644 keV (see Fig. 27) has been observed and its four members have been identified. The value of the K quantum number, calculated with Eq. (3), comes out to be (3.5 ± 0.3). In the γ-α coincidence experiments a 644-keV γ-ray was identified. The α-γ coincidence experiments show that only $\approx$ 20% of the alpha population to this band de-excites to the ground state band and the rest depopulates to the 5/2+(622↑) and 9/2-(734↑) bands. In the present studies we could not distinguish whether the 644-keV level decays to the 252.7-keV state or to 388.2-keV state or to both. This is because of the fact that the α-particles in coincidence with the transitions to the 5/2+(622↑) and to the 9/2-(734↑) bands will also be in coincidence with the γ-rays de-exciting these levels themselves.

In the Nilsson diagram (Fig. 9) two K=7/2 orbitals are available in this energy region: the 7/2-(743↑) hole state and the 7/2+(613↑) particle state. From the α intensity pattern (see Table XXVI) and the excitation energy, both are equally suitable. In absence of the information about the multipolarities of the transitions de-exciting this band, it is not possible

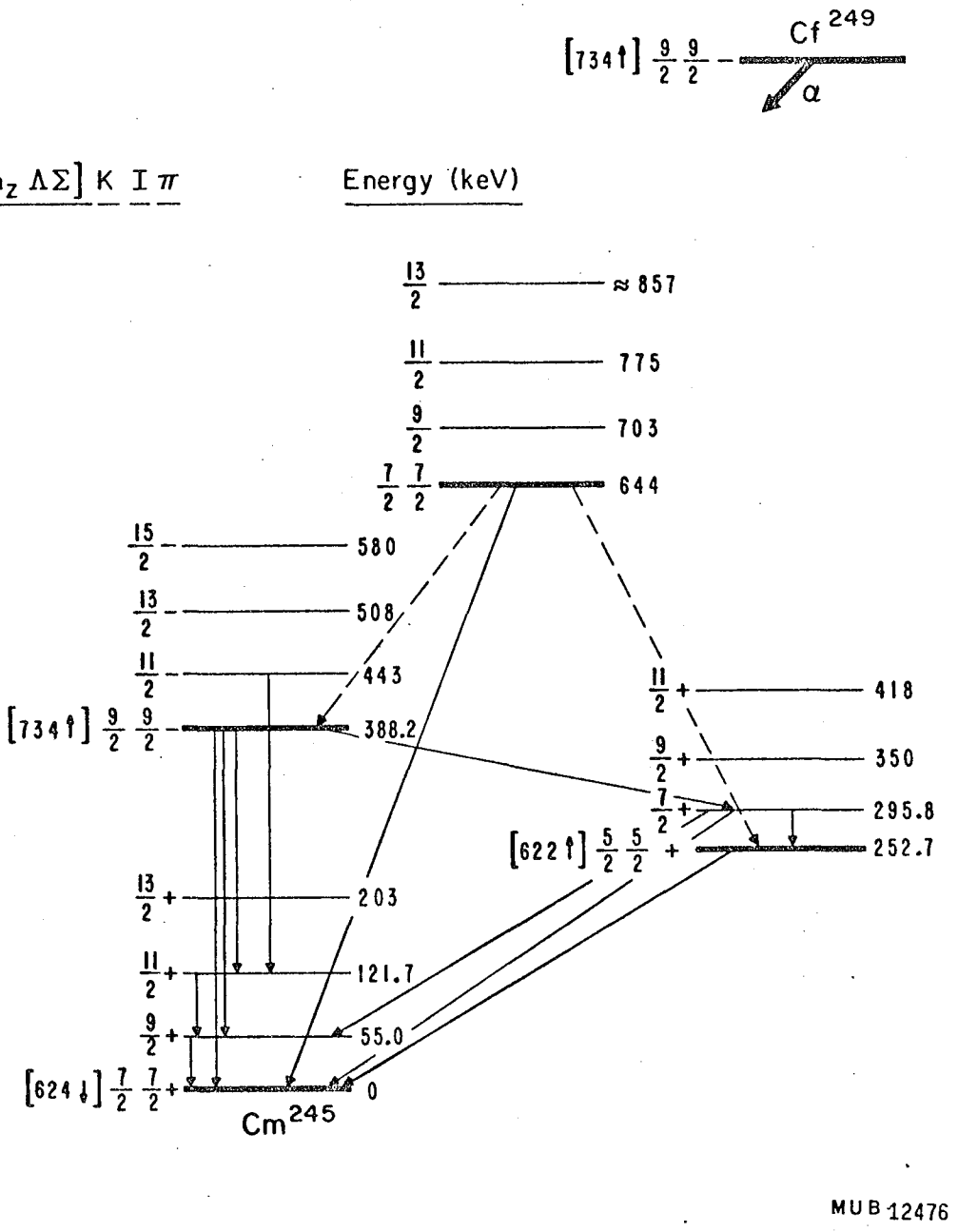

Fig. 27. Decay scheme of Cf^{249}.

to make a definite assignment. However, the assignment of the band as 7/2-(743↑) is preferred for the reason that if it were a 7/2+(613↑) state, we would have expected a stronger transition to the ground state. The relative alpha populations to the members of both bands are calculated and these are given in Tables XXVI.D. and XXVI.E.

F. Alpha Decay of Fm^{255}

The isotope Fm^{255}, the discovery of which constituted the discovery of element 100, was first identified by Ghiorso et al.[57] in the heavy-element samples collected from the thermonuclear explosion "Mike". Various measurements[20] of the half life and the alpha spectrum of this isotope have been made. The most recent and thorough investigation of Fm^{255} has been made by Asaro, Bjørnholm, and Perlman,[58] using magnetic spectrographs for alpha and electron-spectra measurements. On the basis of their results these authors have formulated a decay scheme (shown in Fig. 28), in which four levels are identified as Nilsson states. The level spacings and the alpha intensity pattern to the rotational members of the bands built on 7/2+(613↑) and 1/2+(620↑) states justify their assignments. The levels at 426 keV and 546 keV were elucidated from α-γ and γ-γ coincidence measurements and were given tentative Nilsson state assignments of 9/2+(615↓) and 11/2-(725↑) respectively. The 546-keV level was found to receive high alpha population and has a hindrance factor of 25. Later, Poggenburg's[8] calculations showed that this state should have an alpha decay hindrance factor about two orders of magnitude higher. Because of this disagreement a reinvestigation of alpha groups populating the higher-lying states of Cf^{251} was undertaken.

1. Gamma Rays

In order to establish the existence of the two states mentioned earlier, it was necessary to identify the 120- and 320-keV γ-rays and show that these

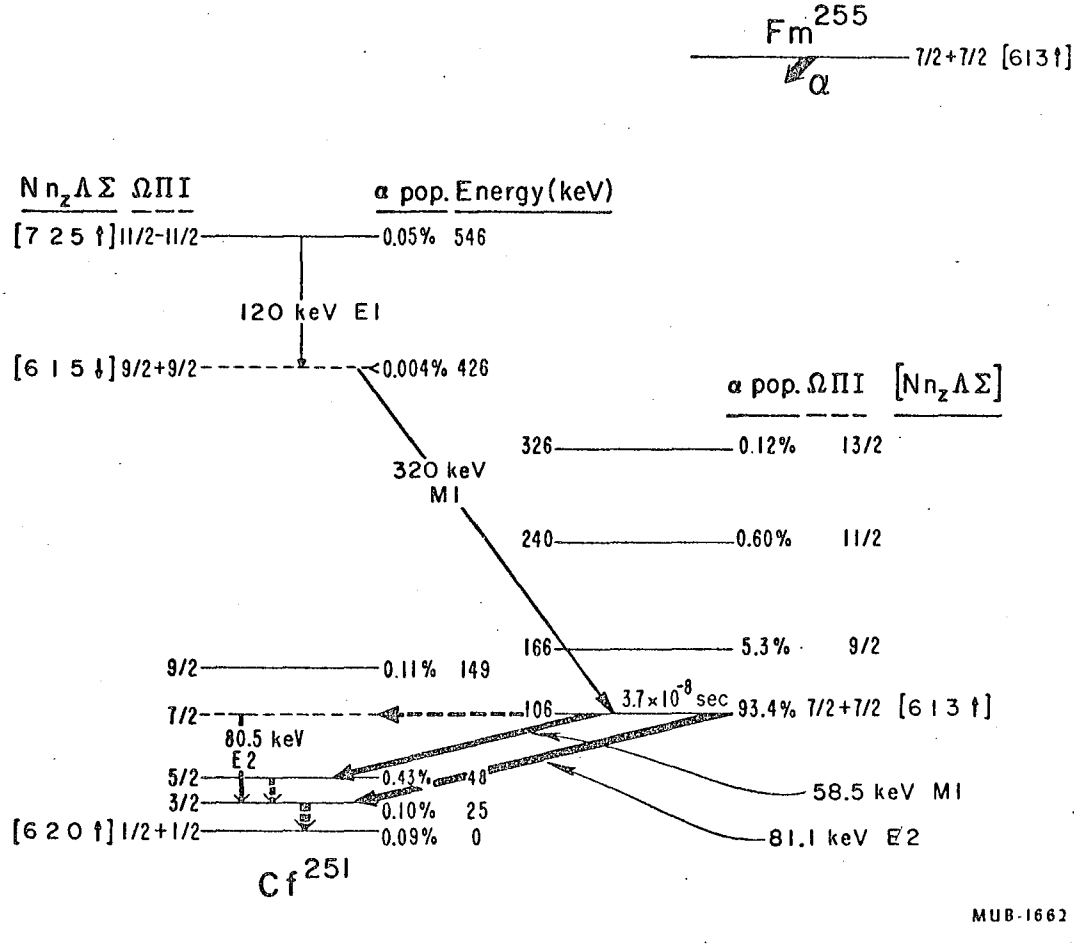

Fig. 28. Fm^{255} decay scheme (from Ref. 58).

are in coincidence. With the sample strength of about 4×10^6 dis/min, it was possible to investigate the low-energy γ-rays with a high-resolution germanium detector. The spectrum taken with a $3 \times 1 \times 0.3$ cm detector is shown in Fig. 29(a). The 131-keV γ-ray in the spectrum is due to an impurity, and disappears in γ-α coincidence experiments. The intensity of the Cf $K_{\beta_2'}$ x-ray is about twice the value expected from theory.[59] This may be due to the presence of a 133-keV γ-ray, which is the transition expected between the I=11/2 and I=7/2 states of the favored band. The energies and intensities of the observed γ-rays are given in Table XXVII. The intensities are normalized to the intensity of the 81.2-keV gamma ray for which the value of (1.1 ± 0.2%) has been used.[58]

The sample was then used for a γ-γ coincidence measurement. The gamma spectrum [as detected by the $3 \times 1 \times 0.3$ cm Ge(Li) detector] was measured in coincidence with 280- to 350-keV γ-rays, as detected with a NaI(Tl) detector. The coincidence spectrum is shown in Fig. 29(b). Californium K x-rays are observed because the high-lying states decay to the 178-keV level (see the decay scheme), which then de-excites to the ground level by an M1 transition. Platinum K x-rays are caused by the source backing which was a 0.002-in. platinum plate. The absence of the 120-keV γ-ray in the singles and coincidence spectra indicate that there is some discrepancy in the previous γ-γ coincidence measurement, and hence the Nilsson quantum number assignments to the 426-keV and 546-keV levels are not justified.

2. α-γ and γ-α Coincidence Measurements

Chemically purified Fm^{255} ($\approx 3 \times 10^6$ dis/min) was electroplated on a 0.002-in. nickel plate for these measurements. The γ-rays were detected with a NaI(Tl) crystal and the α-particles with a semiconductor detector at a geometry of 4%. The α-γ and γ-α coincidence experiments were performed simultaneously, and both alpha and gamma pulses were stabilized. The α-singles spectrum, which was taken to give the source strength and the

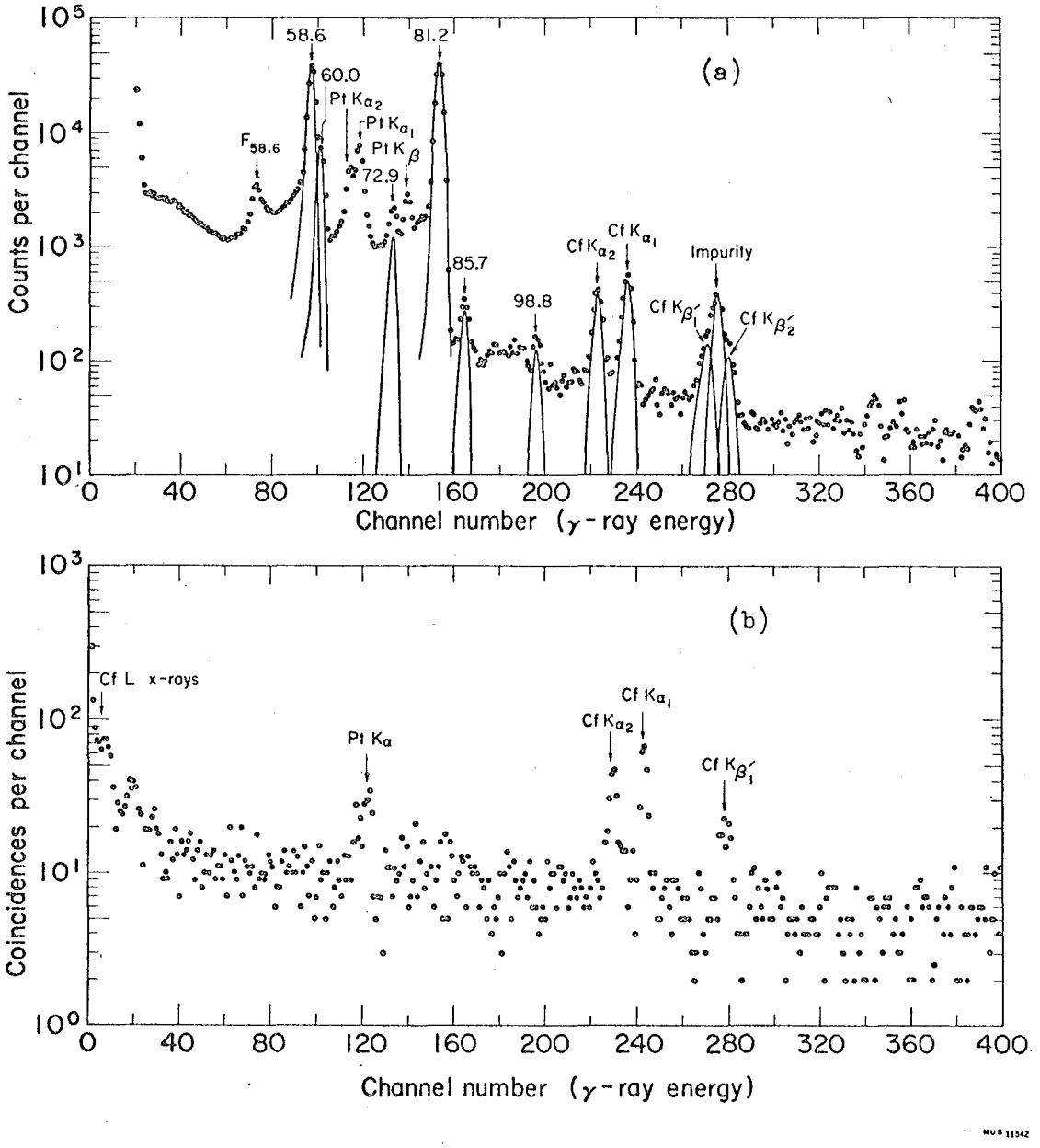

Fig. 29a,b. γ-ray spectra of Fm^{255}.
(a) Low-energy portion of γ-singles spectrum.
(b) Low-energy γ-rays in coincidence with 280- to 350-keV γ-rays.

Table XXVII. Gamma rays of Fm^{255}.

Energy (keV)		Intensity (photons per 10^2 Fm^{255} α-particles)
58.6 ± 0.2		0.75 ± 0.08
60.0 ± 0.2		0.15 ± 0.02
72.9 ± 0.2		$(3.0 \pm 0.5) \times 10^{-2}$
81.2 ± 0.2		1.1 (norm)
85.7 ± 0.2		$(6 \pm 2) \times 10^{-3}$
109.4 ± 0.2	(Cf $K\alpha_2$)	$(2.0 \pm 0.2) \times 10^{-2}$
114.7 ± 0.2	(Cf $K\alpha_1$)	$(3.0 \pm 0.3) \times 10^{-2}$
128.5 ± 0.4	(Cf $K\beta'_1$)	$\approx 1.4 \times 10^{-2}$
133.0 ± 0.5	(Cf $K\beta'_2$) + (240 → 107 transition)	$\approx 1 \times 10^{-2}$
178 ± 1		$(7 \pm 2) \times 10^{-3}$
≈ 185		$\approx 2 \times 10^{-3}$
≈ 336		$\approx 3 \times 10^{-3}$
≈ 372		$\approx 5 \times 10^{-3}$
≈ 437		$\approx 3 \times 10^{-3}$
≈ 493		$\approx 3 \times 10^{-3}$

energies and intensities of the intense alpha groups, is shown in Fig. 30(c). The alpha spectra measured in coincidence with (i) γ-rays greater than 82 keV and (ii) γ-rays greater than 35 keV (to exclude Cf L x-rays) are shown in Fig. 31. In the first experiment the gate was selected so as to cut down the intensity of the alpha groups populating the rotational members of the K=7/2 band and thus identify the high-lying states. The purpose of the second experiment was to observe the alpha groups populating higher members of the favored band. Both these spectra are complex and the resolution of the peaks has been achieved by using the combined information from the three alpha spectra. The broadening of the peaks at the higher energy side is due to the intense conversion electrons of 58.6- and 81.2-keV transitions, which are in coincidence with the favored alpha groups. All alpha groups except α_{493} and α_{520} seem to be definite; the α_{520} may be the 17/2 member of the favored band. The results of these spectra along with the hindrance factors are given in Table XXVIII. The α-particle energies are measured relative to the Es^{253} α_0 group, which was taken as 6.640 MeV.

The γ-α coincidence spectra were taken in order to identify the transitions de-exciting the higher-lying states. The γ-ray spectra in coincidence with (i) all Em^{255} alpha groups and (ii) 6.49- to 6.76-MeV alpha particles are shown in Fig. 30. Although the structure is complex, four high-energy γ-rays have been resolved. In spectrum (b) the ratio of the K x-ray intensity to the total intensity of these γ-rays is found to be 0.7, which is in excellent agreement with the theoretical value for M1 transitions. In Fig. (a) a γ-ray of energy (178 ± 1) keV is observed, and most likely there is another γ-ray of 185 keV energy. The K x-ray intensity relative to the intensity of the (178+185) keV γ-rays is (6 ± 1), which suggests that these transitions are pure M1 in character. The results of these spectra are included in Table XXVII. The 178-keV γ-ray was also observed with a 3 × 2 × 0.8 cm Ge(Li) detector.

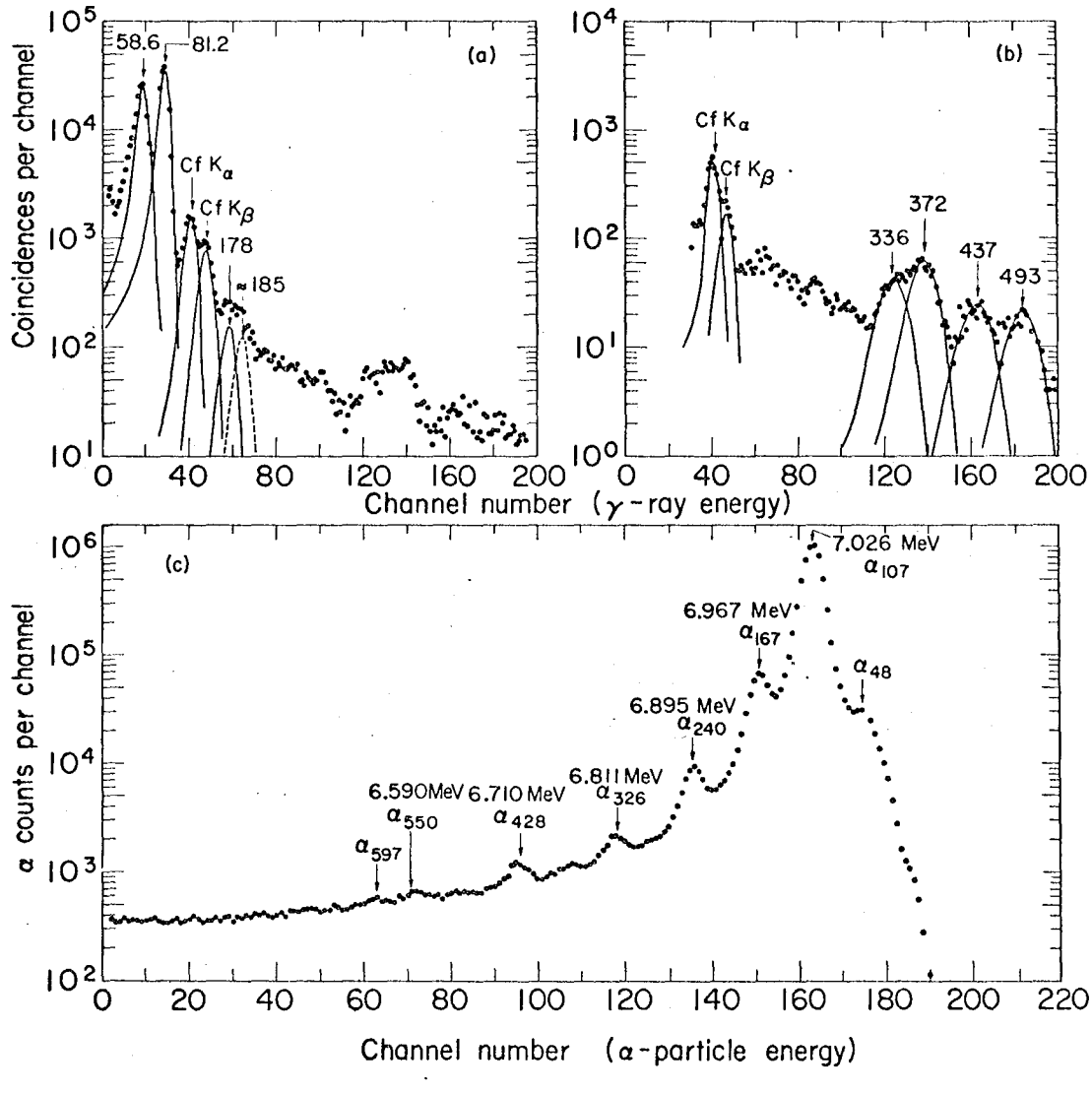

Fig. 30a,b,c. γ-ray and α-particle spectra of Fm^{255}.
(a) γ-rays in coincidence with all Fm^{255} α-particles.
(b) γ-rays in coincidence with 6.49- to 6.76-MeV α-particles.
(c) α-singles spectrum.

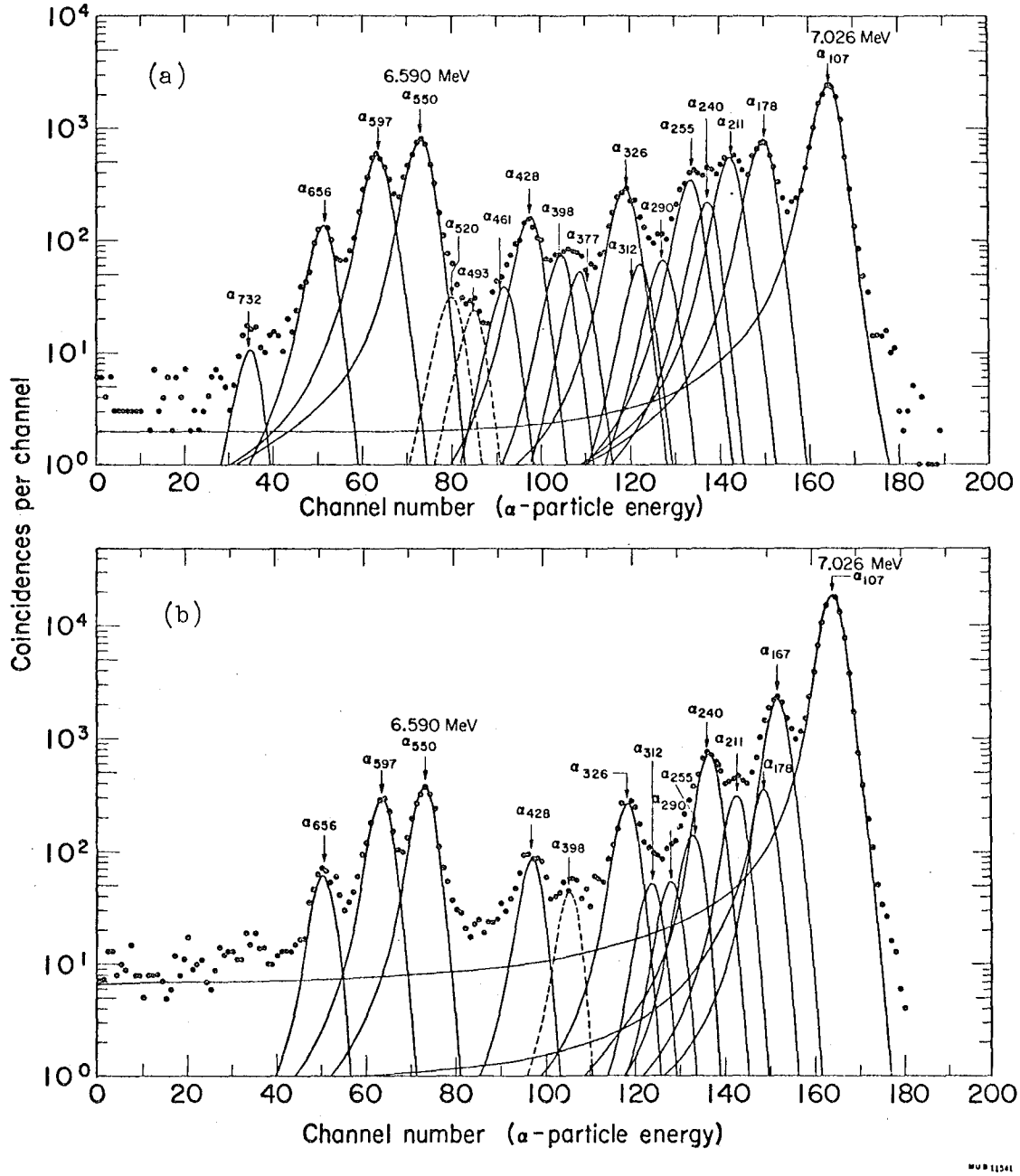

Fig. 31a,b. Fm^{255} α-γ coincidence spectra.
(a) α-particles in coincidence with γ-rays > 82 keV.
(b) α-particles in coincidence with γ-rays > 35 keV.

Table XXVIII. Fm^{255} alpha groups measured in the present work.

α-particle energy (MeV)	Excited state energy (keV)	Intensity (%)	Hindrance factor[22]
7.026 ± 0.003	107	93.3 ± 0.3	1.2
6.967 ± 0.003	167	5.2 ± 0.1	12.4
6.956 ± 0.004	178	$(2.4 \pm 0.4) \times 10^{-2}$	2.4×10^{3}
6.923 ± 0.004	211	$(1.7 \pm 0.4) \times 10^{-2}$	2.5×10^{3}
6.895 ± 0.004	240	0.60± 0.03	53
6.880 ± 0.004	255	$(1.3 \pm 0.4) \times 10^{-2}$	2.1×10^{3}
6.845 ± 0.007	290	$\approx 2 \times 10^{-3}$	9.7×10^{3}
6.824 ± 0.007	312	$\approx 2 \times 10^{-3}$	7.6×10^{3}
6.811 ± 0.004	326	0.11± 0.02	1.2×10^{2}
≈6.760	≈377	$(1.2 \pm 0.5) \times 10^{-3}$	6.8×10^{3}
6.739 ± 0.007	398	$\approx 2 \times 10^{-3}$	3.3×10^{3}
6.710 ± 0.004	428	$(4 \pm 1) \times 10^{-2}$	1.2×10^{2}
≈6.677	≈461	$\approx 6 \times 10^{-4}$	5.8×10^{3}
≈6.646 ?	≈493 ?	$\approx 5 \times 10^{-4}$	5×10^{3}
≈6.619 ?	≈520 ?	$\approx 8 \times 10^{-4}$	2.4×10^{3}
6.590 ± 0.004	550	$(2.0 \pm 0.4) \times 10^{-2}$	69
6.544 ± 0.004	597	$(1.5 \pm 0.3) \times 10^{-2}$	56
6.486 ± 0.004	656	$(3.5 \pm 0.8) \times 10^{-3}$	127
6.411 ± 0.006	732	$(3 \pm 1) \times 10^{-4}$	650

3. Decay Scheme

The energies and intensities of the alpha groups populating the rotational members of the K=1/2 and K=7/2 bands are more accurately measured with the magnetic spectrograph.[58] The level spacings and the abundances to these states are consistent with the assignment of the Nilsson quantum numbers. The level at 428 keV, observed in the present experiments, has the right energy and alpha intensity for the I=15/2 member of the favored band. In Fig. 31(a) the alpha population to the 240-keV state is higher than that expected for the I=11/2 member of the K=7/2 band. The additional intensity of $\approx 1 \times 10^{-2}\%$ is, presumably, due to an alpha transition to the I=11/2 member of K=1/2 band, which de-excites through γ-rays > 82 keV. This is further supported by the identification of a 290-keV state, the 13/2 member of this band. The estimated alpha intensity to this state is given in Table XXVIII and is in agreement with the theoretical prediction.[8]

As there is only one prominent γ-ray of energy 178 keV and there is a fairly intense alpha group 178 keV lower in energy than the Fm^{255} α_0 group, this suggests the possibility of the 178-keV state being the base member of a rotational band. Since this state de-excites to the ground state through an M1 transition it must have spin and parity 1/2+ or 3/2+. The high alpha-decay hindrance factor to this state suggests that the intrinsic spin of the state should be opposite to that of the ground state of the parent nucleus.[60,61] The only state in the Nilsson diagram close in energy to the 7/2+(613↑) state and satisfying these requirements is 3/2+(622↓). The levels at 211, 255, and 312 keV fit well as rotational members of this band. The levels at 377 and 461 keV may also be members of the band. The energies of the rotational members, calculated from Eq. (3), with a rotational constant of 6.4 keV are given in Table XXIX.A. The relative alpha intensities, calculated from Eq. (4) are also compared with the observed intensities in this table. It should be noticed that

Table XXIX. Energy spacings and alpha population of the Cf^{251} levels.

A. Final state = 3/2+(622↓).

Iπ	Excited state energy (keV)		Alpha intensity (%) × 10^2			
			Exp.	Cal.[b]		
	Exp.	Cal.[a]		L=2	L=4	Σ
3/2+	178	178	2.4	2.24	0.16	2.4
5/2+	211	210	1.7	1.10	0.60	1.7
7/2+	255	255	1.3	0.28	0.71	0.99
9/2+	312	312	≈ 0.2	0.035	0.39	0.42
11/2+	≈ 377	383	0.12	0.002	0.11	0.11

[a]The energies are calculated from Eq. (3) with $\hbar^2/2\Im$ = 6.4 keV.

[b]The relative intensities are calculated from Eq. (4) and the hindrance factors for L=2 and L=4 alpha waves are found to be 1.3×10^3 and 1.2×10^3 respectively.

B. Final state = 5/2+(622↑).

Iπ	Excited state energy (keV)		Alpha intensity (%) × 10^2			
			Exp.	Cal.[b]		
	Exp.	Cal.[a]		L=2	L=4	Σ
5/2+	550	550	2.0	1.96	0.04	2.0
7/2+	597	597	1.5	1.15	0.11	1.26
9/2+	656	657	0.35	0.25	0.10	0.35
11/2+	732	731	0.03	0.015	0.037	0.05

[a]The energies are calculated from Eq. (3) with $\hbar^2/2\Im$ = 6.7 keV

[b]The relative intensities are calculated from Eq. (4) and the hindrance factors for L=2 and L=4 alpha waves are found to be 29 and 49 respectively.

the experimental intensities to the 211- and 255-keV levels are somewhat higher than the calculated values. This can be attributed to the Coriolis mixing[7] of this band with the 1/2+(620↑) band. The hindrance factors of the alpha groups populating the I=3/2 and the I=5/2 members of the ground band are known to be 2.5×10^3 and 4.7×10^2 respectively.[58] The theoretical calculations indicate that the alpha abundance to the 7/2+ member of this band should be comparable to the alpha intensity to the 5/2+ level. The above values of the hindrance factors indicate that the Coriolis interaction of the 3/2+(622↓) band with the ground state band will enhance the alpha intensities to the I=5/2 and I=7/2 member of the K=3/2 band, significantly. This is consistent with the experimental result. As the energies of the levels and the alpha abundance to them are not known accurately, it is not possible to make any detailed calculations.

The intensity pattern of the alpha groups below 6.950 MeV clearly indicates that the levels at 550, 597, 656 and 732 keV belong to a rotational band built on the 550-keV intrinsic state. The only values of K quantum number consistent with the energy spacings of these levels are 5/2 and 7/2. In the γ-α coincidence experiment, these states were observed to decay to the members of K=7/2 and K=3/2 bands by M1 transitions. To do so the 550-keV level should be the base member of Kπ=5/2+ band. The only Kπ=5/2+ single-particle state in this vicinity is 5/2+(622↑), the ground state of Cm^{243}. The small hindrance factors of the alpha transitions to these states further support the assignment of the 5/2+(622↑) state. The energies of the members of this band, calculated from Eq. (3), with a rotational constant of 6.7 keV is given in Table XXIX.B. Also given in this table are the relative alpha abundances to these states calculated from Eq. (4). In the table the observed alpha intensity to the 597-keV member of the band is slightly higher than the calculated value. This could be explained by assuming Coriolis interaction of this level with the favored band. The alpha intensities to the levels of K=5/2 bands are not known accurately enough to make any quantitative estimate of the mixing.

The high excitation energy of the $K\pi = 5/2+$ band makes one suspect that the band might have some vibrational character. The low hindrance factors of the alpha groups to this band indicate that the vibrational band must be built on the favored band ($K\pi=7/2+$). The value of the K quantum number of the 550-keV band rules out any possibility of its being a beta- (00+) or an octupole (01-) vibrational band. The alpha transition to the gamma-vibrational band is usually more hindered (hindrance factor $\approx$ 200) and has not been observed in most of the nuclei.

The energy-level diagram of Cf^{241}, constructed on the basis of the previous measurements and the present work, is shown in Fig. 32. The 398-keV level, identified in the α-γ coincidence experiments, does not fit as a rotational member of any of the bands discussed so far. This indicates that this level belongs to a new band, perhaps, as a base member. The Nilsson states (Fig. 9) expected in this region are 11/2-(725↑) 9/2-(615↓), and 9/2-(734↑). As the states are expected to receive comparable alpha population and the decay properties of the 398-keV level is not known, it is not possible to make any assignment.

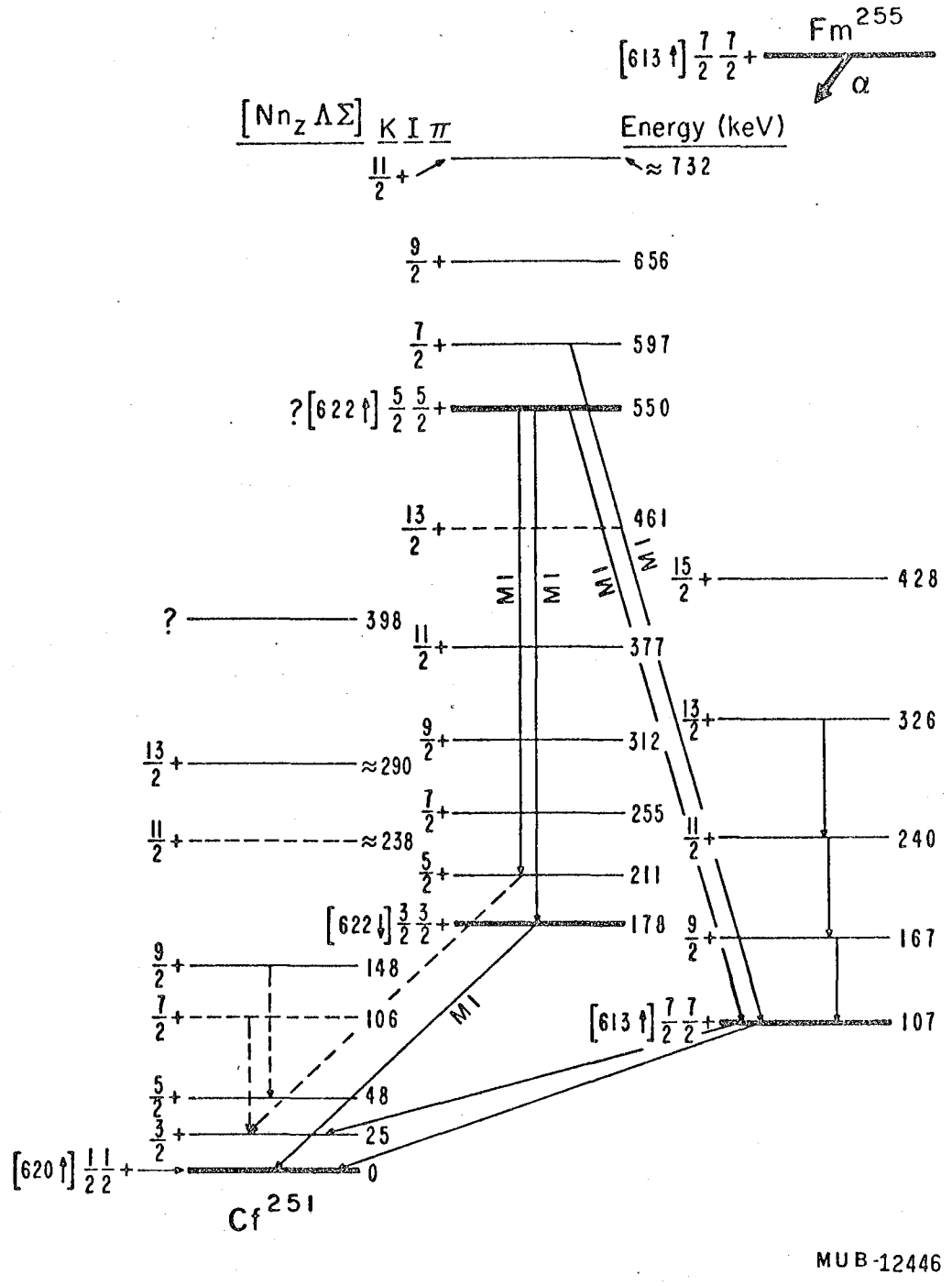

Fig. 32. Decay scheme of Fm^{255}.

V. THEORY AND DISCUSSION

In this chapter the theories used for the interpretation of our results are briefly discussed. This description is provided to give a background for the use of certain terms in the text.

1. Level Energies

It has been concluded from the measurements of quadrupole moments, enhanced electric quadrupole transitions, and the energy dependence of the rotational levels on I(I+1) term that the nuclei in certain mass regions are permanently deformed. In the heavy-element region the permanent deformation starts at a mass number of about 225. These deformed nuclei have been found to have a prolate spheroidal shape which has also been explained by theory.[2,62] The nuclei can rotate in space without changing the shape or the internal configuration. The rotational energy of the nucleus is given by the equation[4]

$$E_I = E_0 + \frac{\hbar^2}{2\Im}\left[I(I+1) + a(-)^{I+1/2}\,(I+1/2)\right] \quad . \qquad (5)$$

In the above equation E_0 is a constant depending on the intrinisc state, $\Im$ represents the effective moment of inertia of the nucleus about an axis of rotation perpendicular to the nuclear symmetry axis, I is the nuclear angular momentum, and K is the projection of I on the nuclear symmetry axis. The second term has non-zero value only for K=1/2 bands and the constant "a" is called a decoupling parameter.

In odd-mass nuclei there is an unpaired nucleon outside the spheroidal core. Nilsson[3] has calculated the eigenvalues and eigenfunctions of the single nucleon in an axially symmetric non-central potential. In the deformed nuclear potential the (2j+1) fold degeneracy of the j^{th} state of the shell model[63] is removed and each state splits into (2j+1)/2 Nilsson states, which are doubly degenerate. In the Nilsson diagrams (Figs. 9 and

16) the intrinsic energies are plotted against the nuclear deformations for each state. Each Nilsson state is characterized by a new set of "asymptotic" quantum numbers which are "good" only in the limit of strong deformation. In addition to Ω (the projection of the particle angular momentum on the nuclear symmetry axis) and π (the parity), these quantum numbers include: N, the total oscillator quantum number; n_z, the number of the oscillator quanta long the symmetry axis; Λ, the component of the total orbital angular momentum along the symmetry axis; and Σ, the component of the intrinsic spin "s" on the nuclear symmetry axis which is limited to the values of $\pm$ 1/2 only.

The Nilsson diagrams have been found to predict correctly the spins and parities of the ground states and the low-lying states of the odd-mass deformed nuclei. The level order of these states were slightly modified by Mang, Poggenburg, and Rasmussen[64] by the introduction of a parity force correlation.

The total rotaional energy, for a general case, can be expressed in a power series in I(I+1). The following equation has been derived by Bohr and Mottelson:[65]

$$E(K,I) = AI(I+1) + BI^2(I+1)^2 + \ldots\ldots\ldots$$
$$(-)^{I+1/2}\,(I+1/2)\,\{A_1 + B_1 I(I+1) + \ldots\ldots\} \quad \text{for} \quad K=1/2$$
$$(-)^{3/2+I}\,(I-1/2)(I+1/2)(I+3/2)\,\{A_3 + B_3 I(I+1)+\ldots\} \text{for } K=3/2 \qquad (6)$$

Similar terms are added for higher values of K. It should be observed that Eq. (5) is a simplified form of Eq. (6). Formula (6) is supposed to take case of various kinds of interactions in the nuclei. The constants for the rotational bands with at least four accurately known level energies are calculated with Eq. (6) and these are listed in Table XXX.

Table XXX. Values of constants A, B, A_{2K}, and B_{2K}.

Nuclide	Band	Value of the constant			
	$K\pi[Nn_z\Delta\Sigma]$	A(keV)	B(eV)	A_{2K}(keV)	B_{2K}(eV)
U^{235}	1/2+[631↓]	6.044	-2.21	-1.74	+2.21
	3/2+[631↑]	6.70	b	-6.67×10^{-3}	b
Pu^{239}[a]	1/2+[631↓]	6.27	-1.41	-3.66	+4.60
Th^{229}	5/2+[633↓]	6.06	-0.25	-0.04×10^{-3}	b

[a] Energies were taken from Ref. 54.

[b] Insufficient levels to determine this parameter.

The constants for K=1/2 bands are determined graphically and those for other bands are obtained from numerical calculations. For the K=1/2 band the quantity $[E(I)-E(I-1)]/2I$ is plotted against the quantity I^2, when two straight lines are obtained. The line connecting the points with the value of (I+1/2) as even has a slope of $(2B+B_1)$ and an intercept on the Y axis of $A+(A_1+B_1/2)$. The slope and intercept of the line passing through the points with the value of (I+1/2) as odd are $(2B-B_1)$ and $A-(A_1+B_1/2)$ respectively. From the slopes and intercepts of the two lines the constants A, A_1, B, and B_1 are evaluated. The values of the parameters for the 1/2+(631↓) band in U^{235} and Pu^{239} are listed in Table XXX. It should be observed that the value of A_1 (which is proportional to the decoupling parameter "a") for Pu^{239} is a factor of 2 higher than that for U^{235}.

2. Alpha Transition Probabilities

It was observed by Bohr, Fröman, and Motelson[24] that if the odd nucleon remains in the same orbital in the daughter as in the parent during the alpha decay, the alpha decay of the odd-mass nuclei will be identical to that of the even-even nuclei to the ground state of daughter. This type of decay is called "favored α decay" and is characterized by a low hindrance factor (between 1 and 4). This phenomenon has been found very helpful in the identification of single-particle states. In such cases, the alpha reduced transition probabilities to various levels are given by the equation[24]

$$P = P_0(Z,E)/N\sum_L \frac{\left|\langle I_i\ L\ K_i(K_f-K_i)\,|I_i\ L\ I_fK_f\rangle+b_L(-)^{I_f+K_f}\langle I_iL\ K_i(-K_f-K_i)\right.}{(HF_L)_{e-e}}$$

$$\left.\frac{|I_iL\ I_f-K_f\rangle|^2}{}\right. \qquad (7)$$

where $P_0(Z,E)$ is the alpha transition probability expected from simple barrier penetration theory,[23] $(HF_L)_{e-e}$ is the hindrance factor of the alpha

wave of angular momentum L, obtained from the adjacent even-even nuclei; the terms in the brackets are Clebsch-Gordon coefficients; and the subscript i and f refer to the initial and final states. The parameter N usually has a value between 1 and 2, and is determined empirically from known alpha intensities. It can also be calculated from the detailed knowledge of the nuclear wave functions. In Eq. (7) the second term is used only when $L \geq K_i + K_f$.

For alpha decay to the members of unfavored bands the same equation is used with the difference that N and $1/(HF_L)_{e-e}$ of Eq. (7) are replaced by a term C_L. The parameter C_L is determined empirically from known alpha intensities. In formula (7) the α-decay matrix element between the ground state of the parent and a certain band in the daughter is the same for all members of the band for an alpha wave of a given angular momentum. The above equation has been used to analyze the alpha intensities to the members of a certain band into alpha waves of different angular momenta. The hindrance factors of the pure L waves, obtained from these analyses, are given in Chapter IV.

The absolute values of alpha decay rates have been calculated by Poggenburg[8] by using the nuclear wave functions. These calculations are very sensitive to the details of nuclear wave functions and hence are quite helpful in the assignment of single-particle states.

The calculations are carried out by resolving the problem into two parts: (i) the formation of the α-particle from the single-particle orbitals at the nuclear surface, and (ii) the emission of the α-particle through the barrier. The total α decay probability amplitude is obtained by summing up the contributions of various neutrons and protons in specific Nilsson orbitals for the formation of α-particles. The wave functions used for these computations are the Nilsson eigenfunctions[3] modified by pairing force correlation. The penetrability factor $P_\ell(\epsilon)$ of the α-particle emission through the isotropic barrier is calculated by the WKB approximation method, using a Woods-Saxon[66] nuclear potential. In the term $P_\ell(\epsilon)$ the

subscript ℓ denotes the angular momentum of the alpha wave and ϵ represents the energy of the α-particle. The anisotropic part of the barrier is taken into account in a matrix, calculated by the method of Froman.[67] The α decay rates listed in Ref. 8 are obtained by normalizing the calculated intensities to the observed intensity of the Pu^{238} α_o group.

The hindrance factors given in Chapter IV are calculated from the spin-independent theory of Preston.[23] In the alpha decay of odd-mass nuclides, the α-particles carry with them different values of angular momentum, which are determined by the selection rules. The angular momentum of the α-particles slows down the transition probability because of the centrifugal barrier. The centrifugal barrier penetrability can be calculated by introducing in the potential experienced by the α-particle an additional term of the form

$$+ \frac{\hbar^2}{2MR^2} L(L+1) \quad ,$$

where L is the orbital angular momentum of the α-particle, M is the reduced mass of the alpha particle, and R is the radius of the parent nucleus. The penetration probabilities for α-particles of various angular momenta have been calculated by Thomas.[68] For nuclides studied in the present work, the angular momentum changes are relatively small. For such cases, Rasmussen[69] has developed a simple approximation which agrees with the rigorous formula up to L=6:

$$P_L/P_0 = \exp[-2.027\ L(L+1)Z^{-1/2}\ A^{-1/6}] \qquad (8)$$

where P_L and P_0 are the penetration probabilities for alpha particles of angular momenta L and 0, Z and A are the atomic number and mass number of the daughter nucleus, respectively.

The hindrance factors determined for various L waves, in Chapter IV, are multiplied by the penetrability factor P_L/P_0, calculated from the

above equation. These quantities (see Table XXXI) are independent of alpha particle energy and the angular momentum carried by them. Thus the reciprocals of these numbers will be proportional to the alpha-decay matrix elements. It should be noted in Table XXXI that there is a definite correlation between the hindrance factor and the change of the intrinsic spin Σ during the alpha decay.

The low hindrance factors of the alpha groups populating the high-lying states of the daughter nuclei indicate the possibility of some vibrational character in them. The data obtained in our measurements are not accurate enough to make any statement about the mixture of vibrational bands in these states. Recently theoretical calculations have been carried out by Malov and Soloviev,[70] and they obtained admixture of vibrational bands in single-particle states for some nuclides. The calculations are not extended to the nuclides investigated in this work and as such no comparison can be made. However, the calculations suggest that the high-lying levels will have some vibrational character and, most likely, it is the mixing of the β vibrational band in the single-particle state which lowers the alpha-decay hindrance factor.

3. Nuclear Coriolis Interaction

The idea of rotation-particle coupling (also known as Coriolis interaction) was first introduced by Kerman[7] in order to explain the deviation from the simple rotational-energy formula, observed in W^{183}. The details of the calculations as applied to the heavy-element region are discussed by McHarris[71] and Holtz.[72] In this section only a brief description of the essential features of the treatment is given.

The Hamiltonian of the single nucleon in the axially symmetry deformed field after some simplification, becomes

$$\mathcal{H} = \mathcal{H}_0 + \frac{\hbar^2}{2\mathcal{I}_3}(I_3 - j_3)^2 + \frac{\hbar^2}{2\mathcal{I}}(\vec{I}^2 - I_3^2 - j_3^2) + \text{RPC} \quad , \qquad (9)$$

where

$$\mathcal{H}_0 = \mathcal{H}_p + \frac{\hbar^2}{2\mathcal{I}}\vec{j}^2 \quad ,$$

Table XXXI. Hindrance factors for different L alpha waves after removal of centrifugal barrier effect.

Parent nuclide	Ground state of the parent	Nilsson state in the daughter	$\Delta\Sigma$	L	P_L/P_0 [a]	(H.F.) $\times$ P_L/P_0 [b]
Bk^{243}	3/2-(521↑)	5/2-(523↓)	1	2	0.609	305
		5/2+(642↑)	0	1	0.848	113
				3	0.371	25
Bk^{245}	3/2-(521↑)	5/2-(523↓)	1	2	0.609	189
		5/2+(642↑)	0	1	0.848	69
				3	0.371	12
Cf^{249}	9/2-(734↑)	7/2+(624↓)	1	1	0.848	1.2×10^4
				3	0.371	1.0×10^3
				5	0.0837	4.5×10^3
		5/2+(622↑)	0	3	0.371	26
				5	0.0837	15
		7/2-(743↑) ?	0	2	0.609	18
				4	0.191	14
Fm^{255}	7/2+(613↑)	3/2+(622↓)	1	2	0.613	800
				4	0.196	240
		5/2+(622↑)	0	2	0.613	18
				4	0.196	29

[a] The penetrability factors are calculated from Eq. (8).

[b] The hindrance factors are taken from Chapter IV.

$$\text{RPC} = -\frac{\hbar^2}{2\Im}\,(I_+ j_- + I_- j_+) \quad ,$$

where I and j are the nuclear and single-particle angular momenta, $I_\pm$ and $j_\mp$ represent the raising and lowering operators, and subscript 3 denotes the component along the symmetry axis. The solutions of the Hamiltonian $\mathcal{H}_0$ give the Nilsson eigenvalues and Nilsson eigenfunctions. In Eq. (9) the RPC term is usually small and hence neglected. The solution of the Hamiltonian (9) without the RPC term gives the simple rotational-energy formula

$$E = E_0 + \frac{\hbar^2}{2\Im}\,[I(I+1)] \quad . \tag{10}$$

It is obvious from Eq. (9) that in cases where the RPC term is large, formula (10) will be inadequate to fit the experimental energies.

The raising and lowering operators $I_\pm$ have non-zero matrix elements only between states differing by one unit in the K quantum number. The matrix element between the states K and K+1 is given by

$$\langle I\ K\ j\Omega \left| \frac{-\hbar^2}{2\Im}\, I_\pm\, j_\mp \right| I\ K\pm1\ j\ \Omega\pm1\rangle = \frac{\hbar^2}{2\Im}\,[I(I+1)-K(K\pm1)]\langle j\Omega \left| j_\mp \right| j\Omega\pm1\rangle \quad . \tag{11}$$

The term $\langle j\Omega \left| j_\mp \right| j\Omega\pm1\rangle$ in the equation is evaluated with Nilsson wave functions.

The effect of the Coriolis interaction can be calculated by the use of variational method. The Hamiltonian (9) can also be written as

$$\mathcal{H} = \mathcal{H}_K + \mathcal{H}_C \quad , \tag{12}$$

where $\mathcal{H}_C$ is the RPC term and $\mathcal{H}_K$ includes the rest of the terms in Eq. (9). The wave function of the total Hamiltonian $\mathcal{H}$ is expressed as a linear combination of the eigenfunctions of $\mathcal{H}_K$. The secular equation obtained from Hamiltonian (12) contains an n × n matrix, where n is the number of states

of different K quantum numbers used in the calculation. The n roots of the secular equation correspond to the energies of the various K states. The simplest case arises when there are only two interacting states with quantum numbers K and K+1. In that case the energies of the two levels with spin I, in the two bands, is given by the relation[7]

$$E(I) = 1/2 \left\{ E_{K+1}(I) - E_K(I) \right\} \pm 1/2 \left[\{ E_{K+1}(I) - E_K(I) \}^2 + 4A_K^2 (I-K)(I+K+1) \right]^{1/2} ,$$

where $A_K = \left| \langle K | \frac{\hbar^2}{2\Im} \vec{J}_- | K+1 \rangle \right|$ (13)

and $J_- = \sum_{\text{particles}} \vec{j}_-$.

As mentioned earlier the matrix element A_K is calculated with the Nilsson wave functions. The values of A_K between the particle and hole state has been reduced in our calculations. The reduction is justified by the fact that for a nucleus with a sharp Fermi surface, A_K between the particle and hole state is zero. The non-zero value of the matrix element between the particle and hole state of a nucleus is due to the diffuseness of the Fermi surface, caused by the pairing force.

Because of the RPC term the state with quantum number K no longer remains pure. The interaction introduces some admixture of the (K±1) states. The wave function, under such circumstances, can be written as

$$\Psi_I = a_I \Psi_{I,K} + b_I \Psi_{I,K+1} , \qquad (14)$$

where $a_I^2 + b_I^2 = 1$.

The admixture coefficient "a" is given by the relation[7]

$$a_I = \left\{ 1 + \left[\pm R + \sqrt{1+R^2} \right]^2 \right\}^{-1/2} ,$$

where $$R_K(I) = \frac{|E_{K+1}(I) - E_K(I)|}{2\, A_K[(I-K)(I+K+1)]^{1/2}} \quad . \qquad (15)$$

It is apparent from Eq. (15) that the closer the states K and K+1 are, the stronger the interaction will be. In our calculations on the Bk^{249} alpha decay, the admixture coefficients for the daughter and the parent were determined with Eq. (15).

ACKNOWLEDGMENTS

It is a pleasure to express my thanks to Professor Isadore Perlman for his advice and direction in the course of this work.

I am extremely indebted to Dr. Frank Asaro for his constant assistance and guidance in every phase of this research. I am also grateful to Duane F. Mosier for his help with electronic problems, Mrs. Helen V. Michel for helping me in the purification and preparation of samples, and calculating hindrance factors. Thanks are also due to Richard E. Parsons for the timely construction of the new coincidence chamber.

The comments and suggestions of the members of the laboratory staff, particularly, Professor John O. Rasmussen and Dr. Frank S. Stephens are highly appreciated.

I am thankful to the Health Chemistry staff, in particular, G. H. Driscoll, A. F. Minter, and E. N. Calhoon for their help in the handling of the radioactive materials. Members of the Chemistry Division Technical Support, particularly, D. F. Mosier, J. E. Arnold, M. N. Firth, and G. W. Kilian deserve thanks for maintaining the electronic components in working order. Thanks are extended to the crew of 88" cyclotron for their assistance and co-operation in the bombardments. Mrs. H. V. Michel and Miss Susanne Halvorsen deserve special thanks for working late hours on the purification of Fm^{255}. I am thankful to the member of the Mechanical Workshop Group, the members of the Semiconductor Group and E. Elad for providing high-resolution detectors.

Thanks are also due to Dr. C. M. Lederer, for his assistance in the initial phase of this work; to Dr. K. J. Poggenburg, Jr., for carrying out some calculations of alpha intensities; to Dr. S. G. Prussin, for helping me in the calibration of γ-ray detectors; and M. D. Holtz for his help in Coriolis calculations.

Lastly I would like to express my appreciations to my many friends, particularly, a few of my Pakistani fellows for keeping me in cheerful mood despite the tedious work.

I am thankful to the members of the Chemistry Division Office staff, in particular, Mrs. Jyl Hagler for typing the thesis.

This work was done under tha auspices of U.S. Atomic Energy Commission.

REFERENCES

1. F. S. Stephens, F. Asaro and I. Perlman, Phys. Rev. 113, 212 (1959).
2. B. R. Mottelson and S. G. Nilsson, Kgl. Danske Videnskab. Selskab, Mat.-Fys. Skrifter 1, No. 8 (1959).
3. S. G. Nilsson, Kgl. Danske Videnskab. Selskab, Mat.-Fys. Medd. 29, No. 16 (1955).
4. A. Bohr and B. R. Mottelson, Kgl. Danske Videnskab. Selskab, Mat.-Fys. Medd. 27, No. 16 (1953).
5. J. M. Hollander, Lawrence Raidation Laboratory Report UCRL-16307 (1965).
6. M. Nakamura and R. L. La Pierre, Nucl. Instr. Methods 32, 277 (1965).
7. A. K. Kerman, Kgl. Danske Videnskab. Selskab, Mat.-Fys. Medd. 30, No. 15 (1956).
8. J. K. Poggenburg, Ph.D. Thesis, Lawrence Radiation Laboratory Report UCRL-16187 (1965).
9. R. C. Pilger, Ph.D. Thesis, Lawrence Radiation Laboratory Report UCRL-3877 (1957).
10. C. P. Ruiz, Ph.D. Thesis, Lawrence Radiation Laboratory Report UCRL-9511 (1961).
11. K. Gunter and F. Asaro, Lawrence Radiation Laboratory, private communication.
12. E. Elad, Nucl. Instr. Methods 37, 327 (1965).
13. C. M. Lederer, Ph.D. Thesis, Lawrence Radiation Laboratory Report UCRL-11028 (1963).
14. G. R. Choppen, B. G. Harvey, and S. G. Thompson, J. Inorg. Nucl. Chem. 2, 66 (1956).
15. L. Phillips and R. Gatti, unpublished data referred to in National Academy of Sciences National Research Council, Nuclear Science Series NAS-NS 3031, 13 (Oct. 1960).
16. This electroplating technique was developed by R. M. Latimer of this Laboratory.

17. A. Chetham-Strode, Jr., Ph.D. Thesis, Lawrence Radiation Laboratory Report UCRL-3322 (1956).
18. R. M. Latimer and J. T. Haley, Lawrence Radiation Laboratory Report UCRL-16191 (1965).
19. S. Fried and H. Schumacher, Lawrence Radiation Laboratory Chemistry Division Annual Report, 1961 (UCRL-10023, Jan. 1962).
20. C. M. Lederer, J. M. Hollander, and I. Perlman, Table of Isotopes (John Wiley & Sons, Inc., New York), to be published.
21. A. H. Wapstra, Nucl. Phys. 57, 48 (1964).
22. H. V. Michel (Lawrence Raidation Laboratory), to be published in Nuclear Data.
23. M. A. Preston, Phys. Rev. 71, 865 (1947).
24. A. Bohr, P. O. Fröman, B. R. Mottelson, Kgl. Danske Videnskab. Selskab, Mat.-Fys. Medd. 29, No. 10 (1955).
25. L. A. Sliv and I. M. Band, Coefficients of Internal Conversion of Gamma Radiation, Academy of Sciences of the USSR, Publication of the Leningrad Physico-Technical Institute: Part I K-Shell (1956), Part II L-Shell (1958); Issued in U.S.A. as Reports 57 ICC K1 and 58 ICC L1 Physics Dept. University of Illinois, Urbana, Illinois.
26. E. Hyde, I. Perlman, and G. T. Seaborg, The Nuclear Properties of the Heavy Elements (Prentice Hall, Englewood Cliffs, N. J., 1964).
27. B. S. Dzhelepov, R. B. Ivanov, V. G. Nedovesov, and Yu. T. Puzynovich, Bull. Acad. Sci. USSR, Phys. Ser. 24, 247 (1961).
28. E. F. Tret'yakov, M. R. Anikina, L. L. Gol'din, G. I. Novikova, and N. N. I. Pirogova, Soviet Phys.-JETP (English translation) 37 (10), 656 (1960).
29. K. V. Vander Sluis and J. R. McNally, Jr., J. Opt. Soc. Am. 45, 65 (1955).
30. V. N. Egorov, Opt. Spect. XVI, No. 4, 301 (1964).
31. E. L. Murri and J. E. Cline, Bull. Am. Phys. Soc. II 6, 239 (1961).

32. S. A. Baranov, V. M. Kulakov, and S. N. Belenki, Soviet Phys.-JETP (English transition) 16, No. 4, 801 (1963); also published in Nucl. Phys. 41, 95 (1963).

33. E. Tret'yakov and L. N. Kondrat'ev, Bull Acad. Sci. USSR (English translation) 29, No. 1, 243 (1965).

34. T. H. Braid, R. R. Chasman, J. R. Erskine, and A. M. Friedman, Phys. Letters 18, No. 2, 149 (1965).

35. B. Bleaney, P. M. Llewellyn, M. H. L. Pryce, and G. R. Hall, Phil. Mag. 45, 773, 991 (1954).

36. F. Asaro and I. Perlman, Phys. Rev. 107, 318 (1957).

37. J. R. Huizenga, C. L. Rao, and D. W. Engelkemeir, Phys. Rev. 107, 319 (1957).

38. J. O. Newton, Physica 22, 1129 (1956); also Nucl. Phys. 3, 345 (1957).

39. R. M. Diamond, M. D. Holtz, J. O. Newton, and F. S. Stephens, Lawrence Radiation Laboratory, private communication (1966).

40. F. S. Stephens, Lawrence Radiation Laboratory, private communication.

41. S. G. Nilsson (Institute of Theoretical Physics, Copenhagen), private communication to F. Asaro (1961).

42. G. Alaga, K. Adler, A. Bohr, and B. R. Mottelson, Kgl. Danske Videnskab. Selskab, Mat.-Fys. Medd. 29, No. 9 (1955).

43. R. Marrus, W. Nierenberg, and J. Winocur, Phys. Rev. 120, 1429 (1960).

44. F. Asaro, F. S. Stephens, S. Amiel, and I. Perlman (Lawrence Radiation Laboratory) unpublished results, cited in Ref. 26.

45. F. S. Stephens, F. Asaro, S. Fried, and I. Perlman, Phys. Rev. Letters 15, No. 9, 420 (1965).

46. V. G. Soloviev and T. Sikolos, Nucl. Phys. 59, 145 (1964).

47. C. J. Orth, Phys. Rev. 148, No. 3, 1226 (1966).

48. P. R. Fields, M. H. Studier, H. Diamond, J. F. Mech, M. G. Ingraham, G. L. Pyle, C. M. Stevens, S. Fried, W. M. Manning, A. Ghiorso, S. G. Thompson, G. H. Higgins, and G. T. Seaborg, Phys. Rev. 102, 180 (1956).

49. J. Milsted and A. M. Friedman, Bull. Am. Phys. Soc. II 7, 353 (1962).
50. F. Asaro, S. G. Thompson, F. S. Stephens, and I. Perlman, Lawrence Radiation Laboratory Report UCRL-9382 (1960); also presented in somewhat different form by I. Perlman in Proceedings of the International Conference on Nuclear Structure at Kingstown, Ontario, Aug. 29-Sept. 3, 1960 (Univerity of Toronto Press), pp. 553-557.
51. M. D. Holtz, Lawrence Radiation Laboratory, private communication.
52. L. B. Magnusson, unpublished data (1957), cited in Ref. 26.
53. F. S. Stephens, F. Asaro, S. G. Thompson, and I. Perlman, Bull. Am. Phys. Soc. Ser. II 2, 394 (1957), and also private communication.
54. G. T. Ewan, J. S. Geiger, R. L. Graham, and D. R. MacKenzie, Phys. Rev. 116, 950 (1959).
55. R. R. Chasman and J. O. Rasmussen, Phys. Rev. 115, 1260 (1959).
56. F. Asaro, F. S. Stephens, J. M. Hollander, and I. Perlman, Phys. Rev. 117, No. 2, 492 (1960).
57. A. Ghiorso, S. G. Thompson, G. H. Higgins, M. H. Studier, P. R. Fields, S. M. Fried, H. Diamond, J. H. Mech, G. L. Pyle, J. R. Huizenga, A. Hirsch, W. M. Manning, C. I. Browne, H. L. Smith, and R. W. Spence, Phys. Rev. 99, 1048 (1955).
58. F. Asaro, S. Bjørnholm, and I. Perlman, Phys. Rev. 133, No. 2B, 291 (1964).
59. A. H. Wapstra, G. H. Nijgh, and R. van Lieshout, Nuclear Spectroscopy Tables (North-Holland Pub. Co., 1959), p. 81.
60. O. Prior, Arkiv Fysik 16, 15 (1959).
61. H. J. Mang, and J. O. Rasmussen, Kgl. Danske Videnskab. Selskab, Mat.-Fys. Skrifter 2, No. 3 (1962).
62. B. R. Mottelson and S. G. Nilsson, Phys. Rev. 99, 1615 (1955).
63. M. G. Mayer and J. H. D. Jensen, Elementary Theory of Nuclear Shell Structure (John Wiley and Sons, Inc., New York, 1955).
64. H. J. Mang, J. K. Poggenburg, and J. O. Rasmussen, Lawrence Radiation Laboratory Report UCRL-10939 (1964).

65. A. Bohr and B. R. Mottelson, Lectures on Nuclear Physics, at Berkeley, Summer 1966.

66. R. D. Woods and D. S. Saxon, Phys. Rev. 95, 577 (1954).

67. P. O. Fröman, Kgl. Danske Videnskab. Selskab, Mat.-Fys. Skrifter 1, No. 3 (1957).

68. R. S. Thomas, Prog.Theor. Phys. 12, 253 (1954).

69. J. O. Rasmussen, Phys. Rev, 115, 1675 (1959).

70. L. A. Malov and V. G. Soloviev, Joint Institute for Nuclear Studies, Dubna, USSR Reprint E-2857 (1966).

71. W. C. HcHarris, Ph.D. Thesis, Lawrence Radiation Laboratory Report UCRL-11784 (1965).

72. M. D. Holtz, Ph.D. Thesis (to be published).